

November 2017

Microbial Dynamics and Design Considerations for Decentralized Microbial Fuel Cell Applications

Cynthia Castro
University of Massachusetts - Amherst

Follow this and additional works at: https://scholarworks.umass.edu/dissertations_2



Part of the [Biotechnology Commons](#), [Civil Engineering Commons](#), [Environmental Engineering Commons](#), and the [Environmental Microbiology and Microbial Ecology Commons](#)

Recommended Citation

Castro, Cynthia, "Microbial Dynamics and Design Considerations for Decentralized Microbial Fuel Cell Applications" (2017). *Doctoral Dissertations*. 1074.
https://scholarworks.umass.edu/dissertations_2/1074

This Open Access Dissertation is brought to you for free and open access by the Dissertations and Theses at ScholarWorks@UMass Amherst. It has been accepted for inclusion in Doctoral Dissertations by an authorized administrator of ScholarWorks@UMass Amherst. For more information, please contact scholarworks@library.umass.edu.

**MICROBIAL DYNAMICS AND DESIGN CONSIDERATIONS FOR
DECENTRALIZED MICROBIAL FUEL CELL APPLICATIONS**

A Dissertation Presented

by

CYNTHIA JEANETTE CASTRO

Submitted to the Graduate School of the
University of Massachusetts Amherst in partial fulfillment
Of the requirements for the degree of

DOCTOR OF PHILOSOPHY

SEPTEMBER 2017

Department of Civil and Environmental Engineering

**MICROBIAL DYNAMICS AND DESIGN CONSIDERATIONS FOR
DECENTRALIZED MICROBIAL FUEL CELL APPLICATIONS**

A Dissertation Presented

by

CYNTHIA JEANETTE CASTRO

Approved as to style and content by:

Caitlyn S. Butler, Chair

James Holden, Member

John Tobiason, Member

Ignacio T. Vargas, Member

Richard N. Palmer, Department Head
Department of Civil and Environmental Engineering

DEDICATION

To my loving parents, Maria Marta and Josue German.

“Queda prohibido no sonreír a los problemas, no luchar por lo que quieres, abandonarlo todo por miedo, [y] no convertir en realidad tus sueños.” –Pablo Nerudo

ACKNOWLEDGEMENTS

Foremost, I would like to thank my academic advisor, Caitlyn Butler, for her unwavering support throughout my time as a graduate student in her lab. She has not only been an excellent advisor and mentor, but also a friend. She has helped me become a better researcher by not only giving me guidance where needed but by also pushing me to achieve excellence so that I can fulfill my academic and career endeavours.

I would like to thank my committee members, John Tobiason, Ignacio Vargas, and James Holden for all their guidance in the past few years. I have always appreciated the writing critiques from Dr. Tobiason, which has improved my writing immensely in the past six years. Dr. Vargas was my mentor and advisor during my time as a visiting researcher in Chile. We had many good conversations about research during our meetings and he always asked insightful questions that instigated thoughtful discussions. As a visitor in a foreign country, I couldn't have asked for a friendlier or kinder advisor than Nacho. I also want to thank Dr. Holden for helping me understand the basic concepts in microbiology. I appreciated his patience as I tried to overcome the huge learning curve I came with as I transitioned from a civil engineering background to a field that required a substantial knowledge of biochemistry and microbiology.

Of course, this work would not have been possible if not for the funding support from the National Science Foundation Graduate Research Fellowship Program (Grant No. S121000000211), The National Science Foundation Graduate Research Opportunities Worldwide, and the Charles F. Perrell Research & Training Award in Environmental Engineering from the College of Engineering.

I would also like to thank all my colleagues in the labs and offices for making my time here at UMass a memorable experience. Specifically, Caitlin, Rosa, Camilla, Varun, and Liz. I'd like to give a special thanks to all the undergrads, especially Dan, Katelyn, Isabella, and Fernanda, who over the years have helped me make the countless liters of media and have even come on weekends to make sure the reactors never stop running. I'd also like to give special thanks to my childhood friends, Jimmy and Diana, for inspiring me to be a better person and to accept the challenges that life gives.

I'd like to thank Jonny for being my partner and friend, and for supporting my pursuit of this degree. It has not been an easy task, to say the least, but he has always had my best interest in mind and continues to motivate me to pursue success. The past few years would not have been as fun if it wasn't for his love of adventure. Thanks for taking me along for the ride.

I'd like to thank German and Jenny for being such awesome siblings. I could not have left Texas if it wasn't for their wholehearted support to follow my dreams. Growing up in our neighborhood and community, not many people went away to school, let alone to graduate school. You both made it possible for me to find the courage to leave our home and pursue these degrees.

Finally, this dissertation is dedicated to my wonderful parents. They fled their beloved El Salvador during the peak of a civil war to survive and give their children a life of opportunity in the United States. I am grateful every day of my life for the sacrifices they have made for my siblings and me. I would have never been able to push past the circumstantial barriers if it were not for their encouragement and faith in my ambitions. I love you both more than words can express.

ABSTRACT

MICROBIAL DYNAMICS AND DESIGN CONSIDERATIONS FOR DECENTRALIZED MICROBIAL FUEL CELL APPLICATIONS

SEPTEMBER 2017

CYNTHIA J. CASTRO, B.S., UNIVERSITY OF TEXAS AT AUSTIN

M.S., UNIVERSITY OF MASSACHUSETTS AMHERST

Ph.D., UNIVERSITY OF MASSACHUSETTS AMHERST

Directed by: Dr. Caitlyn S. Butler

The purpose of this dissertation was to assess the practicality of using microbial fuel cells (MFCs) as alternative sanitation systems for wastewater treatment and energy recovery, focusing on identifying key design considerations for treating high strength wastewaters and managing alternative metabolic pathways.

We evaluated the energetic outputs of a lab-based pilot MFC designed to treat complex organics present in both synthetic feces and municipal wastewater. The pilot MFC produced two energetic products, methane and electricity, when treating two types of complex wastewaters. The energetic products associated with anode respiration and methanogenesis were simultaneously observed and yielded a combined energy output of $3.3 \pm 0.64 \text{ W/m}^3$ when treating synthetic feces wastewater and $0.40 \pm 0.07 \text{ W/m}^3$ when treating municipal wastewater.

We also evaluated the impacts of electrolytes (primarily as conductivity and pH) on the electrochemical performance of MFCs using augmented inoculums. Under electrolytically-stressed anode environments, bioaugmenting the inocula (primary

wastewater) with microorganisms from acidic and high-salts environments improve the electrochemical performance of a MFC under high conductivities (5.2-37 mS/cm) and low pH (4.1-6.2).

The final section is focused on the role of external resistances, or external load, and its impact on electrochemical performance in MFCs when methanogenesis inhibitors are present in the anode. Our study observed that external resistance had a significant influence on the anode potential and power and current densities. When MFCs are operated at low external resistances (17 and 170 Ω), the addition of 2-BES caused anode potential to decrease to values between -0.1 and 0 mV vs SHE. An increase in current density and CE during these periods suggest that shifts to lower anode potentials triggered c-type cytochromes that are only active within that specific range of redox potential. During periods when nitrate was present in the anode, CE and current densities decreased at all external resistances except at 1800 Ω .

Although higher power and current densities were observed at low external resistances, they were not sustained throughout the experimental period. Consistent current output was more readily observed at high external resistances (820 and 1800 Ω), demonstrating the electrochemical robustness of the biofilms exposed to perturbations of the anode environment at more negative anode potentials.

TABLE OF CONTENTS

	Page
ACKNOWLEDGEMENTS.....	v
ABSTRACT.....	vii
LIST OF TABLES.....	xii
LIST OF FIGURES	xiii
LIST OF SYMBOLS AND ABBREVIATIONS	xix
 CHAPTER	
1. INTRODUCTION	1
2. MICROBIAL FUEL CELLS.....	6
2.1 Overview and Application.....	6
2.2 Anode Respiring-Bacteria	9
2.3 Influence of Anode Potential.....	12
2.4 Organic Substrates in MFCs.....	16
2.5 Syntrophic Interactions and Competing Metabolisms	18
2.6 Methanogenesis and Anode Community Competition	23
2.7 Methanogenesis Inhibition Strategies	26
2.8 Conclusions	28
3. DECENTRALIZED WASTEWATER TREATMENT USING A BIOELECTROCHEMICAL SYSTEM FOR THE PRODUCTION OF METHANE AND ELECTRICITY*	29
3.1 Introduction	29
3.2 Methods	32
3.2.1 MFC Construction and Startup	32
3.2.2 Batch enrichment studies	33
3.2.3 MFC Operation	34
3.2.4 Chemical Analysis	35
3.2.5 Electrochemical Analysis.....	36
3.2.6 Mass Balances and Power Production	36
3.3 Results and Discussion	38

3.3.1	Methanogenesis within Communities Enriched from the Anode...	38
3.3.2	COD Removal and Nitrate Reduction in the MFC	39
3.3.3	Electrical Power Production in the Pilot-scale MFC	42
3.3.4	SCFA and Methane production in the MFC Anode	43
3.3.5	Methane as an Alternative Energy Source.....	44
3.4	Conclusion.....	46
4.	ANDEAN SOIL ENRICHMENTS FOR COMPLEX CARBOHYDRATE DEGRADATION AND POWER PRODUCTION IN A MFC—EFFECTS OF PH AND CONDUCTIVITY	48
4.1	Introduction	48
4.2	Objective	51
4.3	Methods	51
4.3.1	MFC Construction	51
4.3.2	Inocula.....	53
4.3.3	Normal Anode Environment.....	54
4.3.4	Stressed Anode Environment.....	55
4.3.5	Performance Analysis	55
4.3.6	Statistical analysis.....	56
4.4	Results.....	57
4.4.1	Degradation of Starch During Normal Conditions	57
4.4.2	Power Production and Coulombic Efficiency During Normal Conditions.....	59
4.4.3	Reactor Performance During Stressed Anode Environment.....	60
4.5	Discussion.....	62
4.6	Conclusions.....	64
5.	EFFECTS OF EXTERNAL LOAD ON MFC ELECTROCHEMICAL PERFORMANCE UNDER SELECT METHANOGENESIS INHIBITORS	66
5.1	Introduction	66
5.2	Objective	69
5.3	Experimental Procedure	70
5.3.1	MFC Construction.....	70
5.3.2	MFC Operation.....	72

5.3.3	Treatment and Electrochemical Performance Evaluation	75
5.3.4	Statistical Analysis	77
5.4	Results	77
5.4.1	Internal Resistance	77
5.4.2	Maximum Power Densities	79
5.4.3	Anode Potential	81
5.4.4	Operational Current Densities	83
5.4.5	Coulombic Efficiency.....	84
5.5	Discussion	87
5.5.1	Internal Resistance Fluctuates with Changes to the Anode Environment	87
5.5.2	High External Resistances Demonstrate the Electrochemical Robustness of Anode Respiring Biofilms	88
5.6	Conclusions	90
6.	DISSERTATION CONCLUSIONS	92
	APPENDIX: SUPPLEMENTARY INFORMATION FOR CHAPTER 5	96
	BIBLIOGRAPHY	102

LIST OF TABLES

Table	Page
2.1 Examples of complex substrate wastewaters for power generation in MFCs (modified from Pandey et al., 2016)	17
4.1 MFC operation parameters under stressed anode environments	55
5.1 Summary of methanogenesis inhibitor addition for each phase of the experiment. Nitrate was added at a ratio 3.7 mg C/ mg N.....	75

LIST OF FIGURES

Figure	Page
1.1 General diagram of an MFC using graphite as the solid electrodes and an abiotic cathode (Franks & Nevin, 2010).....	3
2.1 Schematic of a MFC with an abiotic cathode representing MFC technology principles (Liu & Cheng, 2014).....	6
2.2 Schematic of potential extracellular electron transfer mechanisms employed by ARB. a) Direct electron transfer by outer membrane cytochromes attached to the anode surface b) electron transfer by soluble electron shuttles and c) electron transfer by conductive pili called nanowires on the extracellular biofilm matrix. (Torres et al., 2010)	10
2.3 Current Densities of Six Different Geobacter Species Under Anode Potentials of -500 to 200 mV vs Ag/AgCl (corresponding to -300 to 400 mV vs SHE) (Modified from Kato 2017)	14
2.4 Microbial Community Distribution for ARB Communities Grown at Different Anode Potentials (Torres et al., 2009)	16
2.5 Flow chart outlining the degradation of complex wastes by anaerobic digestion (modified from Sang et al., 2012).....	19

2.6 Electrical interplay between microorganisms and minerals.	
Microorganisms use minerals that contain metal ions as terminal electron acceptors for respiration (part a), electron and/or energy sources for growth (part b), electrical conductors that facilitate electron transfer between microbial cells of the same and different species (part c) and electron-storage materials, or batteries, to support microbial metabolism (part d) (Shi et al., 2016)	21
2.7 Diagram of substrate degradation pathways in MFCs (Velasquez-Orta et al., 2011)	25
3.1 Schematic of the MFC design (not to scale). The wastewater and the nitrate media were each pumped directly into the anode and cathode chambers, respectively. Both chambers contained granular graphite as their electrode material.	33
3.2 Methane production in the headspace of batch reactors enriched with microbial communities from the large-scale MFC, containing either graphite granules, plastic beads, or neither (suspended) (adapted from Jack, 2015)	39
3.3 Average anode chamber influent and effluent COD concentrations for (A) Case F and (B) Case W with standard errors. The percentages above the bars represent average removal efficiencies during each operational period.	41

3.4 Alternative energetic by-products during the degradation of complex substrates in Case F in the large-scale MFC	43
3.5 Comparison of power recovery from methane and electricity normalized by the COD consumed in the anode and presented with standard errors.	45
4.1 Single chamber MFC with graphite granules as the anode electrode and a carbon cloth air cathode.	53
4.2 COD removal in inoculated, co-inoculated, and non-inoculated reactors during normal conditions. All reactors observed high COD removal, over 60% of the initial batch concentrations.	58
4.3 Power density across 12 batch cycles for reactors WW-only, AR-WW, and the control.	59
4.4 Average coulombic efficiency for WW-only, AR-WW, and control reactors with standard deviations across all batch cycles. There was no statistical difference between WW-only and AR-WW.	60

4.5 Charge transferred during stressed anode environment conditions per batch cycle A) changes in anode bulk liquid conductivity and B) changes in anode bulk liquid pH. When conductivity changes, the pH remained at 6.2. When the pH was changed, the conductivity remained at 5.2 mS/cm. For each reactor, statistical differences ($p < 0.05$) of means between the highlighted operational conditions are shown with either (*) or (■) above the bar. All other relationships had no statistically difference in means.....	61
5.1 Reactor setup during the full length of the experiments. One reactor was narrower and taller, but the liquid volume and the surface area remained the same across all reactors. All subsequent power and current densities were normalized to the available surface area during each phase of the experiment.	72
5.2 Internal resistances at the end of each phase for reactors R_17, R_170, R_820, R_1800 for all phases of the experimental period. Internal resistances were determined by LSV. Standard error is shown for all calculated internal resistances. Internal resistance was not available for R_820 during phase VI.	78

5.3 Maximum power densities attainable at the end of each phase for reactors operating with 17, 170, 820 and 1800 Ω . No maximum power density is shown for R_820 during phase VI. During the experiment, baseline anode conditions were re-established during Phase V and VII and comparison were made in regards to Phase I.	81
5.4 Anode potentials across all experimental phases for reactors R_17, R_170, R_820 and R_1800 Ω	83
5.5 Current density across all phases for reactors R_17, R_170, R_820, and R_1800.	84
5.6 Coulombic efficiency and electron sinks due to dissimilatory nitrate reduction occurring at the anode across all phases. Error bars represent standard deviations.....	86
A.1 Polarization curves for determining internal losses and maximum power densities at each phase for all reactors described in Chapter 5.	96
A.2 Power density curves used for determining maximum current density attainable if the internal resistance matched the external resistance. Data shown for reactors R_17, R_170, R_820, and R_1800 for all phases (Chapter 5). Data for R_820 during Phase VI was not available.	97

A.3 Maximum power densities obtained at the end of phase I, V, and VII	
when no inhibitor was presented.	98
A.4 Photographic images of the anode electrodes at the end of the	
experiment. A) R_17; B) R_170; C) R_820; D) R_1800. Biofilms are	
circled.	99

LIST OF SYMBOLS AND ABBREVIATIONS

ARB:	Anode Respiring Bacteria
BESs:	Bioelectrical Systems
2-BES:	2-Bromoethanesulfonate
CE:	Coulombic Efficiency
COD:	Chemical Oxygen Demand
cDNA:	complementary Deoxyribonucleic Acid
DIET:	Direct Interspecies Electron Transfer
DNA:	Deoxyribonucleic Acid
EAB:	Electrochemically-Active Bacteria
F:	Faraday's Constant, 96485.3 C/mol
GC:	Gas Chromatography
gDNA:	genomic Deoxyribonucleic Acid
ΔG :	Gibbs Free Energy
HRT:	Hydraulic Retention Time
LCFAs:	Long Chain Fatty Acids
LSV:	Linear Sweep Voltammetry
MFCs:	Microbial Fuel Cells
mcr:	Methyl-coenzyme M reductase
NO ₃ :	Nitrate
NO ₂ :	Nitrite
NO:	Nitric Oxide
N ₂ O:	Nitrous Oxide

PTFE: Polytetrafluoroethylene

SHE: Standard Hydrogen Electrode

TCD: Thermal Conductivity Detector

USEPA: United States Environmental Protection Agency

CHAPTER 1

INTRODUCTION

There are 1.1 billion people worldwide that have absolutely no access to improved drinking water, and over 2.4 billion people who lack access to an improved sanitation system (WHO/UNICEF JMP, 2015). Much of the affected people reside in developing nations across sub-Sahara Africa, while others reside in South and Central America, and South and Southeast Asia. As of 2015, the Millennium Development goals aiming to halve the population that live under environments lacking safe drinking water and basic sanitation were unmet. With Africa projected to account for over half of the global population growth in the next 34 years (United Nations, 2015), it is imperative to establish viable sanitation and wastewater treatment solutions that remove pathogens and other harmful contaminants while returning treated effluent back to the environment.

One of the major humanitarian movements of today is to assist low-income countries by providing decentralized drinking water and sanitation systems to prevent the spread of disease. Engineers have assisted in combating waterborne illnesses by providing on-site drinking water treatment using low-cost filtration and disinfection techniques (Montgomery & Elimelech, 2007) and improved sanitation by relying on aerobic and anaerobic biological treatment of wastewater using latrines (Mihelcic, 2009) and biogas systems (Chen et al., 2010).

Preventing the spread of bacterial and pathogenic disease is not the only concern when it comes to water and wastewater treatment. The increase in anthropogenic nitrogen pollution has also had significant impacts to the global nitrogen cycle, not only affecting aquatic ecosystems but also human health. Nitrate is typically used as a fertilizer for

agricultural use and can contaminate livestock feed, leading to nitrogen-rich animal waste through consumption. Other nitrogen species are also readily found in human and animal waste in the form of ammonium (NH_4^+) and urea. Nitrogen compounds from fertilizers used in agricultural fields can percolate through soils and contaminate groundwater sources. Nearly half of the drinking water sources worldwide originate as groundwater (Reilly et al., 2008), making these users more susceptible to potential nitrogen exposure. The consumption of nitrates in water has been linked to methemoglobinemia, a fatal condition affecting infants (Schlesinger, 2009) as well as associated with various cancers, birth defects, and diabetes (Ward, 2009).

Nitrogen species in surface water runoff can cause eutrophication and algal blooms of nearby water systems, impacting the ecosystem of aquatic life and impairing the aesthetics of recreational waters. Nitrogen species can also reach surface waters from wastewater treatment systems. Treatment methods for nitrogen-rich wastewaters in centralized wastewater treatment systems include the use of aerobic and/or anoxic reactors. These reactors utilize aerobic nitrifying bacteria to oxidize ammonium to nitrate and anaerobic denitrifying bacteria that reduce nitrate to inert nitrogen gas (Rittmann & McCarty, 2001).

In energy-yielding wastewater treatment systems, such as anaerobic digesters designed to treat highly concentrated waste streams for methane production, nitrogenous species are not directly treated and their presence can actually inhibit the anaerobic microbial metabolic processes (Fricke et al., 2007). This can lead to inefficiencies in treatment and energy recovery. It is estimated that 25 Tg N/year from human waste is discharged into aquatic systems worldwide, where 61% is discharged from decentralized

wastewater treatment systems alone (Oakley et al., 2010). Decentralized treatment systems do not often include nitrogen removal as a primary goal, thus, further research in this area is still required in order to control nitrogen pollution from human waste.

Microbial fuel cells (MFCs), novel biological treatment alternatives, have been designed for treatment of a multitude of organic and inorganic pollutants while also attempting to recover electrical energy from organic-rich wastewaters. In MFCs, anaerobic oxidation of organic constituents from a variety of wastewater sources is facilitated by microorganisms known as anode-respiring bacteria (ARB). These bacteria

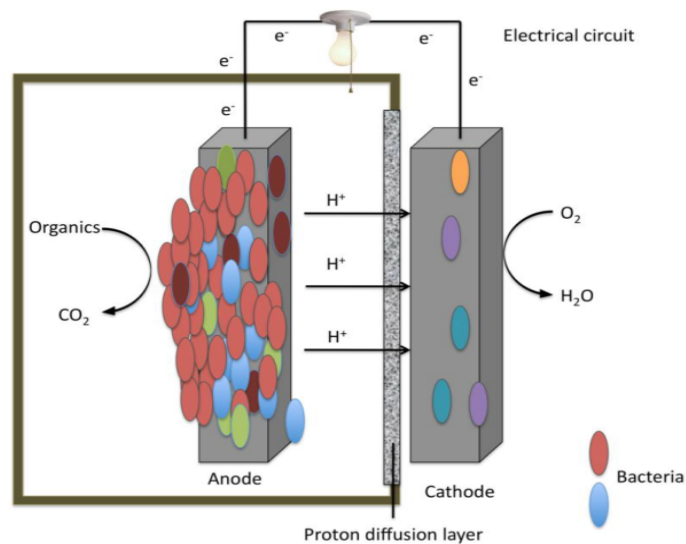


Figure 1.1 General diagram of an MFC using graphite as the solid electrodes and an abiotic cathode (Franks & Nevin, 2010)

can respire a solid electrode, transporting electrons from an anode to a cathode without the need for additional external mediators to facilitate the process (Figure 1.1). By decoupling the oxidation and reduction process into two separate reactions using solid conductive electrodes, electricity can be recovered.

MFC technology has the potential to achieve multiple treatment goals using a wide range of wastewater sources while also recovering energetic byproducts. Although electricity and power yields have increased significantly since their first inception, the anticipated scalability of these yields from bench-scale to full-scale have yet to be reached. Much of the research in this field has continued to focus on understanding the limitations of electricity production, while also shifting focus to developing variants of MFCs that generate chemical byproducts such as hydrogen, peroxides, and for desalination applications (Cao et al., 2009; Cusick et al., 2011b; Liu et al., 2005; Wang & Ren, 2013). Yet, MFCs as a treatment method for centralized municipal wastewater continues to be appealing because MFCs can utilize a large range of organic substrates as their energy source, produce electricity, all while reducing the high costs of aeration that would otherwise be used during the conventional activated sludge process. Unfortunately, very few studies have looked at the implications of developing MFCs as small-scale decentralized treatment systems, suitable as incentivized alternatives to current sanitation systems in developing areas of the world where harvesting energy and directly treating human waste can have meaningful and direct impacts to the livelihood of small communities.

Motivated by the direct need for promoting improved sanitation systems across the globe, the purpose of this dissertation is to assess the practicality of using MFCs as alternative sanitation systems in developing areas for wastewater treatment and energy recovery. This dissertation also highlights several design considerations for developing MFCs to treat high strength wastewaters as well as assess their feasibility for nitrogen

removal. The work presented has been divided into three separate sections with the following objectives:

1. *To determine the feasibility of coevolving methane and electricity in a pilot-scale MFC (Chapter 3; the work presented is a modified version of the published peer-reviewed journal article— C. Castro, V. Srinivasan, J. Jack, & C. Butler.(2016). Decentralized wastewater treatment using a bioelectrochemical system to produce methane and electricity, J. WaSH Dev., 6(4) 613-621)*
2. *To determine if inocula augmentation from extreme environments can improve electron recovery in MFC anodes operating under low pH and high conductivities (Chapter 4)*
3. *To assess the impact of external load on the electrochemical performance of MFCs when operated under sequential methanogenesis inhibitors (Chapter 5)*

The collective work pertains to MFC performance when used as a sanitation system to treat human waste, and comments on design considerations needed to optimize energetic byproducts for decentralized MFC applications. As we further understand the limitations of reactor design parameters and anode microbial dynamics that govern the performance of MFCs, we can develop resilient biofilms to improve energy recovery while discharging treated effluent into the environment.

CHAPTER 2

MICROBIAL FUEL CELLS

2.1 Overview and Application

MFCs are a novel technology that utilize microorganisms to recover energy in the form of electricity. At the anode, an anaerobic environment allows heterotrophic bacteria to oxidize organic matter and reduce a solid electrode (Figure 2.1). During this process, electrons are transported from the anode to the cathode across an external load or resistance, producing a current. The anode and cathode are typically separated by a proton exchange membrane or other means of partitioning to allow diffusion of protons to the cathode, maintaining electroneutrality between compartments. At the cathode, electron acceptors can either be reduced abiotically or biologically (biocathodes).

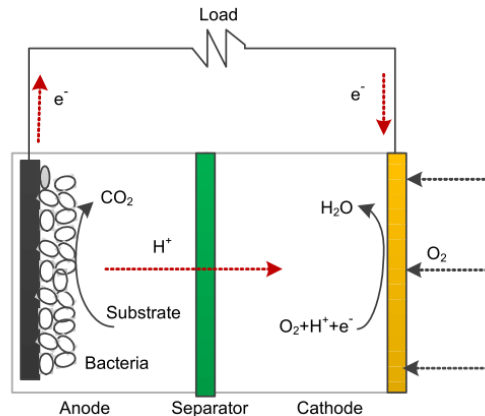


Figure 2.1 Schematic of a MFC with an abiotic cathode representing MFC technology principles (Liu & Cheng, 2014)

Extensive research has been conducted at the bench-scale, exploring various organic substrates, inocula, electrode materials, and reactor configurations for power optimization to ultimately make full-scale wastewater treatment by MFC technology a reality. In recent years, large-scale reactors have consisted of modular MFCs, encompassing a multitude of sequential liter-scale reactors for wastewater treatment and power production. These systems have been specifically designed to treat various wastewaters: sewage from a septic tank, municipal wastewater, and human urine (Alzate-Gaviria et al., 2016; Ge & He, 2016; Ieropoulos et al., 2016). MFC technology is attractive for centralized wastewater treatment because it provides an alternative method to the conventional activated sludge process that requires an intensive external addition of oxygen to promote microbial growth and meet organic carbon, biological nitrogen, and biological phosphorus effluent requirements. It is estimated that 30-60% of a plant's energy use is towards biological treatment (Willis, 2010). Although piloting MFC systems for real-world applications is ongoing, power production does not scale linearly as compared to bench-scale reactors (Castro et al., 2016; Cusick et al., 2011a; Li et al., 2013; Logan, 2010; Zhang et al., 2013). It is difficult to compare performance between bench-scale reactors as the relatively few pilot and large-scale systems that have been conducted have very different configurations, substrate sources, cathode types, and inocula.

Clearly, there are still inefficiencies in scaling up MFC designs to obtain energy for practical use. Most pilot MFC reactors have been constructed with expensive materials such as ion exchange membranes and abiotic cathode catalysts (Alzate-Gaviria et al., 2016; Janicek et al., 2014; Logan, 2010; Zheng, et al., 2012). The potential operational costs of pilot-scale MFCs still far outweigh the power-yielding capabilities that have been reported (Logan, 2010; Zhou et al., 2013). Although no life cycle assessments (LCA) have been conducted on current pilot-scale MFC designs, a preliminary comparison of MFC technology to microbial electrolysis cells (MECs) and anaerobic reactors for centralized wastewater treatment provides evidence that MFCs are not yet more environmentally conscientious than other biological treatment processes (Foley et al., 2010). Although energy recovery from MFCs is still not suited for large-scale centralized wastewater treatment, MFC technology could present an optimal opportunity for decentralized applications to meet sanitation needs in rural areas and provide usable energy in areas where these resources are lacking. Human waste is abundant in organic substrates and nitrogenous compounds which could be utilized to power MFCs (Castro et al., 2014) and recover energy. Anaerobic digesters can also treat organic matter by providing energy as methane, but the presence of nitrates can inhibit the methanogenesis process. MFCs are a promising technology for treating organic and nitrogenous compounds while also recovering energy.

Research is still ongoing to make MFC technology environmentally and economically feasible while trying to further understand its limitations. One of the most important design aspects of MFCs treating complex organic substrates from wastewater are the consortia of microorganisms that facilitate the oxidation process of organic

compounds at the anode. Understanding the microbial ecology of the anode biofilm can give insight into which key electrochemically active microorganisms are present and active, how they interact with non-electrochemically active microbes to complete various metabolic pathways, and how to optimize the anode environment to yield the desired energetic outputs.

2.2 Anode Respiring-Bacteria

Electrochemical activity by microorganisms was first studied by Michael C. Potter (Potter, 1911). Dissimilatory, metal-reducing bacteria from aquatic sediments were first studied to observe the electrochemical activity for harvesting electricity production. Under anaerobic conditions, these electrochemically-active bacteria (EAB) respire solid mineral oxides, such as Fe(III) and Mn(IV), to complete their electron transport chain (Lovley & Phillips, 1988). It wasn't until 2002 that the oxidation and reduction process of these electricity-producing microorganisms was decoupled using a MFC to generate a current across an external load (Bond & Lovley, 2003). Thus, the nomenclature to describe bacteria that can respire a solid electrode are designated as anode respiring bacteria (ARB).

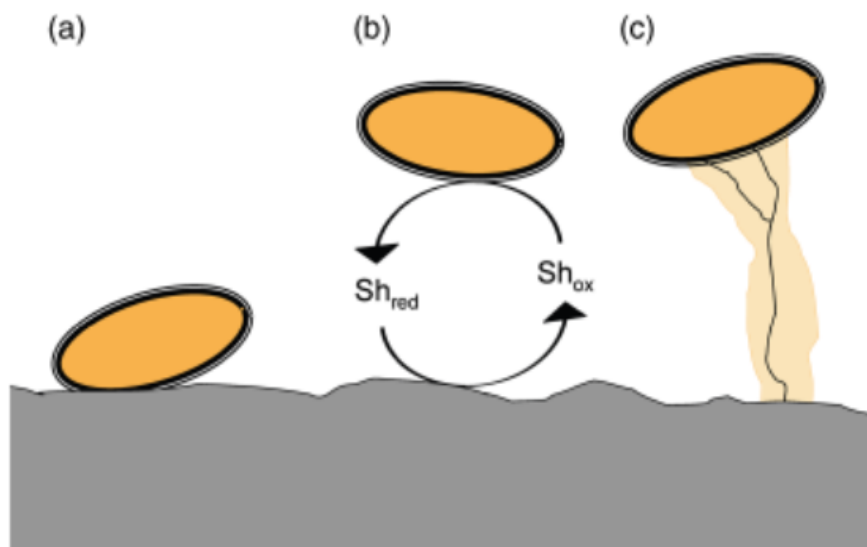


Figure 2.2 Schematic of potential extracellular electron transfer mechanisms employed by ARB. a) Direct electron transfer by outer membrane cytochromes attached to the anode surface b) electron transfer by soluble electron shuttles and c) electron transfer by conductive pili called nanowires on the extracellular biofilm matrix. (Torres et al., 2010)

There are currently three main mechanisms by which ARB can convey electrons from the cell to a solid electrode (Figure 2.2). The first is by direct contact by the outer-membrane c-type cytochromes of ARB with the solid electrode. This type of mechanism has been studied in Gram-negative bacteria such as *Shewanella* and *Geobacter* species and *Desulfovibrio desulfuricans* (Kang et al., 2014; Newton et al., 2009; Zacharoff et al., 2016) as well as a Gram-positive bacteria *Thermincola potens* (Carlson et al., 2012). Bacteria that utilize this mechanism require direct contact with the electrode surface. The second is by utilizing either self-produced or artificial soluble electron shuttles or mediators such as neutral red, thionine, benzylviologen, various phenazines,

phenothiazines, phenoxoazines, iron chelates, pyocyanin, flavins, and quinones to shuttle electrons from the inner cell to the solid electrode terminal electron acceptor (Lovley, 2006; Rabaey et al., 2005; Torres et al., 2010). The third mechanism involves direct contact with a solid electrode but instead through solid conductive or semi-conductive pili that act as nanowires to transport electrons from the cell to the electrode (Boesen & Nielsen, 2013; El-Naggar et al., 2010; Gorby et al., 2006; Reguera et al., 2006). *Geobacter* species can employ all three mechanisms to complete their electron transfer chain.

Studies have now isolated various EAB known to produce electricity through extracellular electron transfer; *Shewanella oneidensis* (Marsili et al., 2008), *Geobacter sulfurreducens* (Bond et al., 2003), *Clostridium butyricum* (Park et al., 2001), *Rhodospirillum rubrum* (Chaudhuri & Lovley, 2003), and *Pseudomonas aeruginosa* are among the most commonly identified and studied. Most belong to the phyla Proteobacteria. The most extensively studied ARBs are the *Geobacter* species and their presence in MFCs is typically used as a biomarker for electrochemical activity (Esteve-núñez et al., 2005; Kato, 2017; Nevin et al., 2008; Reguera et al., 2005; Rotaru et al., 2014). Extensive research has also been undertaken to explore not only the diversity of anode-respiring bacteria that can be utilized for energy recovery, but also the ecology of these bacteria and their ability to thrive in mixed community environments through competitive or synergistic relationships.

2.3 Influence of Anode Potential

From chemistry, we know that a redox reaction cannot occur unless there is an electron donor to be oxidized and an electron acceptor to be reduced. During catabolism, the same redox principles apply for MFCs where the microorganisms catalyze the redox reactions between organic substrates and a solid electrode. Thermodynamics tells us that at standard conditions (pH 7 and 25°C), each oxidation and reduction half reaction has a theoretical free energy (Gibbs Free Energy) that can be released during the reaction process. The difference in redox potential between the substrate and electrode can be directly correlated to the change in Gibbs Free Energy by the following relationship:

$$\Delta G^{\circ'} = -nF(E^{\circ'}_{\text{substrate}} - E^{\circ'}_{\text{anode}}) \quad \text{Equation 2.1}$$

where $\Delta G^{\circ'}$ is the change in Gibbs Free Energy, n is the number of electrons transferred, F is Faraday's constant (96485.3 C/mol), $E^{\circ'}_{\text{substrate}}$ is the standard potential of the substrate utilized and $E^{\circ'}_{\text{anode}}$ is the standard potential of the anode electrode (Wei et al., 2010). Thus, for a thermodynamically favorable reaction, where $\Delta G^{\circ'} < 0$ yields a spontaneous reaction, the reaction is driven forward. In this case, the solid electrode in a MFC anode behaves as the electron acceptor when the redox reaction is thermodynamically spontaneous. The potential of the anode can be controlled in two ways: either by imposing an external voltage to “poise” the anode potential or by controlling the external resistance to regulate the voltage generated (Jung & Regan, 2011).

The influence of the anode potential on microbial activity, structure, and growth kinetics have been studied but it is not yet fully understood (Aelterman et al., 2008;

Dennis et al., 2016; Goud & Mohan, 2013; Kato, 2017; Rismani-yazdi et al., 2011; Torres et al., 2009). Researchers have primarily studied the effects of anode potential on biofilm development and MFC electrochemical performance by poisoning the anode potential and observing changes during start up and during longer operational periods. Aelterman et. al (2008) poisoned the anode potentials at -200, 0, and +200 mV vs a standard hydrogen electrode (SHE) and observed that biomass activity increased at more negative anode potentials during the early weeks of operation (2 weeks), but after a longer period (4 weeks) biomass activity at all potentials decreased and stabilized to similar values (Aelterman et al., 2008). The highest maximum power density during this study was observed at -200 mV vs SHE. Torres et. al. (2009) also observed that current densities as well as microbial activity by ARB were greatest at lower anode potentials (-150 and -90 mV vs SHE) (Torres et al., 2009). Conversely, a recent study observed that during initial start up conditions, thin biofilms under high positive anode potentials (+800 mV vs SHE) generated more biomass per unit charge (Dennis et al., 2016). Over the course of their experiment (40 days in total), biofilms at this high anode potential were thinner than biofilms grown at +300 and +550 mV, transferred less charge, and were less effective at removing substrates.

Maximum power generation at lower anode potentials (typically in the range of -300-0 mV vs SHE) have been linked to *Geobacter* species activity (Kato, 2017; Torres et al., 2009). Not only does the anode potential affect the activity of these model electrochemical bacteria, but it also affects the composition of active species. Kato (2017) highlighted the significance of anode potential on current generation by *Geobacter* species (Figure 2.3). The study observed that *G. sulfurreducens* and *G. metallireducens*

could generate relatively high current densities at a range of anode potentials greater than -100 mV vs SHE where as two other species (*Geobacter daltonii* and *Geobacter chapellei*) could also generate current at these potentials but to a lesser extent (Kato, 2017). *G. bemidjensis* and *G. pelophilus* could only generate current at a small range of -100 to 0 mV vs SHE.

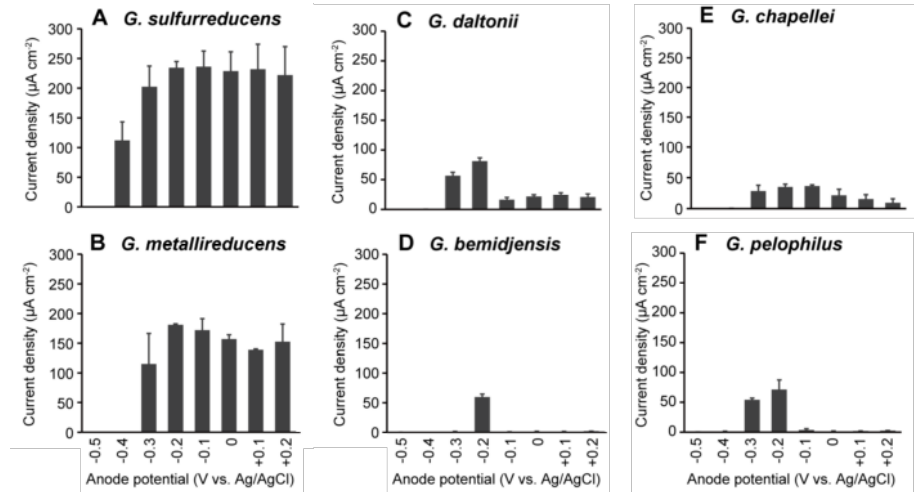


Figure 2.3 Current Densities of Six Different *Geobacter* Species Under Anode Potentials of -500 to 200 mV vs Ag/AgCl (corresponding to -300 to 400 mV vs SHE)
(Modified from Kato 2017)

The difference in current generation was attributed to the extracellular electron transfer (EET) pathways available to each species at different anode potentials. Cytochromes, electron shuttling proteins located within the cell membrane, can be triggered at a variety of anode potentials (-200 – 400 mV vs SHE) within different *Geobacter* species (Kato, 2017; Levar et al., 2014, 2017). *G. sulfurreducens* generating the highest current densities are theorized to have a single, major EET pathway that is highly independent of anode potential. *G. daltonii* and *G. chapellei*, on the other hand, can switch between positive and negative EET pathways depending on the anode

potential. *G. bemidjensis* and *G. pelophilus* differed in that positive and negative EET expression was observed but low current generation occurred under a small range of negative anode potentials.

The alpha diversity of bacterial communities under different anode potentials has only been studied by two groups (Dennis et al., 2016; Torres et al., 2009). Torres et al. focused on operating MFCs at anode potentials between -150 and +370 mV vs SHE while Dennis et al. focused on high positive anode potentials of +300, +550, and +800 mV vs SHE. Results showed that at more negative anode potentials (less oxidative stress), *G. sulfurreducens* are present in higher abundance than other bacteria (Figure 2.4), while at higher potentials the community diversity increases and a decrease in electrochemical performance is observed. At the higher anode potentials (+800mV) anode biofilms were thin, less effective at oxidizing substrates, transferred less charge to the anode, but were able to generate more biomass per unit charge. There was also no effect to alpha diversity at anode potentials +300 and +550 mV vs SHE.

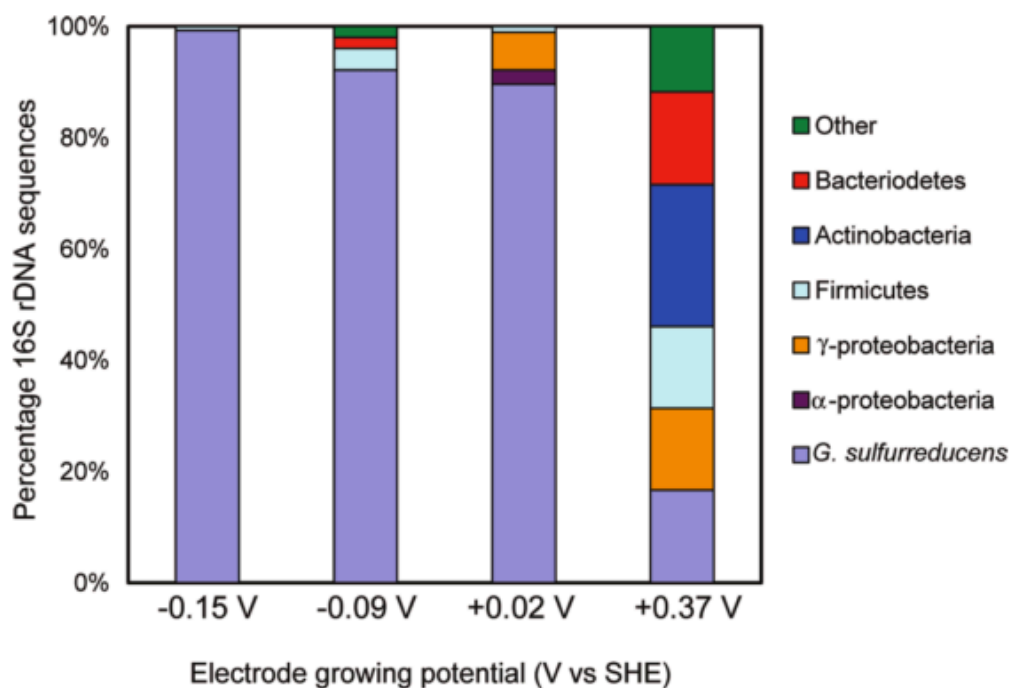


Figure 2.4 Microbial Community Distribution for ARB Communities Grown at Different Anode Potentials (Torres et al., 2009)

2.4 Organic Substrates in MFCs

The number of different substrates that have been tested in MFCs for energy production, whether simple or complex, is extensive (Pandey et al., 2016). The composition of organic substrates used in MFCs have also varied greatly. Low-carbon organic acids and sugars such as acetate, propionate, butyrate, glucose, fructose, sucrose, and xylose in defined medias (Bond et al., 2003; Chaudhuri et al., 2003; Freguia et al., 2010; Jang et al., 2009) have been used for electricity production. In addition to treating domestic and municipal wastewater, MFC technology has also been applied to various other types of complex or undefined wastewaters (Table 2.1). Complex organic substrates consisting of a mixture of fatty acids, starch, cellulose, and mix carbohydrates from swine

waste, manure slurry, human excreta, sludge, and landfill leachate have also been used (Castro et al., 2014; Gálvez et al., 2009; Lee & Nirmalakhandan, 2011; Zhuang et al., 2012).

Table 2.1 Examples of Complex Substrate Wastewaters for power generation in MFCs (modified from Pandey et al., 2016)

Wastewater	Substrate Concentration	Coulombic Efficiency (%)	COD removal (%)	Reference
Paper Wastewater				
Cellulose	2 g COD/L	50	70	(Cheng et al., 2011)
Paper recycling	1464 mg COD/L	16	76	(Huang & Logan, 2008)
Pharmaceuticals				
Recalcitrant Pharmaceuticals	7.98 kg COD/m ³	NA	85	(Velvizhi & Venkata Mohan, 2012)
Steroidal Drugs Industrial Effluent	1340 mg COD/L	30	82	(Ru Liu et al., 2012)
Livestock				
Cattle Waste	NA	52	NA	(Zheng & Nirmalakhandan, 2010)
Slaughterhouse	4850 mg COD/L	64	93	(Katuri et al., 2012)
Dairy Industry				
Real field Dairy	4.44 kg COD/m ³	4.3	95.5	(Venkata Mohan et al., 2010)
Industrial Dairy	53.22 kg COD/m ³ -d	37.2	90.5	(Mansoorian et al., 2014)
Food & Food processing				
Acidogenic Food waste leachate	1000 mg COD/L	20	>87	(Li et al., 2013)
Corn stover hydrolysate	1000 mg COD/L	26.9	70	(Zuo et al., 2006)
Mining				
Coking	3150-3200 mg COD/L	17	50	(Huang et al., 2010)
Coal Tar	2013 mg COD/L	NA	88	(Park et al., 2012)

Although various sources of real wastewaters have been tested, power production is typically optimized by using defined mediums containing simple organic substrates that can be directly oxidized by ARB. MFCs producing the highest recorded power outputs have done so while treating synthetic wastewaters with acetate as the primary carbon source (Fan et al., 2012; Nevin et al., 2008). Real wastewaters, on the other hand, may contain a mixture of simple and complex organic and inorganic compounds. Coulombic efficiency (CE), the ratio of electrons transferred from anode to cathode to the electrons available from substrate degradation, is lower when complex organics are used as substrates. MFCs using monosaccharides have reported 22-34% CE (Catal et al., 2008), 10-28% when using polyalcohols (Catal et al., 2008), and 19% when using starch (Herrero-Hernandez et al., 2013). The presence of inhibitory compounds and complex organics in these mixed wastewaters can highly limit MFC reactor performance (Janicek et al., 2014).

2.5 Syntrophic Interactions and Competing Metabolisms

Although common ARB are not known to oxidize complex organic matter directly, MFC anodes with mixed culture inoculums can provide an environment for symbiotic relationships between ARB and other microorganisms to effectively degrade complex organics. In the absence of oxygen, a mixed community of microorganisms begin to breakdown complex organics in a series of processes coupled as anaerobic digestion. For simplicity, anaerobic digestion of organic matter takes place in four main steps (Figure 2.5). The first step involves hydrolyzation of large macromolecules, such as

carbohydrates, proteins, and lipids into sugars, amino acids and fatty acids (Sang et al., 2012). In the second step, acidogenic bacteria convert the amino acids and sugars into organic acids, alcohols, carbon dioxide, and hydrogen. In the third step, acetogenic bacteria convert organic acids into acetic acid, carbon dioxide and hydrogen (White, 2007). Lastly, methanogenic archaea convert acetic acid, hydrogen, carbon dioxide, formic acid, methanol, methylamines, dimethyl sulfide, and methanethiol into methane gas. This hierarchy of microbial pathways in anaerobic environments allows for the co-existence of various microorganisms to degrade complex organics to simple substrates, usable by ARB to produce electricity. Within this hierarchy, ARB can utilize short chain fatty acids, organic acids, and acetate for direct electricity production.

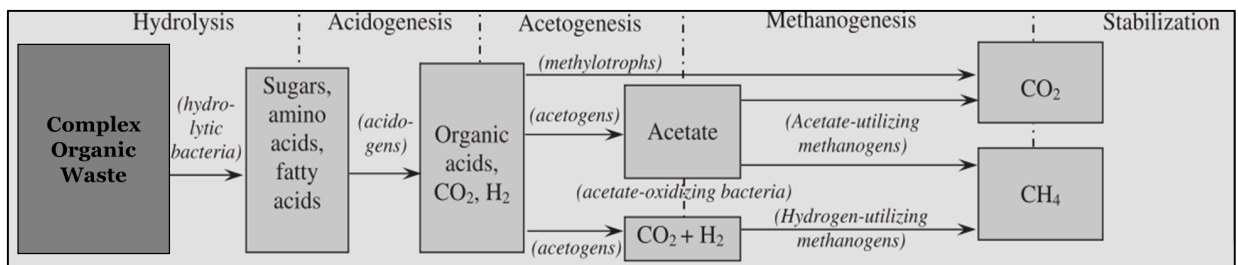


Figure 2.5. Flow chart outlining the degradation of complex wastes by anaerobic digestion (modified from Sang et al., 2012)

In anaerobic mixed communities, it has been known that symbiotic relationships exist between fermenters, specifically obligate proton-reducing acetogens that oxidize organic compounds such as butyrate, propionate, and ethanol to acetate, H_2 , and CO_2 , and hydrogen scavengers (White, 2007). This relationship is called interspecies hydrogen transfer. Hydrogen scavengers utilize H_2 and keep levels low to drive the thermodynamically unfavorable oxidation reactions (at pH 7 and $25^\circ C$) forward.

In a similar manner, recent research has also observed the syntrophic relationship between species of electrochemically-active *Geobacter*. This relationship was first observed between *G. metallireducens*, and *G. sulfurreducens* (Summers et al., 2010). In pure cultures, *G. metallireducens* can use ethanol as an electron donor but cannot use fumarate as an electron acceptor and vice versa for *G. sulfurreducens*. Both species were co-cultured with only ethanol as the electron acceptor and only fumarate as the electron donor. Together, these bacteria were able to oxidize ethanol using fumarate as the electron acceptor by forming aggregates and using conductive pili and cytochromes to transport electrons from one species to another (Kouzuma et al., 2015). This direct interspecies electron transfer (DIET) has also been observed between *Geobacter* species and *Methanosaeta* and *Methanosarcina* species (Chen et al., 2014; Fanghua Liu et al., 2012; Morita et al., 2011; Rotaru et al., 2014; Zhao et al., 2015) and *G. sulfurreducens* and *Thiobacillus denitrificans* (Kato et al., 2012) in the presence of conductive material such as granular activated carbon, graphite, and magnetite nanoparticles (Figure 2.6).

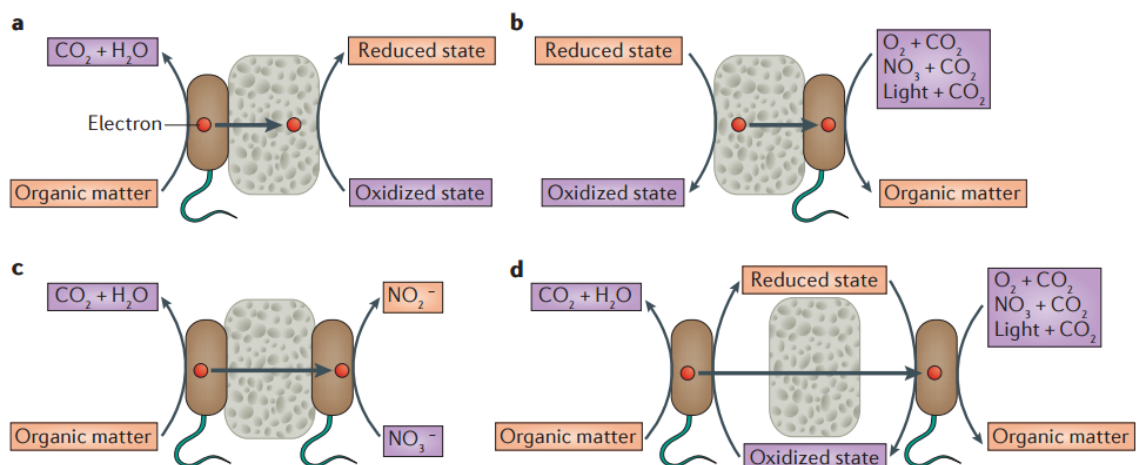


Figure 2.6. Electrical interplay between microorganisms and minerals.

Microorganisms use minerals that contain metal ions as terminal electron acceptors for respiration (part a), electron and/or energy sources for growth (part b), electrical conductors that facilitate electron transfer between microbial cells of the same and different species (part c) and electron-storage materials, or batteries, to support microbial metabolism (part d) (Shi et al., 2016)

The ability of microorganisms to not only respire conductive materials for current collection but to utilize these surfaces as vessels for syntrophic relationships across the same or different domains exemplifies the versatility of microbes for bioremediation and biotechnology applications. Although ARB prefer to oxidize simple carbon substrates, such as acetate, ethanol, and formate (Fan et al., 2007a; Liu et al., 2005; Parameswaran et al., 2010a; Speers & Reguera, 2012), these symbiotic relationships among ARB and other microorganisms can lead to effective treatment of complex waste streams. For electricity-harvesting applications, these symbiotic relationships may lead to diversion of electrons away from electrodes, generating less electricity than desired.

MFCs that use fermentable substrates such as glucose have reported methane and hydrogen production in the headspace, demonstrating that fermentation and methanogenesis is occurring (Jung & Regan, 2011; H. Lee et al., 2008). Minimal research has been conducted to understand the symbiotic relationship of ARB, methanogens, and fermenters (Parameswaran et al., 2009, 2010b). In mixed inocula MFC reactors fed glucose, *Geobacter* and *Desulfuromonas sp.* have been observed to coexist among fermentative genus *Enterococcus* and methanogenic archaea *Methanosaetaceae* and *Methanomicrobiales* within the anode biofilm (Jung & Regan, 2011). Methane production was reported in all the glucose reactors, accounting for 14-18% of electrons and the overall CE of the MFCs ranged from 23-62%. Parameswaran et al. (2009) studied the relationships between the three types of microorganisms in a microbial electrolysis cell (MEC) to showcase that a fermentable substrate, ethanol, was not directly degraded by ARB but rather fermented to acetate and hydrogen by fermenters. Hydrogen was then metabolized by hydrogenotrophic methanogens, *Methanobacteriales*, to produce methane. Electron flow to methanogenesis accounted for 26% whereas the overall CE was 60%. When methane was inhibited, the CE increased to 84%. Methanogens can also utilize acetate through the acetoclastic methanogenesis pathway, directly competing with ARB for substrate. It is evident that methanogenesis is an electron sink that can divert electrons from electricity production to methane production either through direct competition of substrate or through symbiotic activity. Although MFC technology applied to treat waste streams with a multitude of simple and complex organics will require a hierarchy of microorganisms to meet treatment goals, understanding the

interaction between the microorganisms will allow for improvements in reactor design and optimization for targeted energetic outputs.

2.6 Methanogenesis and Anode Community Competition

Under anaerobic conditions, methanogens are likely to be present in wastewaters containing complex organics. An important factor for improving electricity production and coulombic efficiency in MFCs treating complex organic wastewaters is to identify which methanogens are present and what metabolic pathways they are taking to divert electrons from electricity production to methane production.

Methanogens consist of a specific group of archaea that can convert organic or inorganic substrates into methane. Methanogenic archaea fall under five phylogenetically distinct orders: Methanobacteriales, Methanomicrobiales, Methanosarcinales, Methanopyrales, and Methanococcales. These methanogens, a group of primarily autotrophs and some heterotrophs, are strict anaerobes that can produce methane by the following three metabolic pathways: acetoclastic, hydrogenotrophic, and methylotrophic (Baptiste et al., 2005). The acetoclastic pathway is a fermentation process in which the acetate ion is cleaved, followed by a reduction of the methyl group and the oxidation of the carbonyl group (Lessner, 2009). In the hydrogenotrophic pathway, methanogens oxidize hydrogen or formate to reduce carbon dioxide and form methane. Lastly, in the methylotrophic pathway methanogens can use single-carbon compounds such as methanol, methylamines, and methyl-sulfides during a dismutation event in which the methyl group from one substrate is oxidized to carbon dioxide and methane, yielding electrons to reduce three other methyl group substrates.

Although there are three known pathways for methanogenesis, not all methanogens can perform all three metabolic pathways. Almost all methanogens can perform hydrogenotrophic methanogenesis, but only members of the order Methanosarcinales have been identified to perform acetoclastic and methylotrophic methanogenesis as well (Bapteste et al., 2005). Genera of methanogens under this order that perform acetoclastic methanogenesis include *Methanosarcina* and *Methanosaeta* (Kendall & Boone, 2006). Genera that can catabolize methyl groups include *Methanosarcina*, *Methanococciodes*, *Methanohalobium*, *Methanohalophilus*, *Methanlobus*, *Methanomethylovorans*, and *Methanosalsum* (Liu & Whitman, 2008).

It is important to understand the main metabolic pathways of methanogens because during the degradation process of complex organics methanogens will have multiple opportunities to divert electrons towards methane production. Hydrogenotrophic methanogens can divert energy by oxidizing hydrogen and reducing carbon dioxide during the fermentation process. Acetoclastic methanogens can also divert energy by utilizing the fermentation byproduct acetate to produce methane (Figure 2.7).

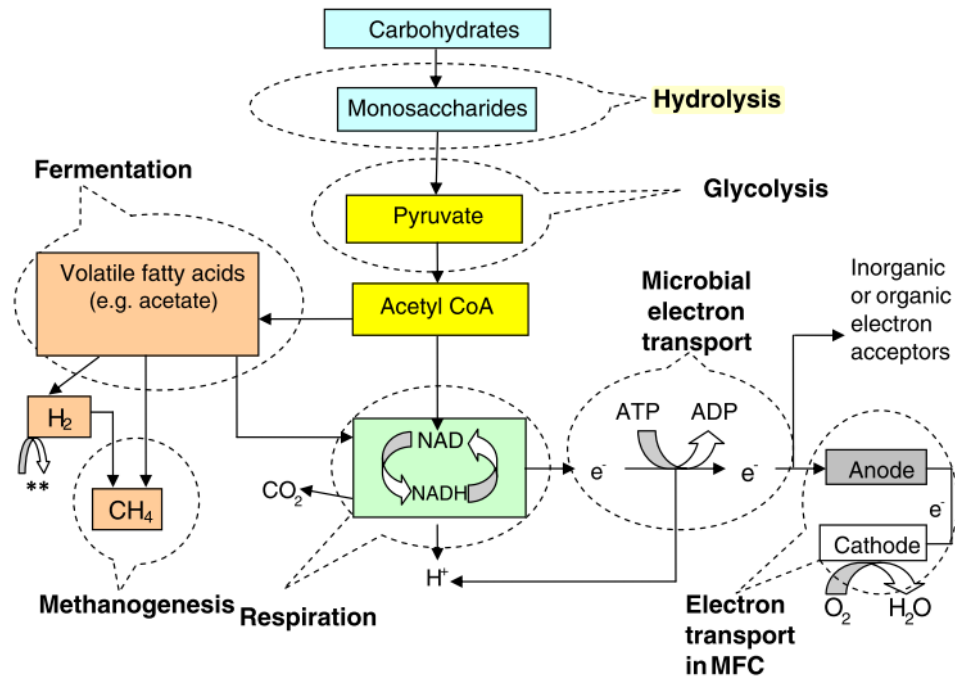


Figure 2.7. Diagram of substrate degradation pathways in MFCs (Velasquez-Orta et al., 2011)

Methanogenesis has been observed in MFC anodes utilizing fermentable substrates. Only a few MFCs that treat complex or fermentable substrates have actually measured and reported methane production in their MFC designs (Freguia et al., 2007; Jung et al., 2011; Katuri et al., 2012; Lee et al., 2008; Rismani-Yazdi et al., 2013; Zhang et al., 2013) and even fewer for pilot-scale reactors (Alzate-Gaviria et al., 2016). When methanogenesis occurs in MFC anodes, it decreases the fuel cell's efficiency to produce electrical energy because energy from the substrate is diverted to other metabolic pathways by mixed consortia of microorganisms when using mixed culture inoculums. Available substrate for ARB may be diverted by methanogens or other acetate-oxidizing bacteria. When methane is measured in MFCs, it has been reported to divert 14-26% of

electrons towards methane production (Jung et al., 2011; Parameswaran et al., 2009).

Members of the order *Methanomicrobiales*, *Methanosarcinales*, and *Methanobacteriales* have been identified in MFC anodes treating complex wastewaters (Parameswaran et al., 2009; Rismani-Yazdi et al., 2013). In order to increase energy recover from MFCs in the form of electricity, methanogenesis must be inhibited.

2.7 Methanogenesis Inhibition Strategies

Although methanogenesis can create inefficiencies when utilizing MFCs to treat organic wastewaters, the process can be inhibited. Methanogenic archaea have one major similarity; the group expresses the enzyme methyl coenzyme M reductase (mcr) which catalyzes the final step in methane production. A chemical compound, 2-bromoethanesulfonate (2-BES), is a structural analog to the mcr enzyme and inhibits the final methane biosynthesis carried out by methanogens (Gunsalus et al., 1978). At concentrations of 0.20 g/L, acetoclastic methanogenesis can be inhibited, while at concentrations of 9.4 g/L, both acetoclastic and hydrogenotrophic methanogenesis can be completely inhibited (Zinder et al., 1984).

Methane production can also be inhibited by nitrogenous species. Free ammonia (NH_3) can cause inhibition of methanogenesis. A hydrophobic molecule, free ammonia can diffuse passively into the cell of microorganisms and cause a proton imbalance or a potassium deficiency, affecting the energy requirements for cell maintenance and suppressing enzyme reactions (Chen et al., 2008; Wang et al., 2015).

Nitrate is also a known inhibitor of methanogenesis. There are two hypotheses for this occurrence: the first, that competition for substrates occur between methanogens and

denitrifying bacteria; second, that toxic denitrifying intermediates such as nitrite (NO_2), nitric oxide (NO), and nitrous oxide (N_2O) inhibit methanogens (Chen et al., 2008; Yang et al., 2016). Studies have shown that the latter is the main mechanism by which methanogenesis is inhibited (Roy & Conrad, 1999). Sodium nitrate has been showed to decrease methane production by 70.1% in *in vitro* cultures of methanogens and cellulolytic bacteria from rumen when added at a concentration of 1.0 g/L (Zhou et al., 2011b). Although 2-BES can inhibit all forms of methanogenesis, sodium nitrate is much less expensive (\$0.08/g NaNO_3) as compared to 2-BES (\$0.97/g Na-BES) while also readily found in nitrogen-rich wastewaters. While nitrate cannot completely inhibit methanogenesis as 2-BES can, it can reach effective levels of inhibition at a fraction of the cost that it takes to inhibit with 2-BES.

In addition to chemical inhibitors, physical changes to the anode environment can also inhibit methanogens. The availability of the anode electrode has been shown to directly correlate with methane production. Jung & Regan (2011) studied the effects of external resistances on methane production in bench-scale MFCs treating glucose and acetate. Three external resistances were tested in identical H-cell reactors: 150 Ω , 970 Ω , and 9800 Ω . Methane production was observed to increase with increasing external resistances when fed glucose but no correlation was observed with acetate. With higher external resistances, the anode availability becomes limited to ARB, and thus methane production is observed to increase with increasing external resistances.

The degradation of complex substrates can also lead to inhibition of methanogens through the production of fatty acids (Koster & Cramer, 1987; Zhou et al., 2011a). Both long-chain fatty acids (LCFAs) and short chain fatty acids (SCFAs) can inhibit

methanogenesis by shifting the anode media pH to a less optimal pH for methanogenic activity (Chen et al., 2008; Wang et al., 2009). While methanogenic activity decreases at a lower pH than 7, the activity of acid-forming bacteria increases. This intermediate step of complex substrate degradation is crucial and complex due to the syntrophic interactions between acetogenic bacteria, methanogenic archaea, and other hydrogen scavengers. The forward reactions of acetogenesis is dependent on hydrogen scavengers consuming excess hydrogen to maintain the hydrogen partial pressure low. Low partial pressure of hydrogen can maintain acetogenesis thermodynamically favorable (Amani et al., 2010). An imbalance in this interaction can inhibit acetate formation and consequently affect acetoclastic methanogenesis.

2.8 Conclusions

MFC technology makes use of electrochemically active microorganisms to recover electrical energy from wastewater sources. Currently, energy recovery for centralized wastewater treatment is not yet feasible because of low power production, high capital costs, and poor long-term stability observed in pilot and large-scale reactors designed using expensive materials (Liu et al., 2014). Alternatively, harvesting these low power yields from MFCs applied for decentralized sanitation purposes can have a significant impact on the livelihood of people who lack or have limited access to sanitation systems and alternative energy sources. Understanding how design parameters affect the microbial dynamics within MFC anode communities that treat complex organics can reveal how best to optimize MFCs to meet multiple treatment strategies and recover multiple forms of energy.

CHAPTER 3

DECENTRALIZED WASTEWATER TREATMENT USING A BIOELECTROCHEMICAL SYSTEM FOR THE PRODUCTION OF METHANE AND ELECTRICITY*

**Modified from the originally published version (Castro et al., 2016)*

3.1 Introduction

The majority of people who lack access to sanitation systems live in developing countries (WHO/UNICEF, 2015). As of 2015, only 68% of the world population used an improved sanitation facility (WHO/UNICEF, 2015), and the majority of people who do practice open defecation live in rural areas. Although the most widely used systems are ventilated improved pit latrines, efforts have been made to develop incentivized sanitation systems. Examples of incentivized systems include composting latrines that produce a natural fertilizer and anaerobic digesters to capture methane gas for heating and cooking purposes (Mihelcic, 2009; Surendra et al., 2014). Although anaerobic digesters and biogas toilets seem feasible in promoting sustainable means for energy recovery, high nitrogen species present in anthropogenic wastewaters have been documented to inhibit the anaerobic microbial degradation process (Fricke et al., 2007).

Bioelectrochemical systems (BESs) and, more specifically, microbial fuel cells (MFCs) have generated significant interest for energy-efficient or energy-yielding wastewater treatment approaches. MFCs decouple the electron donor and the electron acceptor, allowing for anaerobic organic degradation by microorganism using the anode as an electron acceptor. Electrons are transported to a cathode via electrical load, where

the reduction of an electron acceptor occurs. Castro et al. (2014) previously designed and implemented a unique three-chamber MFC system that oxidized organic matter from feces in the anode chamber and utilized a biological cathode to reduce nitrate-rich effluent from a nitrification chamber fed urine. It was designed for retrofitting composting latrines. The MFC Latrine incentivizes sanitation by producing compost, electricity, and treated effluent water as the three main outputs. Although the system produced all three products, electricity recovery was low.

One explanation for the reduced power production at larger scale MFC is alternative, anaerobic microbial metabolisms in the anode compartment. Some anode-respiring bacteria (ARB), like many anaerobic, chemotrophic bacteria, prefer to oxidize acetate because of its low oxidation state (-1) (Thauer et al., 1989). However, the degradation of complex organic matter requires hydrolyzation of large organic macromolecules, followed by fermentation, producing simple organic acids and hydrogen. Symbiotic relationships between anode-respiring bacteria and fermenters have been linked to efficient conversion of organic substrates to electricity (Parameswaran et al. 2009). In contrast, methanogenesis is often cited as a barrier to full-scale implementation of MFC technologies, as methanogens and ARB are often in direct competition for end products of fermentation. Methane has been observed to be a major contributor to inefficiencies at the anode even when simple substrates, such as glucose and sucrose are used (He et al., 2006; Jung and Regan, 2011).

Methanogens have recently been documented to work synergistically with ARB. In the presence of conductive surfaces, direct interspecies electron transfer (DIET) has been reported between known anode-respiring species, *Geobacter sp.*, and the

methanogens *Methanosaeta sp.* and *Methanosarcina sp.* (Liu et al., 2012; Zhao et al. 2015). Furthermore, enhanced methane production has been documented in anaerobic digester aggregates in the presence of conductive material such as graphite (Morita et al. 2011). This suggests that the conductivity of the anode could offer a pathway to divert electrons from electricity production in favor of methanogenesis.

Although not appropriate for all MFC applications, co-evolving methane with electricity is practical for developing countries where methane could be used for heating or cooking and electricity could be stored and used for lighting. Nearly three billion people still use cooking methods that involve burning locally available biomass such as firewood, animal excreta, and kitchen waste, producing harmful indoor air pollution (Surendra et al. 2014). MFCs employed to generate both biogas and electricity at ambient temperatures could allow for on-demand electricity production and storable energy as methane.

This study evaluates the potential for methane production in MFC anode communities and the co-evolution of methane and electricity in a lab-based pilot MFC that is a 1-to-1 representation of the MFC paired with a composting latrine in Ghana (Castro et al., 2014). Methane production, electricity production, and treatment performance were evaluated for two different wastewater conditions: synthetic feces and municipal wastewater. Microbial enrichments from the operating pilot-scale MFC anode were incubated under ambient conditions to explore the role of conductive material on methane production. This BES delivers two additional outputs that a conventional anaerobic digester or biogas toilet cannot produce: direct electricity production and nitrogen removal.

3.2 Methods

3.2.1 MFC Construction and Startup

A hydraulically partitioned, two-chamber MFC, was constructed (Figure 3.1). The laboratory MFC was designed to emulate operational conditions when paired with a composting latrine (Castro et al. 2014). Each chamber consisted of a capped 56.8 L polypropylene tank, containing two baffle walls evenly spaced within the tank for mixing. Effluent from the anode chamber directly flowed into the cathode, where a separate nitrate media was fed to cathode-oxidizing, nitrate-reducing biofilm. Nitrate was added to the cathode to simulate the conditions of the field deployed MFC, which contained an additional aerobic nitrifying chamber for the conversion of ammonia in human urine to nitrate. We chose to eliminate the nitrifying chamber and feed a constant concentration of nitrate to allow focus on the anode chamber in this study. In this design, no proton exchange membrane was used to simplify the design and reduce costs associated with building MFCs in the developing world. Synthetic granular graphite (EC 100 3/8x10, Graphite Sales) was used as the electrode material for both the anode and cathode. Each tank was filled with 45.5 L of the granular graphite. The estimated liquid volume of each electrode chamber was 23 L and the surface area of each electrode was 29.2 m². Three graphite rods (Graphite Store, OD: 1.6 cm; L: 61 cm) were placed in each chamber as current collectors. Wires connected to the graphite rods of each tank were linked together via an external resistor box. The anode and cathode chambers were both inoculated with 4.0 L of primary wastewater obtained from the Amherst Wastewater Treatment Plant (WWTP) (Amherst, MA) and 1.0 L of pond water and sediments from

the campus pond at the University of Massachusetts (Amherst, MA). The MFC initially operated under a 1000 mg/L acetate growth media in a 16 mM phosphate solution.

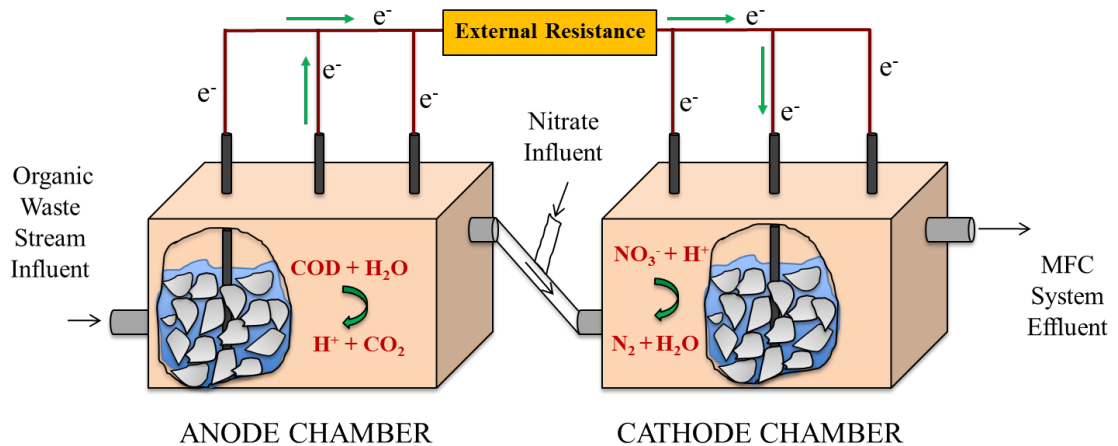


Figure 3.1 Schematic of the MFC design (not to scale). The wastewater and the nitrate media were each pumped directly into the anode and cathode chambers, respectively. Both chambers contained granular graphite as their electrode material.

3.2.2 Batch enrichment studies

To assess enhanced methane production at room temperature in the presence of conductive surfaces, enrichment studies were performed with anode effluent from the pilot MFC. In the enrichment studies, acetate served as the carbon source in a 16 mM phosphate buffer solution. Enrichment bottles were prepared in the presence of graphite granules, non-conductive plastic beads, or with no attachment surface present (suspended). The study was conducted in 12 sealed 150 mL serum bottles, with five replicate cultivations for bottles containing graphite granules, duplicate cultivations for

bottles containing plastic beads and five replicates with no additional attachment surfaces present (suspended growth). Each bottle was capped and purged with nitrogen gas prior to inoculation. The growth media consisted of a 16 mM phosphate buffer containing 1000 mg/L of acetate and 1 mL/L of a calcium-iron and trace mineral solutions. All bottles were autoclaved and cysteine (31.5 mg/L) was added to remove any residual oxygen. All bottles were covered in foil to prevent phototrophic growth, incubated at 22°C, and continuously shaken for 31 days.

3.2.3 MFC Operation

Simultaneous electricity production and methanogenesis was evaluated using the pilot MFC reactor while treating two types of organic wastewaters: synthetic feces wastewater (Case F – 54 day operation), and municipal wastewater (Case W – 50 day operation). Case F media consisted of 8.0 g of starch, 2.50 g of casein, 4.34 g of KH_2PO_4 , 1.09 g of Na_2HPO_4 , 0.310 g of NH_4Cl , 0.130 g of KCl , and 5.0 g of oleic acid per litre of reverse osmosis (RO) water (Du et al. 2011). The pH was 6.3 ± 0.003 and conductivity was $4700 \pm 150 \mu\text{S/cm}$. For Case W, effluent was obtained from the primary clarifier of the Amherst WWTP and used as the influent to the anode. The pH was 7.2 ± 0.08 and conductivity was $640 \pm 30 \mu\text{S/cm}$. The cathode chamber was fed with nitrate in a 16 mM phosphate buffer with the following recipe: 0.710 g Na_2HPO_4 , 1.50 g KH_2PO_4 , 0.050 g MgSO_4 , and 0.605 g NaNO_3 per litre of RO water. All anode and cathode media were purged with nitrogen gas for at least 30 minutes before being introduced into their respective compartments. Media was pumped continuously, with a hydraulic retention

time (HRT) of 8 days for the anode chamber and 4 days for the cathode chamber to reflect operation when connected to a composting latrine superstructure similar to a ventilated improved pit latrine (Castro et al., 2014). Both the anode and cathode biofilms were established prior to operation under both conditions and the MFC has been in operation for the past 4 years. At the completion of each wastewater scenario, visual inspection of the anode and cathode was performed by opening each of the chambers. During Case F, minimal precipitated starch at the top layer was removed when visible but the interior remained intact as to not disturb the biofilms around the granular graphite electrodes.

3.2.4 Chemical Analysis

Samples were collected from the inlets and outlets of the anode and cathode. All samples were filtered through 0.45 μm syringe filters prior to analysis. An ion chromatograph (850 Metrohm) was used to measure nitrite and nitrate. Chemical oxygen demand (COD) was measured according to standard methods using Hach kits (Hach Method 8000). An Agilent gas chromatograph (GC) (7890A model) was used to measure the following short-chain fatty acids (SCFAs): acetic, propionic, isobutyric, n-butyric, isovaleric, n-valeric, isocaproic, n-caproic, and heptanoic acids (standards from Matreya LLC, Pleasant Gap, PA). Liquid samples for SCFA analysis were filtered with a 0.45 μm syringe filter and acidified with 6 N of sulfuric acid for large sample quantities or 12 N of HCl for small sample quantities before analyzing. The GC was also used to measure methane and carbon dioxide gases using a HP-PLOT-Q column. Gas samples for

methane were collected from the headspace of the anode chamber and stored in gas-tight bags before analysis. Duplicate injections were made for each sample.

3.2.5 Electrochemical Analysis

Voltage production was monitored using a Keithley Model 2700 Multimeter with a 7700 Switching Module (Keithley Instruments Inc., Cleveland, OH, USA). Readings were collected every 10 minutes across the external resistance. Polarization curves for determining internal resistance were conducted by linear sweep voltammetry (LSV) using a Gamry Series G750 Potentionstat/Galvanostat/ZRA (Gamry; USA). LSV was run for three cycles at a scan rate of 1 mV/s from zero to the open circuit potential. Current was determined using Ohm's Law, $I = V/R$, where I is the current in amps (A), V is the voltage in volts (V), and R is the resistance in ohms (Ω). Power was determined using $P = I^2R$, where P is power in watts (W). Power densities were normalized to the anode surface area or anode liquid volume, where specified, and reported with standard errors.

3.2.6 Mass Balances and Power Production

In order to compare the alternative end-products produced by the continuous flow MFC anode, all influent and effluent products in and out of the anode chamber were converted to mass rates of electron equivalents as COD. Average current produced by the MFC over the operational period was converted to mg COD/min using the following relationship:

$$\text{Electron equivalents as COD} \left[\frac{\text{mg COD}}{\text{min}} \right] = \frac{I}{Fn} \times MW_{O_2} \quad \text{Equation 3.1}$$

where I is current (C/min), F is Faraday's constant (96485 C/e⁻ eq), n is the electron equivalent for COD (O₂) which is 8 e⁻ eq/mol COD and MW is the molecular weight of oxygen (32 g/mol). The mass rate of soluble methane production was calculated by the following relationship:

$$m_{CH_{4,s}} \left[\frac{\text{mg COD}}{\text{min}} \right] = C_{CH_{4,s}} \times Q \times 64 \frac{\text{g COD}}{\text{mol CH}_4} \quad \text{Equation 3.2}$$

where $C_{CH_{4,s}}$ is the soluble methane concentration in mol/L determined by Henry's Law using K_H , 1.4×10^{-5} mol/m³_{aq}-Pa (Sander, 2014), and the measured partial pressure of methane in the headspace, Q is the flowrate into the reactor (2 mL/min), and 64 g COD per mole of CH₄ assuming by complete oxidation of methane by oxygen. The rate of methane production in the headspace was determined by collecting 1 L of gas from the headspace on consecutive days and determining the amount of methane produced between days. Conversion factors for the mass of each SCFA and methane to mass of COD were obtained from Pitter & Chudoba (1990). The estimated power from methane production was determined by using the average net heating value of methane, 1000 BTU/ft³ (EPA 1995), and the conversion factor of 3.41 BTU-h⁻¹/W (EPA, 1995). Power values were presented in two ways: normalized to the COD consumed during each wastewater treatment scenario or by the liquid volume of the anode.

3.3 Results and Discussion

3.3.1 Methanogenesis within Communities Enriched from the Anode

In consideration of methanogenesis within the anode environment, batch cultivations were used to assess the role of graphite granules in methanogenesis at ambient temperature. Microbial communities obtained from the previously operating pilot MFC anode were transferred into one of three batch enrichments: acetate growth media only, acetate growth media with graphite granules, or acetate growth media with plastic beads. Methane production was observed in all three enrichments. Methane production comprised $19 \pm 9.5\%$ of the headspace gas when granular graphite was present, which was greater than the suspended growth and plastic bead enrichments. The methane concentration in suspended growth cultures was $5.0 \pm 1.6\%$ in the headspace (Figure 3.2). The plastic beads enrichments were most similar to the suspended growth enrichment, with $8.1 \pm 0.65\%$ headspace methane. This suggests that the conductivity of graphite may have led to the greater methane production. Our findings are supported by other studies which have determined that conductive surfaces, such as activated carbon, can support DIET between *Geobacter* species, associated with anode-respiration, and methanogens (Liu et al., 2012; Zhao et al., 2015).

Increased methane production from anode microbial communities in the presence of graphite granules have implications for most MFC applications. Methane is well documented as a competing metabolism for anode-respiring communities, but the results from this study suggests that anode environments may be even more favorable to methanogenesis than conventionally thought. For optimization of energy production in MFC technologies, there are two approaches to consider. Methanogenesis could be

suppressed in the anode to increase electricity production, which may be appropriate in large-scale industrial or municipal applications. Methane could also be captured as a co-evolved, value-added product, which may be useful for applications in developing areas where resources are limited and simplified reactor design and operation are required.

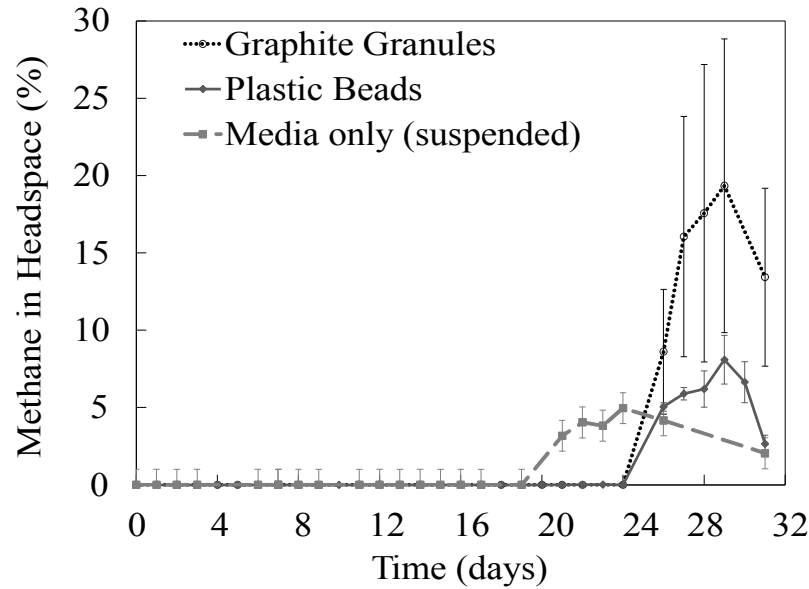


Figure 3.2. Methane production in the headspace of batch reactors enriched with microbial communities from the large-scale MFC, containing either graphite granules, plastic beads, or neither (suspended) (adapted from Jack, 2015)

3.3.2 COD Removal and Nitrate Reduction in the MFC

In order to evaluate the potential for decentralized wastewater treatment and energy recovery, a pilot-scale MFC was operated continuously through two sequential, influent wastewater conditions: synthetic feces wastewater (Case F) and municipal wastewater (Case W). The membraneless, hydraulically-partitioned MFC was designed

for direct human waste treatment (Castro et al., 2014), resulting in a relatively long, 8-day- HRT in the anode chamber. During both cases, nitrate was fed separately to the cathode for biocathodic denitrification. Treatment performance was evaluated based on COD removal in the anode and in the system and nitrate removal in the cathode. Organic matter was removed in the anode chamber when treating influent waste streams (Figure 3.3). COD removal efficiencies were $76 \pm 24\%$ (8200 ± 2000 mg/d) for Case F and $67 \pm 21\%$ (290 ± 56 mg/d) for Case W. These COD removal efficiencies are similar or higher than other large-scale MFC reactors (Jiang et al. 2011; Alzate-Gaviria et al., 2016; Ge and He, 2016). Removal is also similar to bench-scale MFCs treating similar substrates. Between 60-98% COD removal has been reported for batch MFCs fed starch (Lu et al., 2009) and 48-93% when fed municipal wastewaters in continuous flow MFCs (Liu et al. 2004; Kim et al., 2015). Although the HRT presented in these cited studies were significantly shorter than this MFC, the 8-day HRT used in this study was purposely designed to replicate low liquid flows when used as a sanitation system in the developing world, and likely contributed to the significant COD removal.

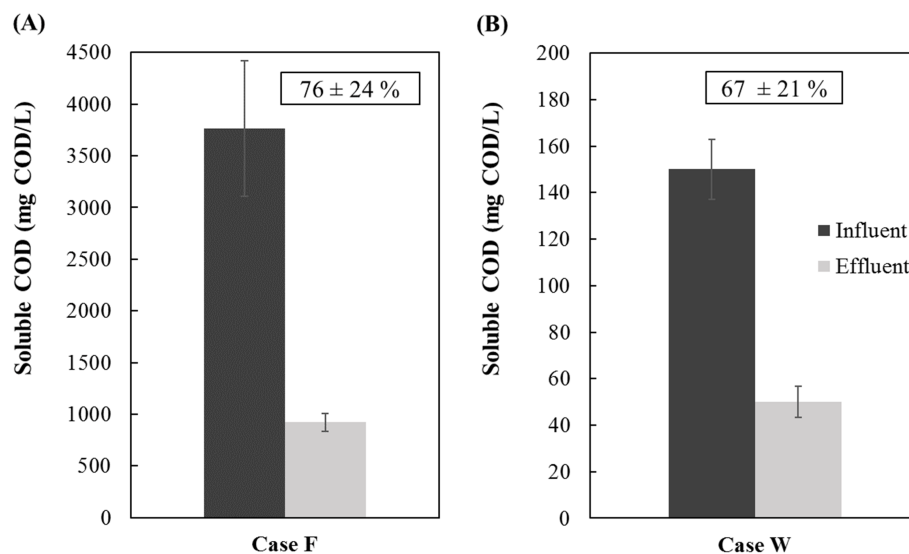


Figure 3.3 Average anode chamber influent and effluent COD concentrations for (A) Case F and (B) Case W with standard errors. The percentages above the bars represent average removal efficiencies during each operational period.

In the cathode chamber, nitrate removal was observed in all cases. Nitrate removal was greater with high organic loading rates at the anode, observing $53 \pm 16\%$ removal in Case F and only $12 \pm 6.9\%$ in Case W. The anode and cathode were hydraulically linked in this MFC configuration and effluent COD not oxidized in the anode was allowed to flow to the cathode, resulting in heterotrophic denitrification. This served as a COD ‘polishing’ step. For Case F, a further $9.6 \pm 4.9\%$ of anode influent COD was removed in the cathode chamber, for a total COD removal in the system of $85 \pm 33\%$. For Case W, an additional $14 \pm 6.7\%$ was removed, for a total COD removal of $86 \pm 13\%$. Power production was lower than expected in all cases and minimal

autotrophic denitrification occurred in the cathode chamber from current delivery to the cathode.

3.3.3 Electrical Power Production in the Pilot-scale MFC

Power production from electricity was observed and sustained during both media treatment cases. Operational power output for Case F and Case W were 4.7 ± 0.46 and $10.6 \pm 0.39 \mu\text{W}/\text{m}^3$. Polarization curves were used to determine the internal resistances and maximum power densities. The internal resistance of the reactor was $42 \text{ k}\Omega$ for Case F and $214 \text{ k}\Omega$ for Case W. Case F had the greatest concentration of organic matter entering the system, at 3800 mg COD/L , while yielding the lowest average operational power output.

Low power output is frequently noted in bench-scale reactors treating complex waste streams. Starch processing waste has yielded $1.4 \text{ W}/\text{m}^3$ ($240 \text{ mW}/\text{m}^2$) (Lu et al., 2009), $4.3 \text{ W}/\text{m}^3$ ($170 \text{ mW}/\text{m}^2$) from swine wastewater (Min et al., 2005), and $1.74 \text{ W}/\text{m}^3$ ($26 \text{ mW}/\text{m}^2$) from domestic wastewater (Liu et al., 2004). Recent large-scale applications of MFCs for wastewater treatment and sanitation purposes have only achieved moderate power output even when utilizing numerous stacked or sequential litre scale MFCs (Alzate-Gaviria et al., 2016; Ge et al., 2016; Ieropoulos et al., 2016). In this study, large external resistances were used to match the internal resistances of the MFC system and to maximize the voltage drop across the resistor to support a LED light and to produce methane. The large external resistances may have limited the anode's availability as an

electron acceptor to ARB, which could lead to increased methanogenesis (Jung and Regan, 2011).

3.3.4 SCFA and Methane production in the MFC Anode

Other microbial metabolisms in the anode were investigated. Dissolved and headspace methane gas accounted for 7.8% of electrons obtained from the oxidation of COD in Case F and 18.9% in Case W. An accumulation of SCFAs was detected in Case F and accounted for a total of 3.1% of the electrons: acetic (1.1%), propionic (0.70%), isobutyric (0.16%), n-butyric (0.24%), isovaleric (0.34%), n-valeric (0.17%), isocaproic (0.11%), n-caproic (0.11%), and heptanoic acid (0.14%) (Figure 3.4). SCFAs were below detection limits for Case W.

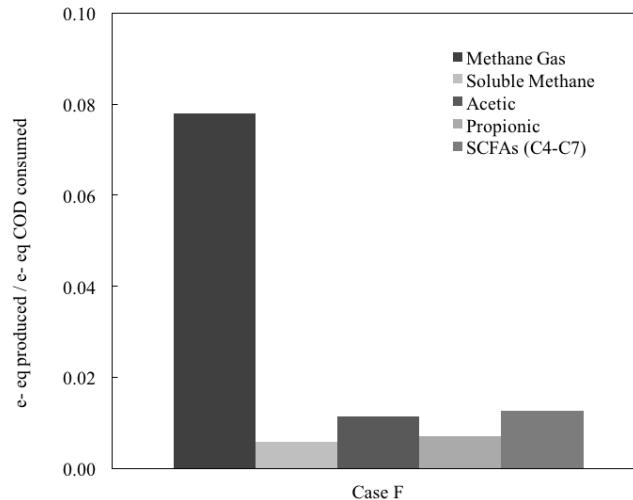


Figure 3.4 Alternative energetic by-products during the degradation of complex substrates in Case F in the large-scale MFC

The major SCFAs found in the effluent of the anode for case F were acetic, propionic, and n-butyric acid, suggesting that large polysaccharides derived from starch were broken down to various sugar forms such as maltose and glucose and further fermented to the simplest short-chain fatty acids. Upon inspection of the anode chamber at the end of Case F, a minor amount of starch had precipitated in the anode and contributed to COD removal. Since it was difficult to separate the small amount of precipitated starch from other volatile solids in the packed bed of graphite granules, we were unable to quantify the accumulation or its contribution to COD removal. Though qualitative inspection leads us to believe it was not a significant component of COD removal.

3.3.5 Methane as an Alternative Energy Source

For large-scale applications of MFC technology, methane production seems inevitable without active suppression of methanogenesis, especially when treating wastewaters with multiple complex organics. The energetic value from a MFC is typically measured by the maximum electrical energy it can produce. Although electrical energy is lowered by competition with methanogens (Torres et al., 2007), an alternate perspective includes methane as a value-added product, particularly in developing areas where biogas can be used as a cooking and heating fuel.

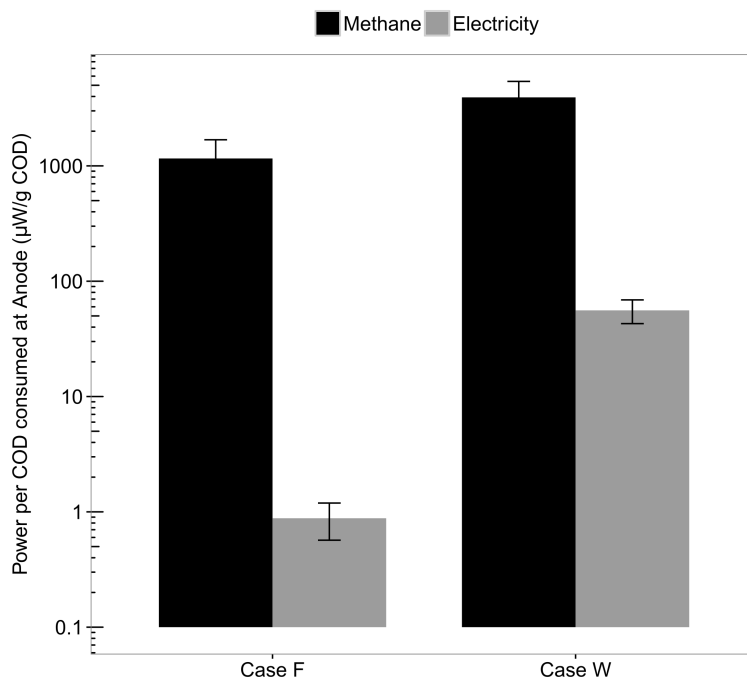


Figure 3.5 Comparison of power recovery from methane and electricity normalized by the COD consumed in the anode and presented with standard errors.

When the MFC anode was fed synthetic feces wastewater (Case F) or municipal wastewater (Case W), it could support the production of 0.008 ± 0.001 and 0.001 ± 0.0002 L CH₄/L_{Reactor-d}, respectively. Power production from methane would yield 2.6 ± 0.31 mW/m² (3.3 ± 0.64 W/m³) for Case F and 0.31 ± 0.06 mW/m² (0.39 ± 0.07 W/m³) for Case W. When power recovered from methane was normalized to the COD removed in the anode, the MFC could produce 1.2 ± 0.53 mW/g COD during Case F and 3.9 ± 1.5 mW/g COD during Case W. Potential power from methane production exceeds the contribution from electrical power in the anode in this system (Figure 3.5). At ambient

temperatures, both methane and electricity production were greater in Case W with low strength municipal wastewater which may allow for other household wastewater to be added to MFC stream fed to MFC anode. In this study, treating municipal wastewater yielded 2.6 times more power from methane and 64 times more electricity (normalize to COD removed) than treating concentrated synthetic feces wastewater. We note that the complexity of starch as the primary carbon source and the unaccountable fraction of starch lost to precipitation in Case F should also be considered when comparing the power output. Based on our results, the complexity of the organic source and concentration in the wastewater should be carefully considered when optimizing power for both methane and electricity.

3.4 Conclusion

Enhanced methane production in the presence of graphite granules was demonstrated within mixed cultures enriched from anode communities. Considering the co-evolution of methane in MFC anode, a pilot-scale MFC produced energetic products in the form of methane and electricity when treating complex wastewaters. The MFC could reliably remove greater than 70% organics when treating two different wastewater streams: synthetic feces wastewater and municipal wastewater. Nitrate removal was also consistently observed in the cathode chamber, and was primarily due to heterotrophic denitrification. Energetic products resulting from anode respiration and methanogenesis were simultaneously observed, yielding a total energy production of $3.3 \pm 0.64 \text{ W/m}^3$ for Case F and $0.40 \pm 0.07 \text{ W/m}^3$ for Case W. Future work will seek to optimize the major metabolic pathways to find the appropriate balance between electrical power and

methane production at the pilot scale. Operational parameters such as HRT, external resistance, temperature, and organic loading could play a role in optimizing the MFC's treatment performance and power output. Simple and low-cost designs for pilot MFCs, coupled with optimization of energy recovery from all potential sources is key to bringing this wastewater treatment technology to fruition for underserved communities.

CHAPTER 4

ANDEAN SOIL ENRICHMENTS FOR COMPLEX CARBOHYDRATE DEGRADATION AND POWER PRODUCTION IN A MFC—EFFECTS OF PH AND CONDUCTIVITY

4.1 Introduction

In Chapter 3, we explored the use of low and high strength wastewaters for the co-evolution of methane and electricity in a large-scale MFC anode. Of particular interest is the use of starch to simulate the composition of real human feces in the synthetic feces wastewater treated by the pilot-scale MFC. Starch is a carbohydrate; an insoluble polysaccharide consisting of mostly amylopectin and some amylose. Both polymers consist of long chains of glucose units linked by glycosidic bonds. Amylopectin is composed of linear glucose chains with uniform branching, whereas amylose is linear and helical making it difficult to break apart (Hoover, 2001). Starches are the major compound of tuber and root crops, which make up a large portion of the global human diet. In humans, the effectiveness of starch digestion is dependent on the amount of amylose in starch initially consumed. Indigestible starch has been observed in human fecal waste (Wolf et al., 1977), which inevitably makes it to wastewater treatment plants. Aside from finding starch in municipal wastewater, starch and other complex organic compounds can also be found in many agricultural and food industry wastes (Kapdan & Kargi, 2006). The use of complex carbohydrates as a fuel source for MFCs at the bench-scale has yielded low power production ($240\text{--}500\text{ mW/m}^2$) (Herrero-Hernandez et al., 2013; Lu et al., 2009) as compared to MFCs that use simple organic substrates such as

acetate (1460-2770 mW/m²) (Fan et al., 2007b, 2012; Nevin et al., 2008). The energy yield decreases even further as reactor scale increases (Castro et al., 2016; Zhang et al., 2013). Most of the studies conducted with starch in MFC anodes have explored the feasibility of using high strength wastes as fuel sources for various types of MFC designs, including single and double chamber reactors, and a few using specific bacterial cultures of *Escherichia coli*, *Clostridium butyricum*, and *Clostridium beijerinckii* (Herrero-Hernandez et al., 2013; Niessen et al., 2004).

Not only is the strength and complexity of organics available as substrate an important factor in power production in a MFC, but also the type of bacterial inoculum used to enrich MFC anodes and the anode environment in which these microorganisms will grow. For most MFC studies, anode media is buffered and maintained around pH 6.8-7 and a conductivity less than 1 mS/cm (Cusick et al., 2011a; Jadhav & Ghangrekar, 2009; Oh & Logan, 2005; Patil et al., 2010). A study by Li et. al. (2013) looked at the electricity production capabilities of MFCs under various inocula of domestic wastewater, activated sludge, or anaerobic sludge. The MFCs operated with each inocula were used to treat acidic food waste leachate, with a pH of 4.76 and a relatively high COD concentration of 1000 mg/L. The CE was highest at 20% using anaerobic sludge as the inoculum. Sequences of PCR-DGGE samples revealed that the anaerobic sludge inoculated reactor contained both fermentative (*Clostridium* sp. and *Bacteriodes* sp.) and putative ARB bacteria (*Magnetospirillum* sp. and *Geobacter* sp.) even at an acidic pH. Although not quantified, hydrogen and methane production may have been significant at this low pH value where some hydrogenotrophic methanogens (Kotsyurbenko et al.,

2007) and most acidogenic bacteria can thrive (Jung et al., 2000), resulting in significant COD removal but low CE.

MFC anodes have been tested under acidic conditions and under high conductivities, both of which have been linked to decreasing bacterial activity and decreasing MFC performance (Kim et al., 2014; Miyahara et al., 2015; Oliveira et al., 2013). *Geobacter* species isolated from freshwater environments, *Geobacter bemidjensis* and *Geobacter psychrophilus*, have been observed to tolerate up to 10 g/L of NaCl without affect to the metabolic activity (Nevin et al., 2005). Miyahara et al. (2015) observed that *Geobacter* species in anode biofilms increased in abundance with increase in sodium chloride concentrations up to 5.8 g/L but decreased remarkably at concentrations of 18 g/L and higher. Most of the studies testing extreme conductivities and pH have used inocula from ambient environments. Although ARB have also been isolated from thermophilic and acidic environments, the extent of existence of other ARB from extreme environments is not yet known (Borole et al., 2008; Jangir et al., 2016; Zavarzina et al., 2007).

It is evident that the specific inocula used in MFCs are important for developing resilient mixed microbial biofilms that can tolerate wastestreams exhibiting extreme conditions that would otherwise hinder microbial activity. Creating resilient biofilms with local inocula from extreme and remote environments can aid in developing MFC technology to meet several goals: 1) the biological remediation of highly contaminated water sources, 2) enhance electricity recovery under stressed anode environments created by such contaminated water sources, and 3) provide incentivized sanitation solutions for small populations living in remote areas that lack such infrastructure.

4.2 Objective

Objective: The objective of this study was to quantify the effects of augmenting wastewater inocula with acidic and salt-polluted sediments on power production, CE, charge transfer, and COD removal under electrolytically-stressed (e.g. pH and conductivity) anode environments.

Hypothesis: I hypothesized that the typical wastewater (WW) inocula obtained from treatment plants can be combined with microorganisms from acid mine drainage sediments to create a more robust anode-respiring biofilm under stressed anode environments (e.g. pH and conductivity) similar to concentrated human waste. Conductivity and pH have both been shown to affect the proton concentration and improve ion transfer from anode to cathode. With an increase in available protons and salt concentrations in the anode solution, MFC power production can be enhanced. The addition of extreme environment microorganisms may improve the threshold tolerance at both acidic and saline conditions.

4.3 Methods

4.3.1 MFC Construction

A single chamber MFC reactor consisted of a 250 mL glass bottle that made up the anode chamber, retrofitted with three sampling ports and a single side arm joined with silicone to the carbon cloth air-cathode (Figure 4.1). The anode and cathode electrodes

were separated using a cloth separator, placed immediately in front of the cathode. The air cathode consists of an activated carbon cloth (Zorflex FM 100, Chemviron Carbon, UK) coated with four PTFE diffusion layers on the air side and a platinum catalyst layer on the liquid side, following the procedures outlined by Cheng et. al. (2006). Each anode chamber was filled with 220 g of synthetic granular graphite (EC-100 3/8 X10, Chagrin Falls, OH) with an average diameter of 4.76 mm. The estimated surface area of each anode was $0.166 \pm 0.002 \text{ m}^2$. When graphite granules were sampled from each reactor, the surface areas were corrected based on the number of granules removed during each sampling point. One graphite rod (11 mm OD; 154 mm L) was used as the electron collector between the graphite granules in the anode and a platinum wire was connected to the cathode. A 240Ω resistor was placed between the anode and cathode electrodes. The liquid volume in the anode was 160 mL in each reactor. The reactors were sampled at the end of each batch cycle and each 15 mL sample was filtered using $0.45\mu\text{m}$ pore filters and stored at -20°C .

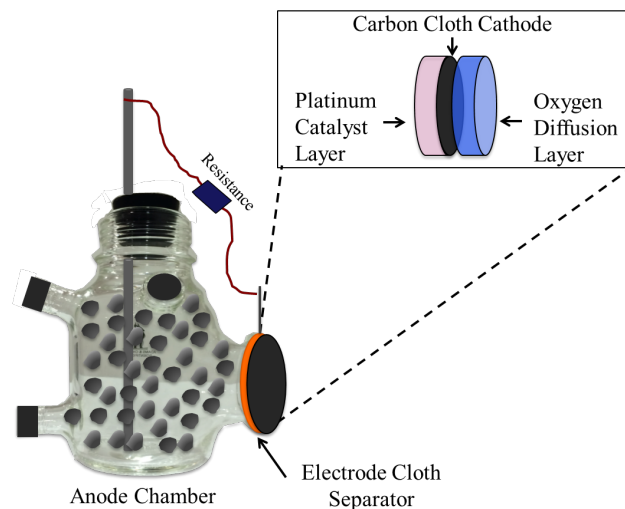


Figure 4.1 Single chamber MFC with graphite granules as the anode electrode and a carbon cloth air cathode.

4.3.2 Inocula

Two different inoculants were tested. One set of duplicates was inoculated with primary wastewater (WW), obtained from La Farfana wastewater treatment plant located in Santiago, Chile while the other set was inoculated with the same wastewater as well as with sediments and liquid from a low pH environment (AR-WW). Sediment samples were obtained from the Azufre River sub-basin, located in the XV Region of Arica and Parinacota in northern Chile. This area is characterized by high concentrations of metals, high salinity, and extremely low pHs due to contamination from arsenic mining of the nearby Tacora crater (Leiva et al., 2014). Liquid and soil samples obtained from the field site were stored at 4°C and used within a week after storing.

Two reactors were inoculated with 33 v/v % WW only, designated as WW-only reactors, while the other two were inoculated with 21 v/v % WW and 12 v/v % Azufre river sediments, and designated as AR-WW reactors. A control with no additional

inoculum was also established. All reactors were fed a synthetic wastewater media containing 0.5 g of starch, 4.3 g of KH_2PO_4 , 1.09 g of Na_2HPO_4 , 0.30 g of NH_4Cl , and 0.13 g of KCl per liter of RO water, unless otherwise noted. Growth enrichment solutions were also added to each media batch. The trace mineral solution consisted of 100 mg $\text{ZnSO}_4 \cdot 7\text{H}_2\text{O}$, 30 mg $\text{MnCl}_2 \cdot 4\text{H}_2\text{O}$, 300 mg H_3BO_3 , 200 mg $\text{CoCl}_2 \cdot 4\text{H}_2\text{O}$, 10 mg $\text{CuCl}_2 \cdot 2\text{H}_2\text{O}$, 10 mg $\text{NiCl}_2 \cdot 6\text{H}_2\text{O}$, 30 mg $\text{Na}_2\text{MoO}_4 \cdot 2\text{H}_2\text{O}$, and 30 mg Na_2SeO_3 per liter of RO water and amended with 1 g $\text{CaCl}_2 \cdot 2\text{H}_2\text{O}$ and 1 g of $\text{FeSO}_4 \cdot 7\text{H}_2\text{O}$ per liter of RO water. pH of the synthetic media was 6.30 ± 0.03 and a conductivity of 4.9 ± 0.42 mS/cm during the start-up period and initial conditions before stressed environments began. The synthetic wastewater was autoclaved the day prior to use and stored at 4°C . Immediately before use, the media was sparged with nitrogen gas for 15 min and maintained under anaerobic conditions. The reactors were covered in foil to prevent light from entering and were kept at 20°C unless otherwise noted.

4.3.3 Normal Anode Environment

During normal conditions, starch concentrations were 500 mg COD/L and batch cycles ranged between 8-15 days. During this period, COD removal, power production, and CE were assessed when the anode environment remained at 5.2 mS/cm and pH 6.2 in order to establish baseline conditions before the anode environment was stressed. Due to the long length of batch cycles, the starch concentration was decreased to 250 mg COD/L for three cycles before stressed anode environments were introduced (Table).

4.3.4 Stressed Anode Environment

Two stressed environments were assessed: 1) high conductivity and 2) low pH (Table 4.1). During the higher conductivity studies, an additional 8 g/L and 16 g/L of NaCl were added to the modified anode media to yield conductivities of 15.5 mS/cm and 37 mS/cm, respectively. For low pH studies, HCl and NaOH were added accordingly to achieve pH levels of 5.5 and 4.1. The pH was continuously monitored with a pH probe until the desired pH was attained.

Table 4.1 MFC operation parameters under stressed anode environments

	pH	Conductivity (mS/cm)	Starch (mg COD/L)
Cond_15.5	6.3	15.5	250
Cond_37.0	6.3	37.0	250
pH_5.4	5.4	5.2	250
pH_4.1	4.1	5.2	250

4.3.5 Performance Analysis

The voltage across the resistor was measured using a Kiethley data acquisition system (M2700, Cleveland, OH). Readings were taken at 10-minute intervals during the entire operational period. Polarization curves were conducted by LSV using a Gamry potentiostat (Warminster, PA, USA). LSV was run for three cycle lengths at a scan rate of 1mV/s from zero to the open circuit potential for each reactor. Current was calculated using ohms law, $I = E / R$, where E is the voltage, I is the current and R is the external

resistance. Power density curves were calculated using $P = EI$. Both the polarization and power density curves were normalized to the anode surface area. Coulombic efficiencies (CE) for each batch cycle were calculated using the following equation (Logan et al., 2006):

$$CE = \frac{8 \int_0^t I dt}{F v_{An} \Delta COD} \quad \text{Equation 4.1}$$

where F is Faraday's constant, v_{An} is the volume of liquid in the anode, ΔCOD is the amount of organic substrate consumed during the batch cycle, and the integral is the number of charge transferred over a period t . The integral was approximated using the trapezoidal rule where:

$$\int_0^t I dt = \sum_{i=1}^t \left(\frac{C_i + C_{i+1}}{2} \right) (t_{i+1} - t_i) \quad \text{Equation 4.2}$$

For chemical oxygen demand (COD) analysis, effluent samples were taken at the end of each batch cycle, filtered through 0.45 μ m syringe filters, and stored at -20°C. COD Hach kits were utilized for measuring COD, following the USEPA Reactor Digestion Method 8000, and were analyzed within a week. Conductivity and pH measurements were conducted using HACH probes and were calibrated each time before use.

4.3.6 Statistical analysis

A two-tailed student t-test was used to determine the probability that statistically significant differences existed between the means of coulombic efficiencies during normal conditions and the mean charge transferred across the stressed anode environments. If the null hypothesis, $H_0: \mu_1 - \mu_2 = 0$, was rejected with a significant level of 0.05 ($p < 0.05$), we assumed that the means were statistically different. Hereafter, when

“statistically significant” is stated, it can be assumed that there’s a 95% confidence level that a type I error (rejecting the null hypothesis when it is true), was not made.

4.4 Results

4.4.1 Degradation of Starch During Normal Conditions

Starch (as COD) was measured at the end of each batch cycle. Batch cycles ranged between 8-16 days during normal conditions. COD degradation was only $6.6 \pm 4.7\%$ greater in the AR-WW reactors than the WW-only reactors (Figure 4.2). The control, lacking both the Azufre river sediments and municipal wastewater, also showed significant starch degradation for each cycle. Although granules for all reactors were acid washed, I hypothesize that non-electrochemical microbial communities may have existed within the anode granules prior to inoculation, growing in the control reactor once the starch media was added. Evidence for this behavior is the high starch degradation in the control while no power production was observed.

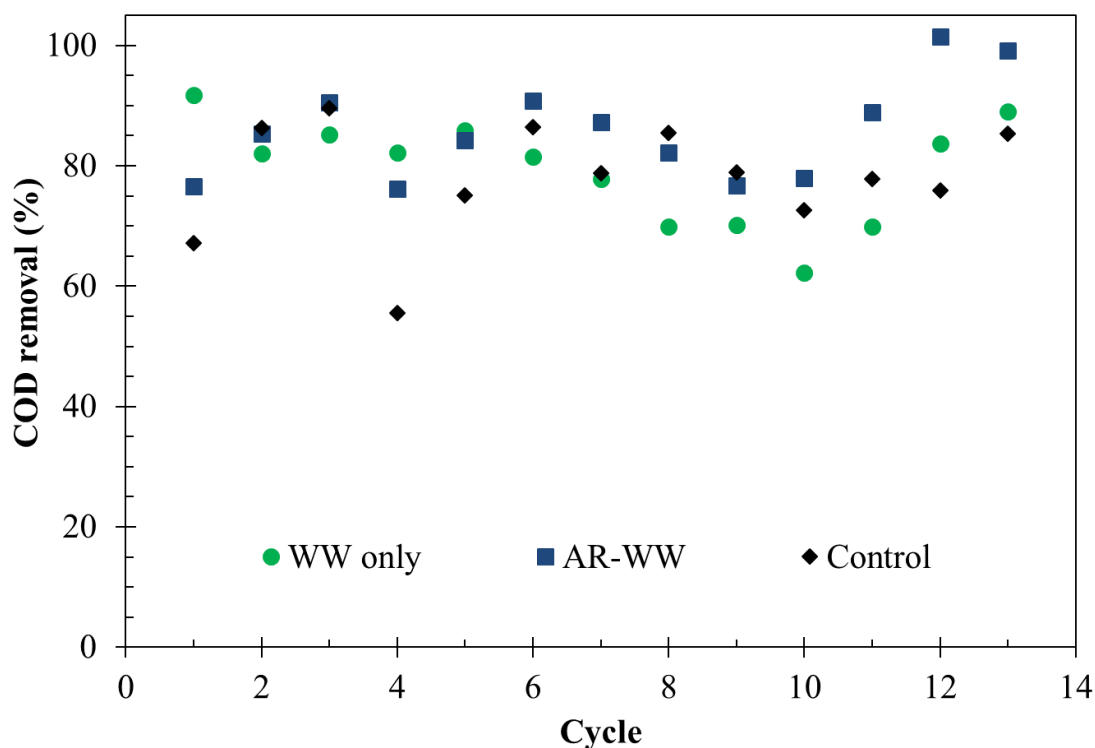


Figure 4.2 COD removal in inoculated, co-inoculated, and non-inoculated reactors during normal conditions. All reactors observed high COD removal, over 60% of the initial batch concentrations.

Batch cycle lengths were long, ranging between 8-15 days with an average length of 11 ± 2.8 days, allowing for sufficient time for substrate utilization. As a comparison, Lu et al. (2009) observed that starch processing waste with a COD concentration of 4850 mg/L had a batch cycle length of approximately 37 days while using processing waste as the inoculum. The batch cycle length observed in this study was comparable to previous studies of starch degradation in anaerobic conditions. All reactors consumed over 60% starch but only reactors that were inoculated with either wastewater or with both wastewater and Azufre River sediments showed power production.

4.4.2 Power Production and Coulombic Efficiency During Normal Conditions

Peak power production fluctuated significantly between batches for both the WW-only and AR-WW reactors across all batch cycles (Figure 4.3). Although this fluctuation occurred, the AR-WW reactor attained higher power densities than the WW-only reactor. No power production was observed for the control during normal conditions, demonstration that anode-respiring communities were not enriched in the control.

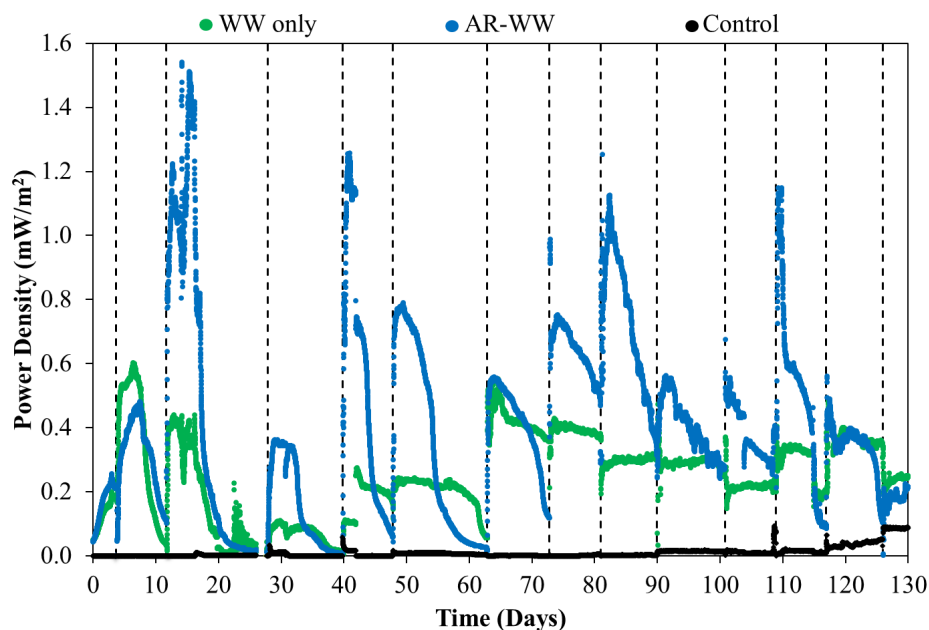


Figure 4.3 Power density across 12 batch cycles for reactors WW-only, AR-WW, and the control.

Although the peak power densities reached by the AR-WW reactor were high ($0.83 \pm 0.36 \text{ mW/m}^2$), the WW-only reactor could sustain a relatively lower ($0.36 \pm 0.14 \text{ mW/m}^2$) but constant power output throughout most batch cycles. Due to these varying

patterns in power density, CE is a more appropriate assessment of reactor performance. CE values were similar for both inoculated reactors (Figure 4.4) but the difference between the AR-WW and WW-only reactor was not statistically significant. During normal conditions, the inocula type did not have an apparent effect on CE.

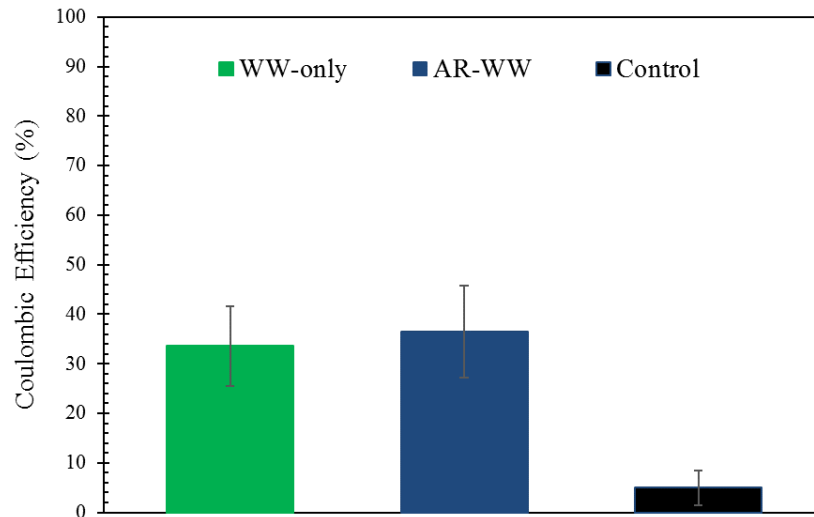


Figure 4.4 Average coulombic efficiency for WW-only, AR-WW, and control reactors with standard deviations across all batch cycles. There was no statistical difference between WW-only and AR-WW.

4.4.3 Reactor Performance During Stressed Anode Environment

Due to the addition of chloride in the form of NaCl to increase the conductivity of the anode solution, chloride interfered with the COD HACH kits for all high conductivity samples and several from the low pH period. For this portion of the study, limited COD removal and the associated coulombic efficiency were reported. As a pseudo measurement of electrochemical efficiency, we presented instead the electrical charge transferred across the system, measured in coulombs, during each batch cycle.

When the conductivities of the anode media were increased from 5.2 to 15.5 mS/cm, the rate of charge transferred per batch cycle increased as compared to the normal conditions for the WW-only reactor (Figure 4.5A). The AR-WW reactor only showed a statistically significant change in charge transfer between conductivities 15.5 and 37 mS/cm. Comparing the WW-only and AR-WW reactors to each other, the charge transfer per batch cycle was higher in the AR-WW reactor than the WW-only reactor for conductivities of 5.2 and 37 mS/cm.

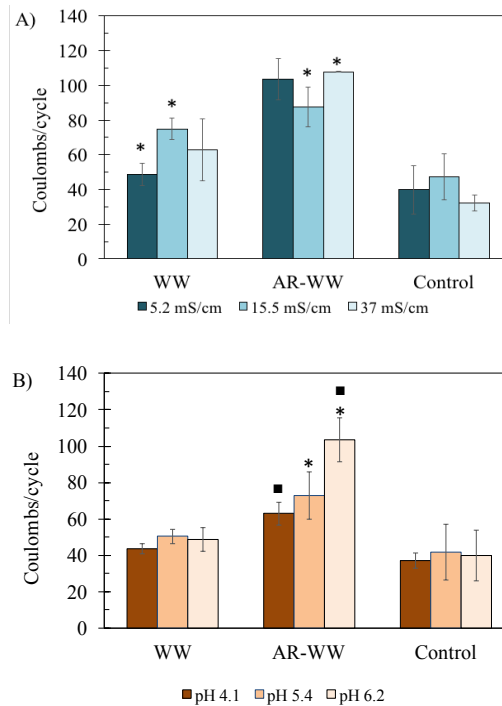


Figure 4.5 Charge transferred during stressed anode environment conditions per batch cycle A) changes in anode bulk liquid conductivity and B) changes in anode bulk liquid pH. When conductivity changes, the pH remained at 6.2. When the pH was changed, the conductivity remained at 5.2 mS/cm. For each reactor, statistical differences ($p < 0.05$) of means between the highlighted operational conditions are shown with either (*) or (■) above the bar. All other relationships had no statistically difference in means.

When the pH was decreased from 6.2 to 5.4 and then further to 4.1, there was a clear distinction in pH effects on charge transferred between the WW-only reactor and the AR-WW reactor (Figure 4.5B). The pH did not significantly affect the charge transferred in the WW-only reactor. However, charge transfer decreased as the pH decreased in the AR-WW reactor but it still delivered a greater number of coulombs than the WW-only reactor. Across all reactors, charge transfer was greatest when the pH remained at 6.2 and when conductivity was between 5.2 and 37 mS/cm.

4.5 Discussion

Based on the results from this study, the AR-WW reactor attained higher peak power densities than the WW-only inoculum reactor under normal conditions. Although observed peak power densities were higher for the AR-WW reactor, both MFCs attained similar CE's of $34 \pm 8.1\%$ for the WW-only reactor and $36 \pm 9.3\%$ for the AR-WW reactor. Operational power density revealed that the kinetics of organic degradation varied between AR-WW and WW-only reactors.

When the anode environments were stressed to acidic or high-salinity conditions, clear distinctions were observed between the performance of the WW-only and AR-WW reactor. The AR-WW reactor had better charge transfer performance than the WW-only reactor at all pHs and conductivities. Changes in pH significantly affected the AR-WW reactor, causing a decrease in charge transfer as pH decreased, while having no effect on the WW-only reactor. Interestingly, where data were available, there was no statistical

difference in CE when pH decreased in the co-inoculated reactor ($9.8 \pm 2.2\%$ at pH 6.2 and $10.5 \pm 1.0\%$ at pH 4.1) or in the WW-only reactor ($5.3 \pm 1.3\%$ at pH 6.2 and $7.2 \pm 0.6\%$ at pH 4.1). This suggests that although charge transfer improved at higher pHs for the AR-WW reactor, so did the microbial community's ability to oxidize the substrate, achieving similar efficiencies at both high and low pHs. MFCs inoculated with only sediments from the same study site, operated in similar air-cathode configurations with pyruvate as the substrate, and at an even lower pH (3.7) than presented in this study, showed a CE of $4.6 \pm 3.9\%$ (Leiva et al., 2016). As such, there is evidence from this study to suggest that using a mixture of Azufre River sediments and primary wastewater enriched for an anode community that could 1) degrade a complex organic substrate that could yield higher CE's than either inoculum on its own at low pH, and 2) tolerate electrolytically-stressed environments more effectively than communities developed from primary wastewater alone.

Under stressed environments, microorganisms can adapt and strategize their physiology in order to maximize the use of their surrounding resources for survival (Brooks et al., 2011). Extreme changes in pH or conductivity can alter the microbial cells physiological characteristics to some extent before causing irreversible damage to the cells. In MFCs, both changes to the anode bulk liquid's pH and conductivity have been studied for reactors operating with inocula from ambient environments (Jadhav & Ghangrekar, 2009; Kim et al., 2014; Miyahara et al., 2015; Nevin et al., 2005). These studies found thresholds, especially for salt concentrations, where microbial activity is completely hindered by microbes from ambient environments. Microbial activity seems to decline at conductivities over 30 mS/cm for some *Geobacter* species (Nevin et al.,

2005). In our study, the co-inoculated reactor had improved performance at 37 mS/cm. It is possible that microbes from extreme environments have physiological capabilities that allow the use of higher salt concentrations to drive their proton motive force, a currency for energy, to promote microbial activity.

4.6 Conclusions

The purpose of the study was to assess whether the addition of sediments from a heavily salt-polluted river would enhance electrochemical performance in MFC anode environments where pH and conductivities were stressed from the typical conditions associated with MFC reactors. For this study, MFCs were inoculated with primary wastewater from a municipal wastewater treatment plant in Santiago, Chile. While one reactor was only inoculated with wastewater, the other contained an additional inoculum of sediments from a heavily salt-polluted and acidic river of northern Chile, the Azufre River.

This study showed that the addition of Azufre river sediments to a municipal wastewater inoculum can improve the electrochemical performance of an MFC with stressed anode environments under high conductivities and low pH than reactors with only municipal wastewater inocula. While much of the MFC research field uses inocula from wastewater treatment plants or other ambient environments, bioaugmentation of inocula with microorganisms that thrive in more extreme environments should be considered for bioremediation of a variety of high strength wastewaters, whether from highly contaminated water sources or mixed human waste streams from latrines.

Developing microbial communities that can adapt to exposure of harsh environments within MFCs may make the technology suitable for in-situ remediation purposes.

CHAPTER 5

EFFECTS OF EXTERNAL LOAD ON MFC ELECTROCHEMICAL PERFORMANCE UNDER SELECT METHANOGENESIS INHIBITORS

5.1 Introduction

One of the major obstacles in utilizing MFC technology for complex wastewater treatment applications, such as the synthetic feces wastewater used in the previous chapters, is the ability of ARB to efficiently convert organic substrate to electricity. MFCs operated to treat defined and simple organic compounds yield high coulombic efficiencies in the range of 70 - 80% (Fan et al., 2007a; Lee et al., 2008; Rabaey et al., 2005). These high CEs have also been observed in MFCs inoculated with effluents of previously-enriched MFCs (parent MFCs) where selective medias have already been used to promote the growth of ARB. In this way, an enriched group of ARB in new MFCs can degrade simple organics more efficiently to maximize current and power yields. While useful for research purposes, it is impractical for full-scale systems and pilot-scale reactors deployed on the field. At the bench-scale, research has focused extensively on increasing power production using simple substrates, such as acetate. When mixed inocula are used in MFC anodes, ARB, along with a multitude of other heterotrophic microorganisms, including acetoclastic methanogens, can compete for the available acetate (Lee et al., 2008; Velasquez-Orta et al., 2011). This competition for substrate can ultimately shift electricity production by ARB to methane production by methanogens.

When MFCs are operated to treat real wastewaters with complex substrates, the CE decreases to 20% or less (Feng et al., 2008; Lu et al., 2009; Majumder et al., 2014; Velasquez-Orta et al., 2011). A handful of studies have observed that when complex substrates are used as the energy source in mixed community MFCs, alternative metabolic pathways to electricity production occur and even dominate. Phylogenetic analyses based on partial bacterial 16S rRNA gene and archaeal specific gene primers of anode biofilms developed from mixed inocula clearly show that a range of microorganisms from sulfur-reducing bacteria to fermentative bacteria to methanogens can coexist and limit the availability of electron donor for ARB to produce electricity (Beecroft et al., 2012; Borole et al., 2009).

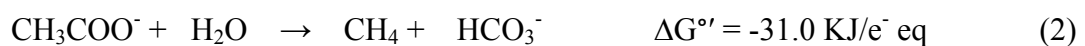
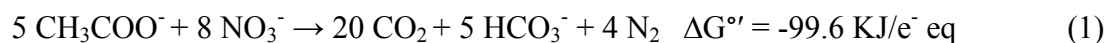
Methanogenesis is a competing metabolism in MFC anodes that treat both simple and complex organic substrates but it is not always recognized or quantified in the MFC literature. To manage substrate competition in MFC anodes, and improve the recovery of electrical energy produced by ARB, methanogenesis can be effectively inhibited with chemical additives that create changes to the anode environment (Parameswaran et al., 2009, 2010a; Zhuang, Chen, et al., 2012). 2-BES has been used to inhibit methanogenesis in several MFC reactors (Kiely et al., 2011; Parameswaran et al., 2009, 2010b; Srinivasan & Butler, 2017; Zhuang et al., 2012), but it is expensive and likely cost-prohibitive in large-scale applications. Nitrate (NO_3^-) has also been shown to inhibit methanogenesis effectively and at lower dosing concentrations than 2-BES (Zhou et al., 2011b) but it is not readily used for MFC applications since nitrate is an alternative electron acceptor for many bacteria that exist in the anode microbiome. Its availability in the anode can

decrease CE and the overall energy produced by the MFC by diverting available electrons towards nitrate reduction.

Nitrate is an economically feasible alternative methanogenesis inhibitor for potential use in large-scale applications of MFC technology where methanogenesis may be a dominant energy sink because it is readily available in contaminated water sources. Nitrogen-rich wastewaters, whether from municipal treatment plants or from decentralized treatment systems, can be coupled with MFC technology to meet dual treatment goals of organic and nitrogen removal and potentially improve energy yields by inhibiting methanogenesis.

While the addition of external chemicals like 2-BES can effectively suppress methanogenesis, alternative inhibitors that are already freely present in wastewater have not been extensively studied for MFC applications. A recent study by Srinivasan & Butler (2017) found that nitrate addition to a MFC anode had minimal effects on the electrochemical performance and microbial community structure when the electron donor was in excess (7.4 mg C/ mg NO₃-N). At a ratio of 3.7 mg C/mg N, ARB and denitrifiers could coexist with minor effects to the electrochemical performance and community structure. Therefore, the presence of nitrate in a MFC anode shows significant promise as an alternative to 2-BES for methanogenesis suppression.

With the presence of nitrate in a mixed community anode, alternative metabolic pathways will be available to microorganisms when acetate is used as the substrate:



where (1) describes the oxidation reaction of acetate by denitrifiers and (2) describes the fermentation process of acetate by acetoclastic methanogens at 25°C and pH 7. Taking thermodynamics into consideration (Equation 2.1; Chapter 2, section 2.3: $\Delta G^{\circ'} = -nF(E_{\text{sub}}^{\circ'} - E_{\text{an}}^{\circ'})$), the Gibbs free energy of the redox reaction for anode respiration is dependent upon the reduction potential of the anode, $E_{\text{an}}^{\circ'}$ when the substrate type and concentration remains the same. Theoretically, for ARB to have a competitive advantage, the larger the difference between substrate potential and anode potential, the greater the Gibbs free energy to out compete alternative metabolisms. The anode potential can be actively controlled by a potentiostat or influenced by the external resistance of the MFC (Aelterman et al., 2008; Dennis et al., 2016; Kannaiah Goud et al., 2013; Kato, 2017; Torres et al., 2009; Venkata Mohan et al., 2010). Therefore, the response and resilience of the anode-respiring community in the presence of alternative metabolic pathways will be highly influenced by the anode potential and the parameters that dictate the reduction potential of the anode electrode (i.e. electrolyte composition and electrode material).

5.2 Objective

Objective: The purpose of this study was to identify the resilience of anode biofilm electrochemical performance to sequential additions of methanogenesis inhibitors to the anode environment in MFCs with different external resistances.

Hypothesis: Theoretically, in an MFC with a constant substrate standard potential of -0.30 V vs SHE when acetate is the substrate, biofilms at the anode will gain more energy with an anode at a standard potential more positive than the minimum of -0.30 V.

Low external resistances will yield a more positive anode potential. I hypothesized that reactors under an external resistance most similar to the internal resistance, where maximum electricity and power are typically observed, will be optimized to produce a more positive anode potential that can yield a favorable and competitive Gibbs Free Energy ($\Delta G < 0$) against other metabolic pathways. These optimized anode potentials will promote the electrochemical activity of ARB, making the overall MFC anode more resilient under additions of methanogenesis inhibitors to the anode environment.

5.3 Experimental Procedure

5.3.1 MFC Construction

Four dual chamber H-type MFC reactors were constructed (Figure 5.1). Although one reactor was slightly different in physical dimensions, the anode surface area and anode liquid volume remained constant across all reactors. A cation-exchange membrane (CMI-7000, Membrane International Inc., Glen Rock) was used to separate the anode from the abiotic ferricyanide cathode. The anodes contained a Ag/AgCl electrode (Basi Inc., West Lafayette, IN). Each reactor contained five carbon felt electrodes (22 mm x 110 mm x 3.2 mm) in each chamber which were attached together via marine-grade platinum wires. The total starting surface area of the anode electrodes was 0.028 m² and decreased by 3.2% of the total surface area when sampled after each phase for future downstream processing of DNA and RNA (Appendix). The final surface area was 0.023 m², decreasing less than 20% by the end of the experiment.

The starting external resistance, or external load, was set to 820 Ω during the initial acclimation period. Although a wide range of external resistances have been used

in MFC applications, ranging anywhere between 1-100,000 Ω , the majority of studies have used external resistances less than 2000 Ω (Beecroft et al., 2012; Castro et al., 2016; Du et al., 2011; Feng et al., 2008; Jung et al., 2011; Rismani-Yazdi et al., 2013). For this study, the start-up external resistance was chosen as a mean value of the most widely used external resistances. The anode chamber was inoculated with a 1:40 dilution by volume of anaerobic digestate from a locally operated anaerobic digester used for methane production (Barstow Farms, Hadley, MA) and diluted into the anode media. The cathode chamber was continuously maintained under a 70 mM ferricyanide in 80 mM phosphate buffer solution.



Figure 5.1 Reactor setup during the full length of the experiments. One reactor was narrower and taller, but the liquid volume and the surface area remained the same across all reactors. All subsequent power and current densities were normalized to the available surface area during each phase of the experiment.

5.3.2 MFC Operation

During the initial start-up period, the reactors were set up in recycle-batch for a minimum of three consecutive batch cycles. Each reactor was fed 500 mg acetate/L in a 16 mM phosphate buffer solution, supplemented with a trace mineral solution as previously described in Chapter 3 at a recycle flow rate of 40 mL/min to promote mixing. Continuous flow conditions were established at a flow rate of 0.20 mL/min.

Reactors ran in continuous mode until MFC voltages and anode potentials had stabilized and remained within one standard deviation of the mean during that period. Once stabilized anode potentials and current production were observed, polarization curves were performed on all reactors to determine the internal resistance by LSV as described in Chapter 3, Section 3.2.5. All reactors of the same physical dimensions had an internal resistance of $170 \pm 0.35 \, \Omega$, while the taller and narrower reactor had a larger internal resistance of $480 \pm 0.09 \, \Omega$. All reactors had the same working anode and cathode liquid volumes and surface areas. The reactor of slightly different initial internal resistance remained at an external resistance of $820 \, \Omega$ throughout the entire experiment (R_820). The remainder of the reactors were set to the following external resistances: $170 \, \Omega$ (R_170) to match the internal resistance, $17 \, \Omega$ (R_17) and $1800 \, \Omega$ (R_1800) to evaluate a log difference from the internal resistance at the start of the experimental conditions. Substrate limiting conditions were tested by decreasing the acetate concentration from 500 to 100, 50, 40, 30, and 35 mg/L to determine at what influent concentration the reactors could sustain power production and also still observe complete substrate removal. This was done to develop a competitive environment under the distinct external resistances. The final acetate concentration of 40 mg/L was selected for all reactors and operated under these conditions for over 180 days prior to the start of the experimental period.

The reactors were operated under sequential addition of two known methanogenesis inhibitors, 2-BES and NO_3^- , to systematically assess the effects on electrochemical performance of the MFCs operating at distinct external resistances in a continuous flow reactor (Table 5.1). Each period ran for at least three HRTs and all

further HRTS during that period were considered steady-state. Concentrations of 2-BES and NO_3^- were chosen based on a previous study that observed minimal effects on electrochemical performance and anode community structure under substrate-limiting conditions when the C/N ratio was maintained at 3.7 mg C/ mg N for prolonged periods of time (Srinivasan et al., 2017). The first three phases (I-III) assessed the effects of NO_3^- as an electron donor competitor to ARB if methanogenesis was inhibited with 2-BES. Phase IV and V were recovery periods for the biofilms to stabilize before being exposed to NO_3^- without the addition of 2-BES (Phase VI) so that the effects of a three-way competitive environment between ARB, methanogens, and denitrifiers on electrochemical performance could be assessed.

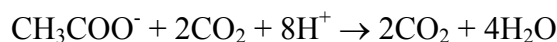
Table 5.1 Summary of methanogenesis inhibitor addition for each phase of the experiment. Nitrate was added at a ratio 3.7 mg C/ mg N.

Phase	Phase Length (Days)	BES Added (mg/L)	NO ₃ ⁻ Added (mg N/L)	Target Effects on Microbial Competition in Anode Biofilms
I	42	0	0	Establish baseline performance
II	19	630	0	Methanogenesis inhibition with BES
III	17	630	4.4	Two-way competition between ARB and denitrifiers
IV	5	630	0	Recovery Period
V	8	0	0	Recovery Period
VI	12	0	4.4	Three-way competition between ARB, methanogens, and denitrifiers
VII	19	0	0	Recovery Period

5.3.3 Treatment and Electrochemical Performance Evaluation

Acetate, nitrate, and nitrite concentrations were evaluated using ion chromatography (IC) (Metrohm 850 Professional, Riverview, FL). A metrosep A Supp 5 separation column was utilized with a 3.2 mM carbonate and 1.0 mM bicarbonate eluent solution. Influent and effluent samples from each reactor were taken on the day of sampling, filtered using a 0.45 µm syringe filter, and immediately stored at -20°C.

Acetate concentrations were converted to mg COD/L using the following stoichiometric relationship:



and using molecular weights of O_2 (32.0 g/mol) and CH_3COO^- (59.0 g/mol) to yield a ratio of 1.08 g O_2 /g CH_3COO^- . Methane gas was measured with a gas chromatograph (Agilent 7890A, Santa Clara, CA) using a HP-PLOTQ column under an isothermal method of 60°C for 7 minutes. A 1 mL sample was taken from the anode bulk liquid and placed into a 1.8 mL vial that was previously sparged and filled with helium. The helium was displaced during addition of the liquid sample using a two-syringe system to maintain a closed controlled volume. The vial was left at room temperature for 24 hours to allow the liquid and gas phases to equilibrate. A 250 μL headspace sample was injected into the GC inlet and detected using a thermal conductivity detector (TCD). Methane was analyzed only for detection purposes, not to quantify, because gas tight conditions were not completely maintained during sampling of the anode influent and effluent, and suspended and attached biomass.

Voltage and anode potential readings were recorded every 15 minutes, unless noted otherwise, using a Kiethley data logger (Model 2700, Beaverton, OR). The anode potential was measured using Ag/AgCl as the reference electrode. All anode potentials are presented in reference to a SHE. Current was calculated using Ohms' Law, $I = E / R$, where E is the measured voltage, I is the current and R is the external resistance. Polarization curves were performed as previously described for each reactor before changing to the next operational condition to determine and monitor fluctuations in the internal resistance and maximum power densities. Power was calculated using $P = E \times I$.

Both current and power were normalized to the projected anode surface area during each phase. CEs were determined using the following equation:

$$CE = \frac{8 I}{F q \Delta COD} \times 100 \quad \text{Equation 5.1}$$

where I is current in Amperes, F is Faraday's constant (96485 C/mol), q is the flow rate in L/s, and ΔCOD is the amount of acetate removed by the reactor (Logan et al., 2006).

CE's are reported as percentages. To determine electron sinks due to the presence of nitrogen in the anode, it was assumed that complete dissimilatory nitrate reduction was the main metabolic pathway by microorganisms present in the anode. Based on stoichiometry, the required acetate was 5 moles per 8 moles of NO_3^- .

5.3.4 Statistical Analysis

For comparisons of mean internal resistance, current density, and coulombic efficiency across the different phases a one-way analysis of variance (ANOVA) was performed for comparisons of two or more means using MINITAB EXPRESS Statistical Software (version 1.5.0) to find statistical differences. The null hypothesis, $H_0: \mu_1 = \mu_2 = \mu_3 = \mu_n$, was rejected if p-value < 0.05, meaning that at least one mean was different according to Tukey's simultaneous tests for difference of means.

5.4 Results

5.4.1 Internal Resistance

The purpose of this study was to observe the resilience of electrochemical performance when MFCs were operated at a range of external resistance and the anode

environment was sequentially exposed to two known methanogenesis inhibitors, 2-BES and NO_3^- . During the start-up period, microbial communities present in anaerobic digester were acclimated to an external resistance of 820 Ω . After four recycle-batch cycles to acclimate the anode communities, polarization curves were conducted to determine the internal resistance of the fuel cells and the external resistances were altered for three of the four reactors to 17 Ω (R_17), 170 Ω (R_170), and 1800 Ω (R_1800) while one remained the same (R_820). The external resistance plays an important role in the development of microbial communities at the anode because it can directly influence the anode reduction potential and its availability to microbial respiration, affecting the subsequent energy generation (Wagner et al., 2010).

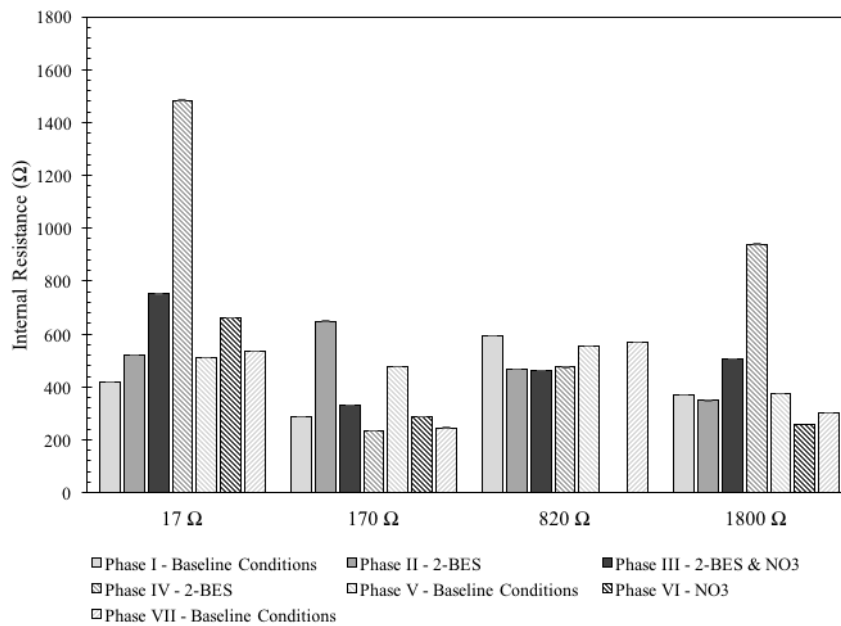


Figure 5.2 Internal resistances at the end of each phase for reactors R_17, R_170, R_820, R_1800 for all phases of the experimental period. Internal Resistances were determined by LSV. Standard error is shown for all calculated internal resistances.

Internal resistance was not available for R_820 during phase VI.

The baseline-conditioning period (Phase I) was performed for each of the defined external resistances after substrate-limiting parameters were established. This was done in order to develop an equilibrium baseline and control period for comparisons of current density, anode potential, and internal resistances to the subsequent phases. The internal resistances varied widely during the experimental phases (II-VI) at the extreme ends of external resistances (17 Ω and 1800 Ω) (Figure 5.2). Reactors with the lowest and highest external resistances in this study observed similar increases in internal resistance when BES was present (Phases II-IV), followed by an immediate drop when BES was no longer present in the anode. The opposite effects were observed for R_820 as methanogenesis inhibitors were added and removed from the anode bulk liquid. An increase in anode ion concentrations due to salt additions can decrease the internal resistance when pH remains constant (Liu et al., 2005), which was the observed effect at 820 Ω . Interestingly, at 170 Ω the internal resistance remained low (average $360 \pm 150 \Omega$), with observed peaks at Phase II and V.

5.4.2 Maximum Power Densities

Although the internal resistances fluctuated significantly at all fixed external resistances, clear positive trends in the maximum power density by the reactors at each phase were observed with increasing external resistance (Figure 5.3). These maximum power densities were determined using LSV and represent the maximum power densities the MFCs could attain if the external resistance matched the measured internal resistance at the end of each phase. With the initial addition of 2-BES in Phase II, maximum power

densities increased by a factor of 22 for R_17. The exponential increase was less notable as the external resistances became greater, increasing by 1.8, 1.7, and 0.58 times for reactors R_170, R_820, and R_1800, respectively. As the anode environments returned to baseline conditions for Phases VI and VII, a clear rise in maximum power density from the initial maximum power density in Phase I was observed, where the increase was most prominent for R_17, increasing from 0.04 to 0.40 and up to 2.7 mW/m² by Phase VII (Figure A.3).

The improvement in electrochemical performance over the experimental period is taken as a pseudo measurement of the activity of anode-respiring biofilms. It is hypothesized that the sequential addition of the methanogenesis inhibitors 2-BES and NO₃⁻ created an unfavorable environment for methanogens to proliferate, giving anode-respiring communities within the biofilm a competitive advantage to develop a robust community over time. The higher the fixed external resistance, the more resilient the biofilm became in the second half of the experiment (Phase V-VII) when NO₃⁻ was the only added inhibitor, noting only a 9% decrease in maximum power density between V and VI for external resistance 1800 Ω. Enrichment of the anode communities with periods of methanogenesis inhibitors in the anode of MFCs may be a useful attribute to improve the activity of anode-respiring communities and develop long-term resilient biofilms that can generate electrical energy.

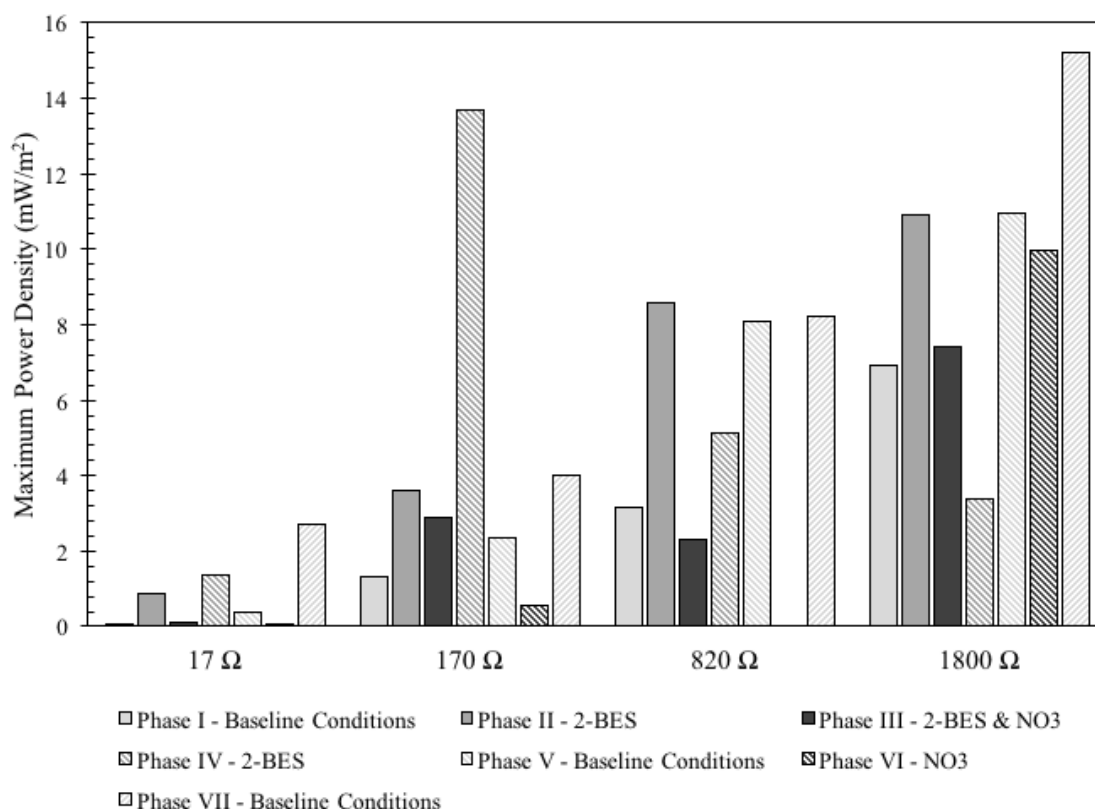


Figure 5.3 Maximum power densities attainable at the end of each phase for reactors operating with 17, 170, 820 and 1800 Ω. No maximum power density is shown for R_820 during phase VI. During the experiment, baseline anode conditions were re-established during Phase V and VII and comparison were made in regards to Phase I.

5.4.3 Anode Potential

The anode potential for each MFC was influenced using fixed external resistances rather than poisoning the anode. In this way, the anode community was completely dependent on the anode potential that evolved at the specified external resistance. The anode potential developed for each reactor was directly associated with the fixed external

resistance. The higher the external resistance, the more positive the anode potential became. The addition or removal of methanogenesis inhibitor at each phase contributed to further shifts in the anode potential (Figure 5.4). For R_17, the anode potential remained positive (0 to +0.3 V) for all phases except the recovery phases (IV and V). During NO_3^- addition periods (Phase III and VI), the potential was the most stable, meaning the anode potentials were linear and within one standard deviation of the mean, and remained constant around $+0.27 \pm 0.01$ V for R_17. Similarly, the anode potential became more negative when 2-BES was in solution (Phase II and IV) for R_170 and R_820. The opposite effect was observed when NO_3^- was added to these reactors in Phase III and VI, observing an increase in anode potential to 0 V or higher. At the highest external resistance, R_1800, the anode potential remained relatively constant around -0.36 ± 0.02 V and observed the least amount of fluctuation in anode potential across all phases except Phase VI where NO_3^- was added without 2-BES. During that period, anode potential increase up to -0.2 V after 15 days, decreasing back to -0.36 once NO_3^- was removed.

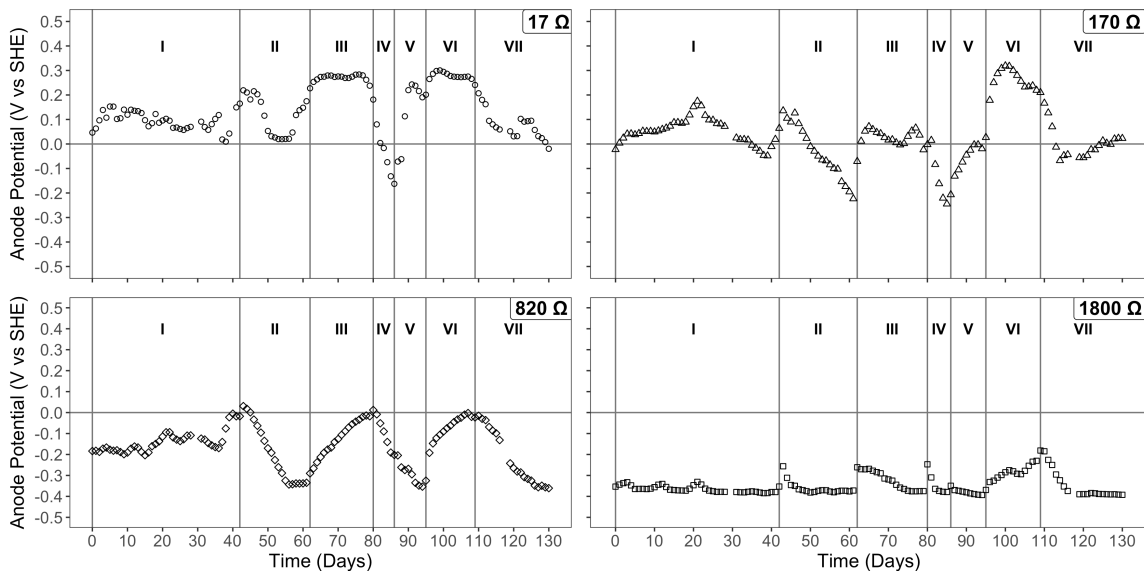


Figure 5.4 Anode potentials across all experimental phases for reactors R_17, R_170, R_820 and R_1800 Ω .

5.4.4 Operational Current Densities

The current densities increased more prominently during periods of 2-BES addition (Phases II & IV) at external resistances 17 and 170 Ω (Figure 5.5). Interestingly, after the anodes were sequentially introduced to 2-BES and NO_3 during Phase II and III, the current density at the recovery period (Phase VI) increased for R_17 and R_170. The highest observed current density was 52 mA/m^2 for R_170 during Phase IV. Although the current density was a significant increase from previous phases, it was not maintained during that period. This could be due, in part, to the biofilm needing a longer stabilization period to reach steady-state than what was allowed (5 days).

For R_1800, minor fluctuations were observed in the operational current density across all phases. These fluctuations were more prominent in R_820 but did not reach

similar power density values as in R_17 or R_170. At the high external resistance (1800 Ω) the current density observed only a small decrease from $10.0 \pm 0.9 \text{ mA/m}^2$ in Phases I-II to $5.8 \pm 0.7 \text{ mA/m}^2$ in Phase III when 2-BES and NO_3 were present in the anode bulk liquid. At all other times, the current densities were maintained and gradually increased from Phase I to Phase VII.

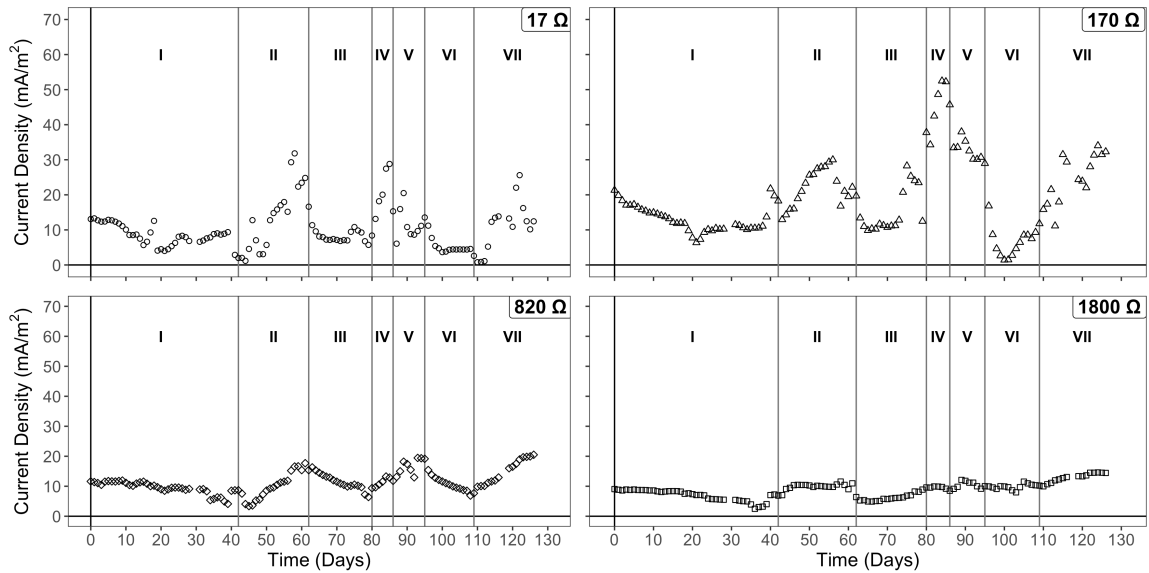


Figure 5.5 Current density across all phases for reactors R_17, R_170, R_820, and R_1800.

5.4.5 Coulombic Efficiency

Before any methanogenesis inhibitors were added to the MFCs, average CE were $15 \pm 2.1\%$, $23 \pm 3.2\%$, $12 \pm 5.0\%$, and $18 \pm 2.9\%$ for R_17, R_170, R_820, and R_1800, respectively (Figure 5.6). During Phase II, 2-BES was added and CE's increased to $38 \pm 11\%$, $37 \pm 7.9\%$, $18 \pm 2.4\%$, and $29 \pm 4.0\%$ for R_17, R_170, R_820, and R_1800, respectively. Although not quantified, methane gas was detected in the headspace of all

reactors in phase I and the increase in CE immediately after 2-BES addition is likely attributed to inhibition of methanogenesis activity. The CE increased more significantly during the initial addition of 2-BES (Phase II) at low external resistances, where the anode potential was closest to 0 mV for R₁₇ and R₁₇₀.

With the high external resistances of 820 Ω and 1800 Ω , there was no statistically significant difference in CE across all phases except between phase II and VI for 1800 Ω . The lower external resistance (17 Ω) exhibited similar results, where CE increased more significantly during the first BES addition in Phase II but returned to the initial CE for the rest of the phases. With 170 Ω , different trends were observed. There was no difference in CE during Phase I-III when BES and NO₃⁻ were present in the anode bulk liquid. A large increase occurred after NO₃⁻ was removed, gradually decreasing for the following Phases (IV-VI), until returning to the original CE as in Phase I.

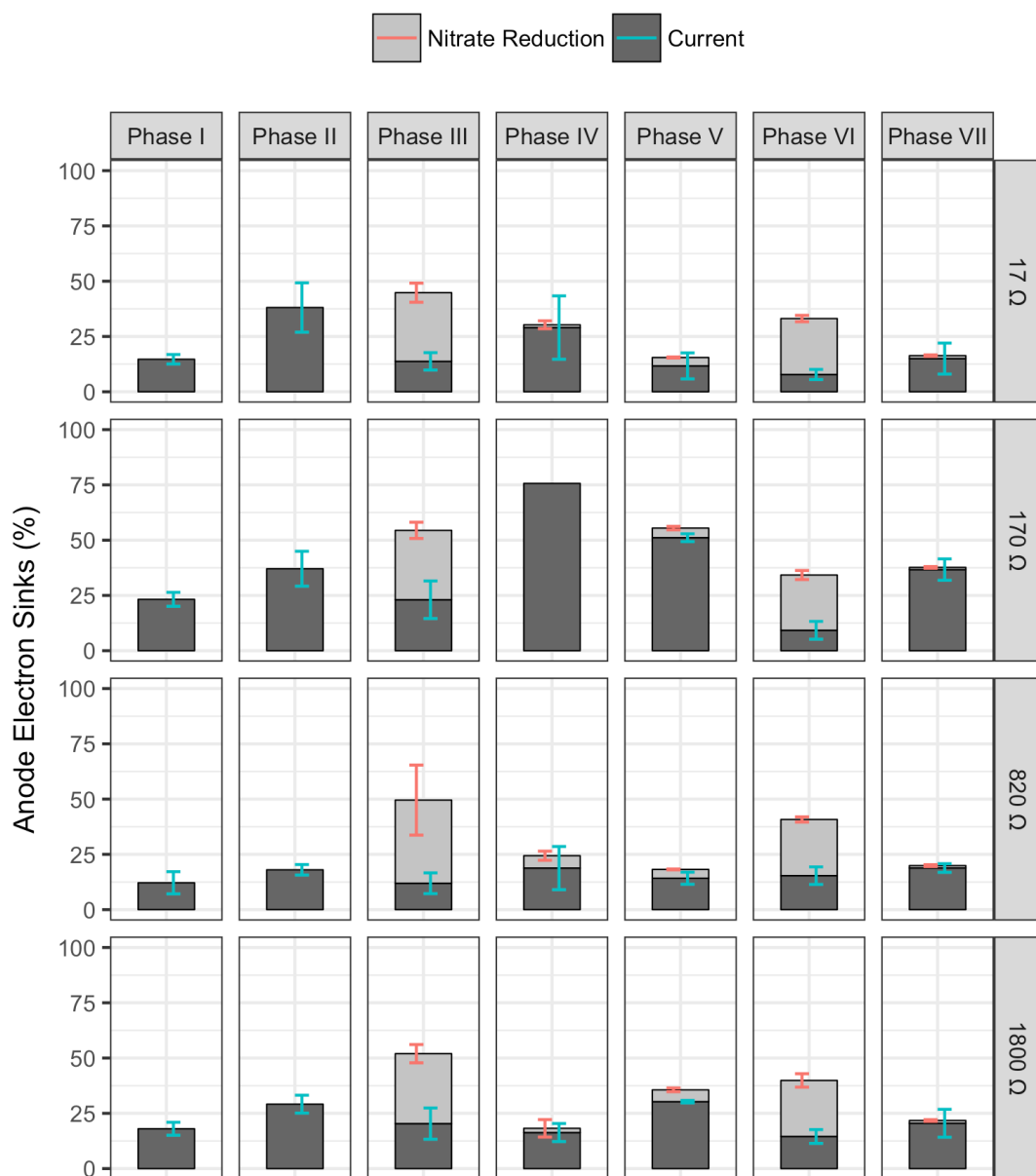


Figure 5.6 Coulombic efficiency and electron sinks due to dissimilatory nitrate reduction occurring at the anode across all phases. Error bars represent standard deviations.

5.5 Discussion

5.5.1 Internal Resistance Fluctuates with Changes to the Anode Environment

The internal resistance of any MFC is comprised of three types of resistance losses: activation or charge transfer losses, diffusion or concentration losses, and ohmic (solution) losses. The dominant loss in most MFCs is ohmic loss, typically observed by conducting polarization curves and monitoring the linearity between the cell voltage and the current density (Logan, 2008). Polarization curves for all reactors at each phase revealed that the internal losses were primarily due to ohmic losses (Figure A.1). Ohmic losses can also be subdivided into three categories: losses due to ion transport within the electrolyte, losses due to electron transport, and losses due to contact resistance (Lee et al., 2008; Revankar & Majumdar, 2014).

In most MFC applications, the primary contribution to ohmic losses is due to ion transport within the anode electrolyte. As such, we can assume that ohmic loss is equal to the ionic resistance, which is a function of electrolyte conductivity, distance between the anode and cathode, and the available surface area of the anode (Vázquez-Larios et al., 2011). The only parameter that was altered across the phases was the electrolyte conductivity. Although the electrolyte conductivity was dynamically changing across phases, the expected fluctuations in internal conductivity are only observed with R_820. It is possible that electron transport losses and contact losses may also be contributing to ohmic losses, although, it was not the scope of this study to quantify these losses.

As hypothesized, the reactor operated with external resistance similar to its own internal resistance observed the highest current densities and coulombic efficiencies. Conversely, the anode potential was still vulnerable to shifts by the addition of

methanogenesis inhibitors in the anode. Peak current densities were observed at very specific anode potentials for the reactor operating at 170 Ω . The community evolved at this external resistance was most active at anode potentials between -0.3 to 0 mV.

5.5.2 High External Resistances Demonstrate the Electrochemical Robustness of Anode Respiring Biofilms

In MFCs, the anode is used by anode-respiring communities as the terminal electron acceptor. Theoretically, the maximum energy that can be obtained from the biologically-catalyzed redox reaction is given by the Gibbs free energy. Intuitively, the larger the difference in redox potentials between the substrate and the anode, the more energy that can be captured. This is not always the case for reactors driven by biological reactions. ARB have a complex mechanism for using energy for anode respiration which is dependent on cofactors, enzymes, and proteins, such as the c-type cytochrome that enable a major component of the electron transport chain (White, 2007).

Extensive studies have been conducted on the model anode-respiring microorganism *G. sulfurreducens* to evaluate the role of anode potential on the electron transfer pathways (Bond et al., 2003; Kato, 2017; Levar et al., 2014, 2017). *G. sulfurreducens* have multiple electron transfer pathways which can switch and dominate depending on the redox potential of the anode (Levar et al., 2014). In our study, the presence of methanogenesis inhibitors significantly altered the anode potentials at lower external resistances (17-170 Ω). Communities acclimated to the lower external resistances from Phase I showed maximum current density when the anode potential shifted to values between 0 and -0.1 V vs SHE. The redox potential for c-type

cytochromes have been cited within these limits for *G. sulfurreducens* and other *Geobacter* species, such as OmcS and omcZ associated with *G. sulfurreducens* (Kato, 2017; Levar et al., 2014; Reguera et al., 2006; Santos et al., 2015).

On the other hand, at 820 Ω , the current density increased when the anode potentials decreased. It is possible that the anode-respiring community utilizes inner membrane c-type cytochromes that are only triggered at low anode potentials (Levar et al., 2017). At the highest external resistance, associated with the lowest observed anode potential, there seems to be no effect to the current density or coulombic efficiency regardless of the type of inhibitor present in the anode. At high anode potentials biofilms are thinner and more diverse than at more negative anode potentials (Wagner et al., 2010). More recent studies have also observed similar trends in microbial diversity across the frequently studied anode potential spectra (-200 to 800 mV vs SHE) (Dennis et al., 2016; Goud & Mohan, 2013; Kato, 2017; Rismani-yazdi et al., 2011). It is speculated that the thicker biofilms developed at 1800 Ω were less diverse than those at more positive anode potentials. This suggests that at more negative anode potentials, enrichment of anode-respiring communities that can utilize cytochromes at highly negative redox potentials may have occurred. Although studies have not explored the activity of *Geobacter* species at anode potentials between -0.3 and -0.4 V vs SHE, c-type cytochromes in *Shewanella oneidensis*, another frequently studied ARB, have been observed to reduce potentials anywhere between -0.1 and -0.4 V vs SHE (Pitts et al., 2003). *S. oneidensis* has 41 c-type cytochromes encoded into its genome, demonstrating the range of electron transfer pathways available.

5.6 Conclusions

External resistances have a large influence on the observed anode potential, governing the availability of the anode as an electron acceptor for anode-respiring communities. The presence of methanogenesis inhibitors in the anode have a more prominent influence in low resistance reactors (17 and 170 Ω) that exhibited high positive anode potentials. When 2-BES was present at these low external resistances, anode potential became more negative and reached values between -0.1 and 0 mV vs SHE, causing an increase in observed current densities. This also correlated with the higher CE's observed at lower external resistances with the presence of 2-BES. We speculate that the communities within these biofilms contain anode-respiring microorganisms that utilize c-type cytochromes that are only triggered at low anode potentials. Interestingly, by alternating the addition of BES and NO_3^- in the anode over time, current densities and maximum power densities when neither inhibitor was present improved at all external resistances.

Although higher polarization power and operational current densities were displayed at low external resistances, they were not sustained. Consistent current output was more readily shown at high external resistances, demonstrating the electrochemical robustness of the anode biofilm to perturbations of the anode environment at more negative anode potentials. Careful consideration of the external resistance should be made when operating MFCs, keeping in mind the application and goal for which it will be utilized. For controlled system where little changes to the anode environment will occur, low external resistances can yield high current densities. For applications where the anode environment will be exposed to fluctuations of electron competitors or other

metabolic inhibitors, higher external resistance may yield more consistent electrochemical performance. Future work will focus on identifying the activity of key anode-respiring microorganisms and the effects of nitrate on the activity of methanogens.

CHAPTER 6

DISSERTATION CONCLUSIONS

The motivation for the work presented in this dissertation was to understand the role of design parameters on the overall electrochemical performance of MFCs and to assess the practicality of using MFCs as an alternative sanitation system in developing areas for wastewater treatment and energy recovery.

In Chapter 3, we evaluated the energetic outputs of a lab-based pilot MFC designed to treat both complex organics present in synthetic feces and municipal wastewater. The pilot MFC produced two energetic products, methane and electricity, when treating two types of complex wastewaters. The energetic products associated with anode respiration and methanogenesis were simultaneously observed and yielded a combined energy output of $3.3 \pm 0.64 \text{ W/m}^3$ when treating synthetic feces wastewater and $0.40 \pm 0.07 \text{ W/m}^3$ when treating municipal wastewater. Our studies showed that methanogenesis was a dominant alternative metabolic pathway in the anode. This was reinforced by demonstrating that enhanced methane production occurred within mixed cultures enriched from the pilot MFC anode communities in the presence of graphite granules. Our work revealed that alternative metabolic pathways in large-scale MFCs treating complex wastewaters may dominate over electricity-yielding pathways. However, the combined energetic output is still a valuable resource and can be a stepping stone for developing incentivized sanitation solutions.

In Chapter 4, the focus shifted towards improving the performance of the anode-respiring communities by assessing whether augmenting the inoculum (primary

wastewater) with microorganisms from acidic and high-salts environments similar to human feces improved the electrochemical performance of MFCs. We also evaluated the effects of electrolyte concentrations (primarily as conductivity and pH) on MFC performance. With an augmented inoculum, the power density generated was greater than MFCs with only primary wastewater as the inoculum. During this period, the initial bulk liquid conditions were maintained at pH 6.2 and conductivity of 5.2 mS/cm. The CEs were similar for both inoculated reactors, $33 \pm 7.8\%$ for the municipal wastewater inoculated reactor and $37 \pm 9.2\%$ for the co-inoculated reactor and their difference was not statistically significant ($p > 0.05$). With increase in conductivity, the charge transfer from anode to cathode improved in the both the wastewater inoculated reactor and the co-inoculated reactor but was highest in the co-inoculum reactor. The pH had no effect on charge transfer in the primary wastewater inoculated reactor. Although the charge transfer was again higher in the co-inoculated reactor than the primary wastewater inoculated reactor across all pHs tested, the charge transfer decreased as the bulk liquid became more acidic. This study found that the addition of sediments from an acidic and high salt-polluted river to municipal wastewater inocula could improve the electrochemical performance of a MFC with stressed anode environments under high conductivities (5.2-37 mS/cm) and low pH (4.1-6.2). It is evident that the type of inocula should be an important design consideration for applications when MFCs treat wastestreams exhibiting extreme environmental conditions that can otherwise hinder microbial activity. Developing resilient mixed biofilms can improve the electrochemical performance of MFCs, and thus the energy that can be recovered.

Chapter 5 focused on evaluating the influence of the anode potential on the electrochemical resiliency of anode-respiring biofilms to additions of methanogenesis inhibitors, 2-BES and NO_3^- . Our study found that external resistance had a significant influence on the anode potential, and power and current densities. When MFCs were operated at low external resistances (17 and 170 Ω), the addition of 2-BES had a large influence over the anode potential, causing it to decrease to values between -0.2 and 0 mV vs SHE. This decrease correlated with an increase in observed current densities. It is speculated that anode potentials at this range triggered c-type cytochromes that are only active within that range of redox potential. This also correlated with the higher CE's observed at lower external resistances with the presence of 2-BES.

Although higher polarization power and operational current densities were observed at low external resistances, they were not sustained during the length of the phase. Consistent current output was more readily observed at high external resistances, demonstrating the electrochemical robustness of the anode biofilm to perturbations of the anode environment at more negative anode potentials. Careful consideration of the external resistance should be made when designing MFCs for applications where the anode environment will be exposed to fluctuations of electron competitors or other metabolic inhibitors. The use of higher external resistances may yield more consistent electrochemical performance but external resistance that matches the internal resistance yield higher current and can potentially improve these yields over long-term operation.

In summary, MFCs targeted towards decentralized sanitation applications can yield dual energetic products, methane and electricity, where methane seems to dominate at the pilot scale. Bioaugmentation of the anode inoculum may improve electrochemical

performance of MFCs that treat waste streams composed of complex organics and high-salts content. Similarly, nitrate can potentially be used as a methanogenesis inhibitor in the anode without detrimentality affecting the electrochemical performance. Although higher external resistances may yield more consistent current, MFCs with external resistances matching the internal resistance of the cell may yield higher current in long-term operation.

The development of the MFC latrine should focus on making the technology capable of producing sufficient electrical energy to meet the user demands. While methane production is a large energy sink in large-scale applications, the use of nitrate as an inhibitor is promising. Although our work showed that by controlling the anode potential via a high external resistance the effects of nitrate on electrochemical performance could be restrained, future work should also consider the complexity of the substrate and its influence on promoting the availability of other metabolic pathways that can also divert energy.

APPENDIX

SUPPLEMENTARY INFORMATION FOR CHAPTER 5

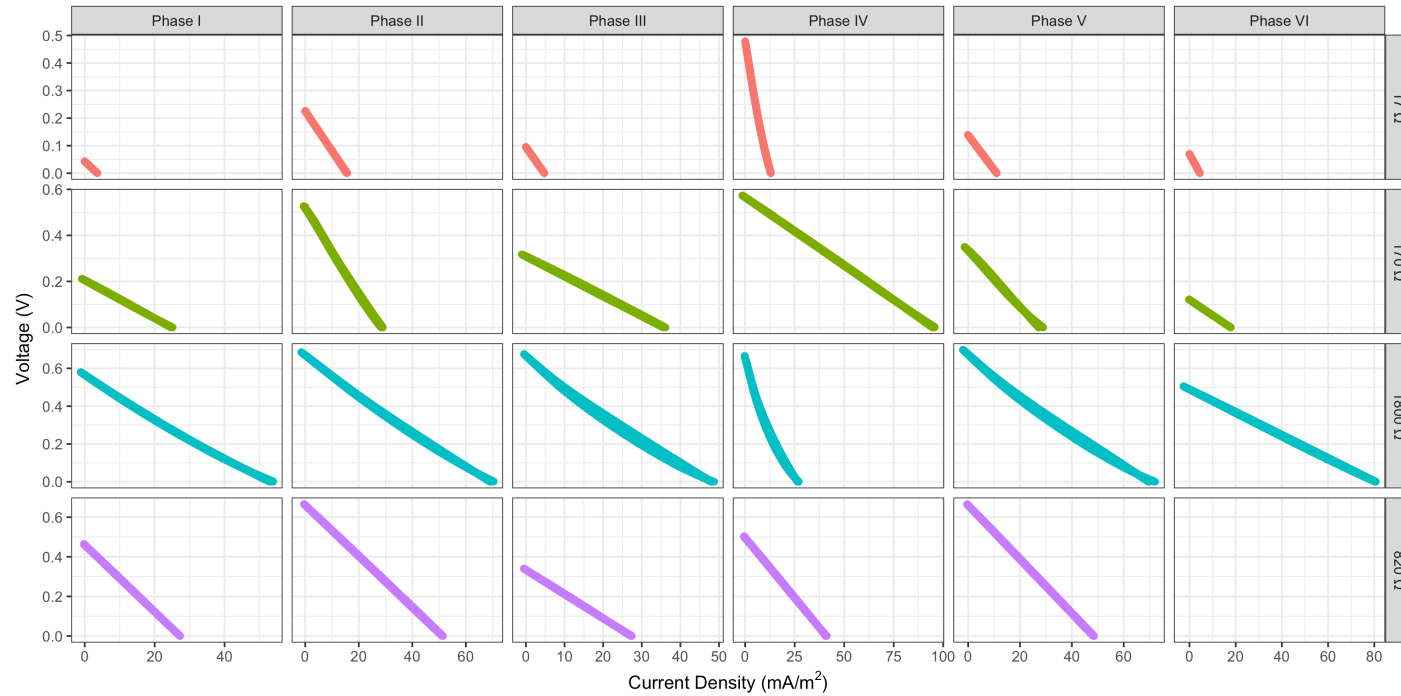


Figure A.1 Polarization curves for determining internal losses and maximum power densities at each phase for all reactors described in Chapter 5.

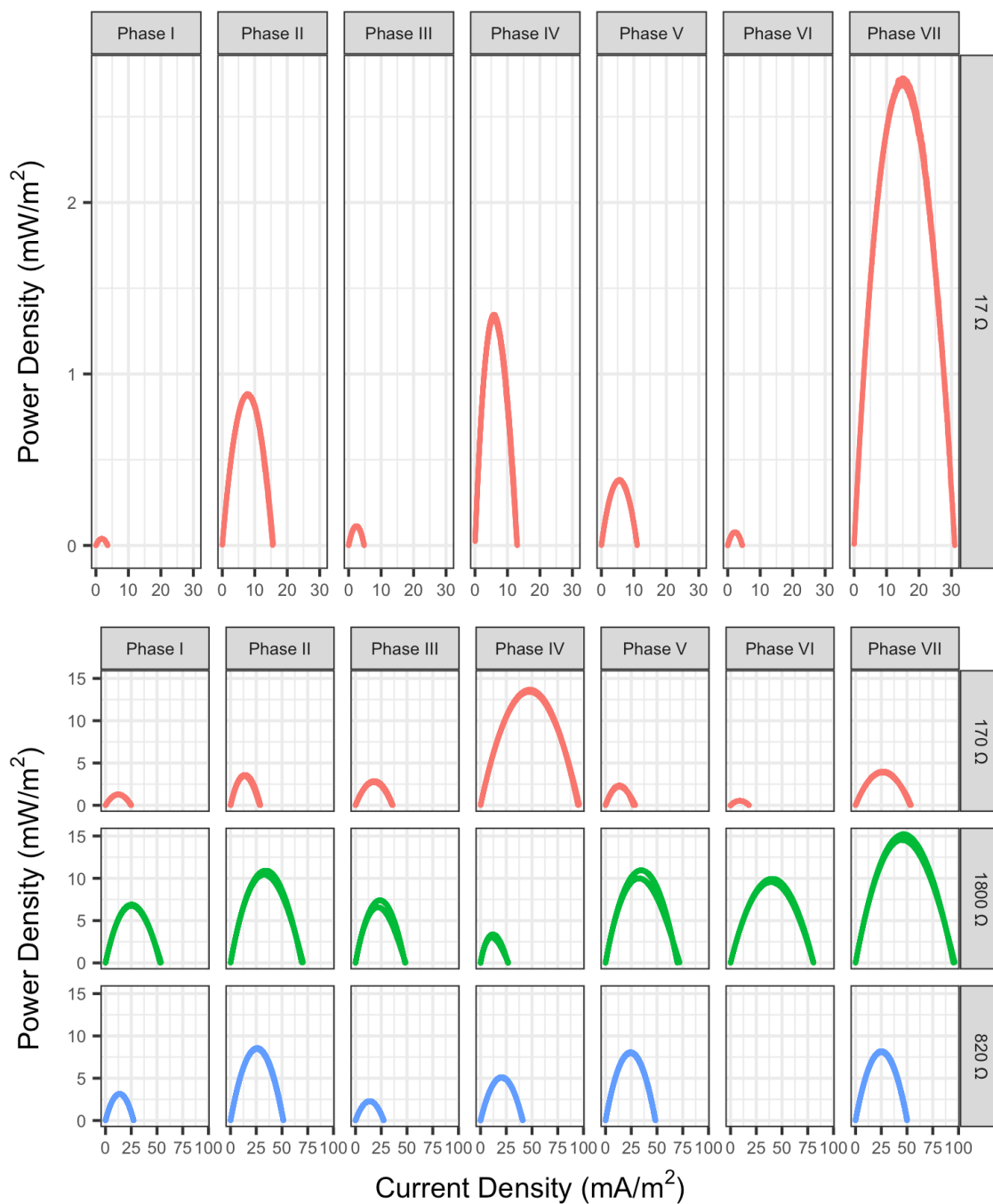


Figure A.2 Power density curves used for determining maximum current density attainable if the internal resistance matched the external resistance. Data shown for reactors R_17, R_170, R_820, and R_1800 for all phases (Chapter 5). Data for R_820 during Phase VI was not available.

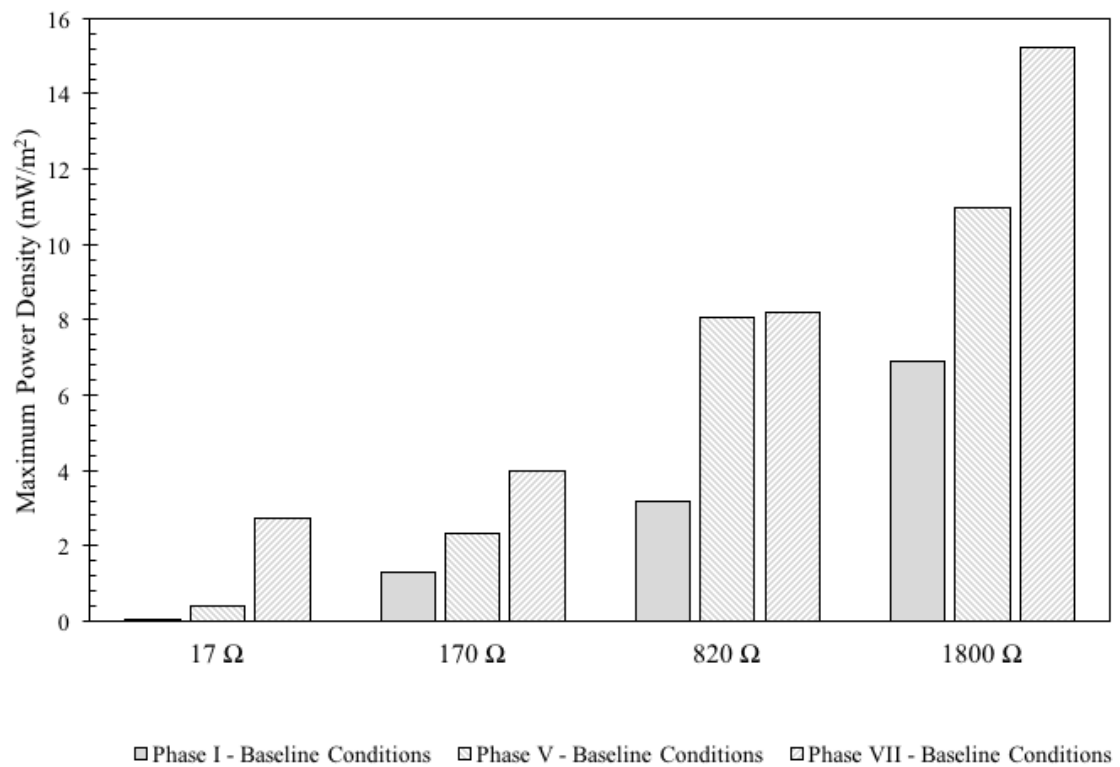


Figure A.3 Maximum power densities obtained at the end of phase I, V, and VII when no inhibitor was presented.

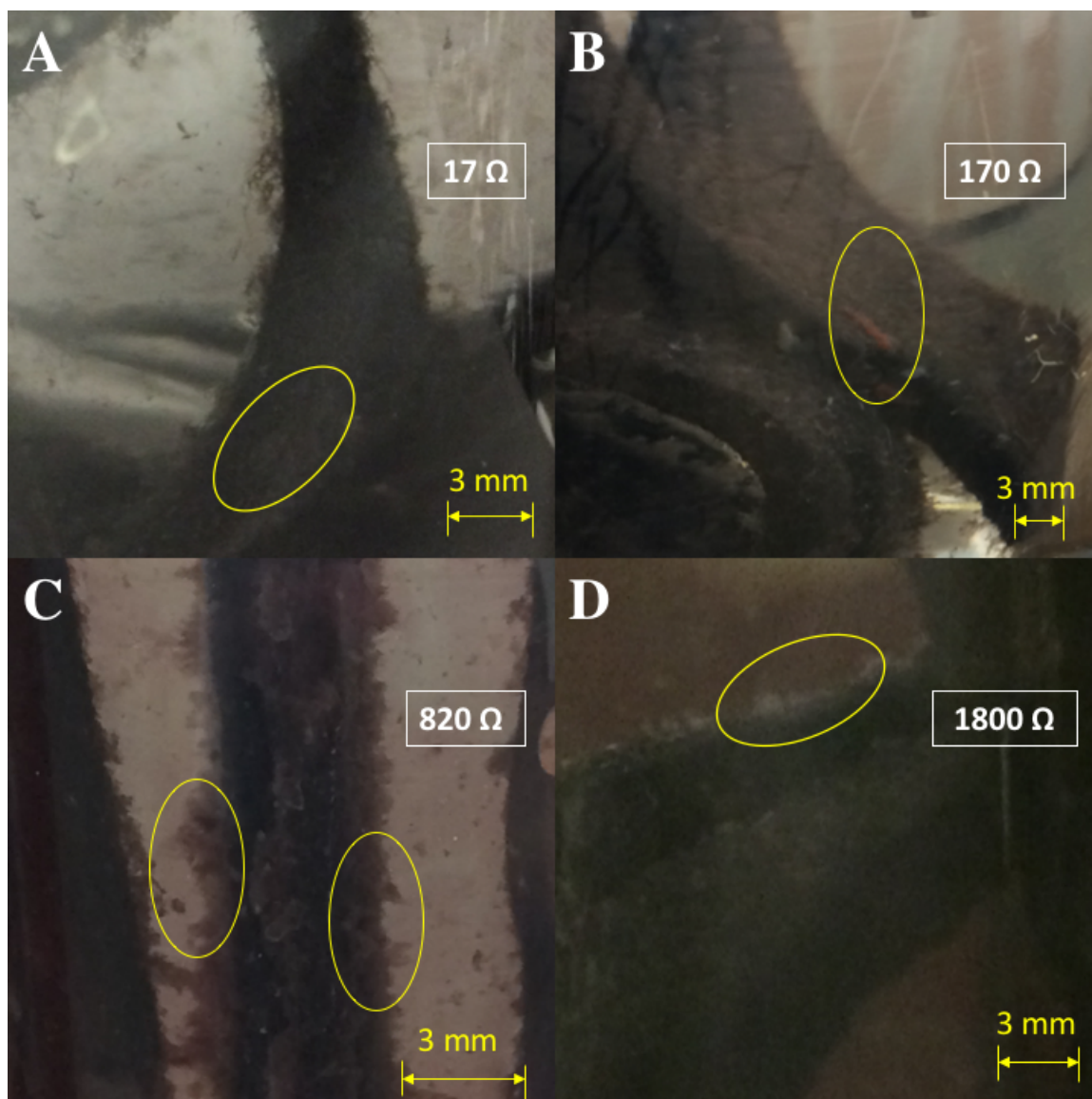


Figure A.4 Photographic images of the anode electrodes at the end of the experiment. A) R_17; B) R_170; C) R_820; D) R_1800. Biofilms are circled.

Methods completed for future work: Biofilm Sampling of External Resistance Reactors

To assess the changes in microbial community in the anode biofilm, gDNA and total RNA were examined to identify which microorganisms were present and active at various time periods of the experiment. Attached and suspended biomass samples were extracted a few hours prior to changing the anode environment to the next phase. In total, seven sampling points from each reactor were obtained. For sampling the attached biomass, a small piece of the carbon felt (4.4 x 22 x 3.2 mm) was cut from each of the five electrodes in the anode under sterile conditions. The pieces were taken from various spots (top, bottom, and sides) to account for the variability in locations where biofilms might form. For sampling the suspended biomass, the anode bulk liquid was mixed and 40 mL were removed and stored in a sterile tube. The bulk liquid with suspended biomass was centrifuged at 4000 rpm for 10 minutes and the liquid was decanted. The remaining biomass pellet was stored in LifeGuard Soil Preservation Solution (Qiagen; Netherlands) at -20°C until processing.

The total RNA was extracted using the RNA PowerSoil® Total RNA Isolation kit (Qiagen), while gDNA was extracted using the RNA Powersoil® DNA Elution Accesory Kit (Qiagen). RNA was treated with DNase Max Kit (Qiagen) to remove contamination of genomic DNA. Concentrations of both mRNA and gDNA were determined using a NanoDrop ND-100 UV/Vis Spectrophotometer (Thermo Scientific, Waltham, MA). Protein and salt contaminations were examined at wavelengths 280 nm and 230 nm, respectively. All samples were within the A_{260}/A_{280} and A_{260}/A_{230} absorbance ratios of 1.7-2.0 and > 1.5 , respectively. Extracted total RNA was converted

to cDNA using a High Capacity cDNA Reverse Transcription Kit (Applied Biosystems, Waltham, MA). The cDNA and gDNA samples were stored at -20 °C for future downstream analysis.

BIBLIOGRAPHY

- Aelterman, P., Freguia, S., Keller, J., Verstraete, W., & Rabaey, K. (2008). The anode potential regulates bacterial activity in microbial fuel cells. *Applied Microbiology and Biotechnology*, 78(3), 409–418. <https://doi.org/10.1007/s00253-007-1327-8>
- Alzate-Gaviria, L., García-Rodríguez, O., Flota-Bañuelos, M., Del Rio Jorge-Rivera, F., Cámara-Chalé, G., & Domínguez-Maldonado, J. (2016). Stacked-MFC into a typical septic tank used in public housing. *Biofuels*, 1–8. <https://doi.org/10.1080/17597269.2015.1118783>
- Amani, T., Nosrati, M., Mousavi, S. M., & Kermanshahi, R. K. (2010). Study of syntrophic anaerobic digestion of volatile fatty acids using enriched cultures at mesophilic conditions. *International Journal of Environmental Science & Technology*, 8(1), 83–96. <https://doi.org/10.1007/BF03326198>
- Bapteste, E., Brochier, C., & Boucher, Y. (2005). Higher-level classification of the Archaea: evolution of methanogenesis and methanogens. *Archaea (Vancouver, B.C.)*, 1(5), 353–63. <https://doi.org/10.1155/2005/859728>
- Beecroft, N. J., Zhao, F., Varcoe, J. R., Slade, R. C. T., Thumser, A. E., & Avignone-Rossa, C. (2012). Dynamic changes in the microbial community composition in microbial fuel cells fed with sucrose. *Applied Microbiology and Biotechnology*, 93(1), 423–437. <https://doi.org/10.1007/s00253-011-3590-y>
- Boesen, T., & Nielsen, L. P. (2013). Molecular dissection of bacterial nanowires. *mBio*, 4(3), e00270-13. <https://doi.org/10.1128/mBio.00270-13>
- Bond, D. R., & Lovley, D. R. (2003). Electricity Production by *Geobacter sulfurreducens* Attached to Electrodes. *Applied and Environmental Microbiology*, 69(3), 1548–1555. <https://doi.org/10.1128/AEM.69.3.1548-1555.2003>
- Borole, A. P., Hamilton, C. Y., Vishnivetskaya, T. A., Leak, D., Andras, C., ... Davison, B. (2009). Integrating engineering design improvements with exoelectrogen enrichment process to increase power output from microbial fuel cells. *Journal of Power Sources*, 191(2), 520–527. <https://doi.org/10.1016/j.jpowsour.2009.02.006>
- Borole, A. P., O'Neill, H., Tsouris, C., & Cesar, S. (2008). A microbial fuel cell operating at low pH using the acidophile *Acidiphilium cryptum*. *Biotechnology Letters*, 30(8), 1367–1372. <https://doi.org/10.1007/s10529-008-9700-y>
- Brooks, A. N., Turkarslan, S., Beer, K. D., Yin Lo, F., & Baliga, N. S. (2011). Adaptation of cells to new environments. *Wiley Interdisciplinary Reviews: Systems Biology and Medicine*, 3(5), 544–561. <https://doi.org/10.1002/wsbm.136>

- Cao, X., Huang, X., Liang, P., Xiao, K., Zhou, Y., ... Logan, B. E. (2009). A New Method for Water Desalination Using Microbial Desalination Cells. *Environmental Science & Technology*, 43(18), 7148–7152. <https://doi.org/10.1021/es901950j>
- Carlson, H. K., Iavarone, a. T., Gorur, a., Yeo, B. S., Tran, R., ... Coates, J. D. (2012). Surface multiheme c-type cytochromes from *Thermincola potens* and implications for respiratory metal reduction by Gram-positive bacteria. *Proceedings of the National Academy of Sciences*, 109(5), 1702–1707. <https://doi.org/10.1073/pnas.1112905109>
- Castro, C. J., Goodwill, J. E., Rogers, B., Henderson, M., & Butler, C. S. (2014). Deployment of the microbial fuel cell latrine in Ghana for decentralized sanitation. *Journal of Water, Sanitation and Hygiene for Development*, 4(4), 663. <https://doi.org/10.2166/washdev.2014.020>
- Castro, C. J., Srinivasan, V., Jack, J., & Butler, C. S. (2016). Decentralized wastewater treatment using a bioelectrochemical system to produce methane and electricity. *Journal of Water, Sanitation and Hygiene for Development*, 6(4), 613–621. <https://doi.org/10.2166/washdev.2016.190>
- Catal, T., Li, K., Bermek, H., & Liu, H. (2008). Electricity production from twelve monosaccharides using microbial fuel cells. *Journal of Power Sources*, 175(1), 196–200. <https://doi.org/10.1016/j.jpowsour.2007.09.083>
- Catal, T., Xu, S., Li, K., Bermek, H., & Liu, H. (2008). Electricity generation from polyalcohols in single-chamber microbial fuel cells. *Biosensors and Bioelectronics*, 24(4), 849–854. <https://doi.org/10.1016/j.bios.2008.07.015>
- Chaudhuri, S. K., & Lovley, D. R. (2003). Electricity generation by direct oxidation of glucose in mediatorless microbial fuel cells. *Nature Biotechnology*, 21(10), 1229–32. <https://doi.org/10.1038/nbt867>
- Chen, S., Rotaru, A.-E., Shrestha, P. M., Malvankar, N. S., Liu, F., ... Lovley, D. R. (2014). Promoting Interspecies Electron Transfer with Biochar. *Scientific Reports*, 4. <https://doi.org/10.1038/srep05019>
- Chen, Y., Cheng, J. J., & Creamer, K. S. (2008). Inhibition of anaerobic digestion process: a review. *Bioresource Technology*, 99(10), 4044–64. <https://doi.org/10.1016/j.biortech.2007.01.057>
- Chen, Y., Yang, G., Sweeney, S., & Feng, Y. (2010). Household biogas use in rural China: A study of opportunities and constraints. *Renewable and Sustainable Energy Reviews*, 14(1), 545–549. <https://doi.org/10.1016/j.rser.2009.07.019>

- Cheng, S., Kiely, P., & Logan, B. E. (2011). Pre-acclimation of a wastewater inoculum to cellulose in an aqueous-cathode MEC improves power generation in air-cathode MFCs. *Bioresource Technology*, 102(1), 367–371. <https://doi.org/10.1016/j.biortech.2010.05.083>
- Cusick, R. D., Bryan, B., Parker, D. S., Merrill, M. D., Mehanna, M., ... Logan, B. E. (2011a). Performance of a pilot-scale continuous flow microbial electrolysis cell fed winery wastewater. *Applied Microbiology & Biotechnology*, 89(6), 2053–2063. <https://doi.org/10.1007/s00253-011-3130-9>
- Cusick, R. D., Bryan, B., Parker, D. S., Merrill, M. D., Mehanna, M., ... Logan, B. E. (2011b). Performance of a pilot-scale continuous flow microbial electrolysis cell fed winery wastewater. *Applied Microbiology and Biotechnology*, 89(6), 2053–63. <https://doi.org/10.1007/s00253-011-3130-9>
- Dennis, P. G., Virdis, B., Vanwonterghem, I., Hassan, A., Hugenholtz, P., ... Rabaey, K. (2016). Anode potential influences the structure and function of anodic electrode and electrolyte-associated microbiomes. *Scientific Reports*, 6(1), 39114. <https://doi.org/10.1038/srep39114>
- Du, F., Xie, B., Dong, W., Jia, B., Dong, K., & Liu, H. (2011). Continuous flowing membraneless microbial fuel cells with separated electrode chambers. *Bioresource Technology*, 102(19), 8914–20. <https://doi.org/10.1016/j.biortech.2011.07.056>
- El-Naggar, M. Y., Wanger, G., Leung, K. M., Yuzvinsky, T. D., Southam, G., ... Gorby, Y. a. (2010). Electrical transport along bacterial nanowires from *Shewanella oneidensis* MR-1. *Proceedings of the National Academy of Sciences of the United States of America*, 107(42), 18127–31. <https://doi.org/10.1073/pnas.1004880107>
- EPA. (1995). *Compilation of Air Pollutant Emission Factors*. Research Triangle Park. Retrieved from <https://www3.epa.gov/ttnchie1/ap42/>
- Esteve-núñez, A., Rothermich, M., Sharma, M., & Lovley, D. (2005). Growth of *Geobacter sulfurreducens* under nutrient-limiting conditions in continuous culture, 7, 641–648. <https://doi.org/10.1111/j.1462-2920.2005.00731.x>
- Fan, Y., Han, S.-K., & Liu, H. (2012). Improved performance of CEA microbial fuel cells with increased reactor size. *Energy & Environmental Science*, 5(8), 8273–8280. <https://doi.org/10.1039/c2ee21964f>
- Fan, Y., Hu, H., & Liu, H. (2007a). Enhanced Coulombic efficiency and power density of air-cathode microbial fuel cells with an improved cell configuration. *Journal of Power Sources*, 171(2), 348–354. <https://doi.org/10.1016/j.jpowsour.2007.06.220>

- Fan, Y., Hu, H., & Liu, H. (2007b). Sustainable Power Generation in Microbial Fuel Cells Using Bicarbonate Buffer and Proton Transfer Mechanisms. *Environmental Science & Technology*, 41(23), 8154–8158. <https://doi.org/10.1021/es071739c>
- Feng, Y., Wang, X., Logan, B. E., & Lee, H. (2008). Brewery wastewater treatment using air-cathode microbial fuel cells. *Applied Microbiology and Biotechnology*, 78(5), 873–880. <https://doi.org/10.1007/s00253-008-1360-2>
- Foley, J. M., Rozendal, R. a, Hertle, C. K., Lant, P. a, & Rabaey, K. (2010). Life cycle assessment of high-rate anaerobic treatment, microbial fuel cells, and microbial electrolysis cells. *Environmental Science & Technology*, 44(9), 3629–3637. <https://doi.org/10.1021/es100125h>
- Franks, A. E., & Nevin, K. P. (2010). Microbial Fuel Cells, A Current Review. *Energies*, 3(5), 899–919. <https://doi.org/10.3390/en3050899>
- Freguia, S., Rabaey, K., Yuan, Z., & Keller, J. (2007). Electron and carbon balances in microbial fuel cells reveal temporary bacterial storage behavior during electricity generation. *Environmental Science and Technology*, 41(8), 2915–2921. <https://doi.org/10.1021/es062611i>
- Freguia, S., Teh, E. H., Boon, N., Leung, K. M., Keller, J., & Rabaey, K. (2010). Microbial fuel cells operating on mixed fatty acids. *Bioresource Technology*, 101(4), 1233–8. <https://doi.org/10.1016/j.biortech.2009.09.054>
- Fricke, K., Santen, H., Wallmann, R., Hüttner, A., & Dichtl, N. (2007). Operating problems in anaerobic digestion plants resulting from nitrogen in MSW. *Waste Management*, 27(1), 30–43. <https://doi.org/10.1016/j.wasman.2006.03.003>
- Gálvez, A., Greenman, J., & Ieropoulos, I. (2009). Landfill leachate treatment with microbial fuel cells; scale-up through plurality. *Bioresource Technology*, 100(21), 5085–5091. <https://doi.org/10.1016/j.biortech.2009.05.061>
- Ge, Z., & He, Z. (2016). Long-term performance of a 200 liter modularized microbial fuel cell system treating municipal wastewater: treatment, energy, and cost. *Environ. Sci.: Water Res. Technol.*, 2(2), 274–281. <https://doi.org/10.1039/C6EW00020G>
- Gorby, Y. A., Yanina, S., McLean, J. S., Rosso, K. M., Moyles, D., ... Fredrickson, J. K. (2006). Electrically conductive bacterial nanowires produced by *Shewanella oneidensis* strain MR-1 and other microorganisms. *Proceedings of the National Academy of Sciences of the United States of America*, 103(30), 11358–63. <https://doi.org/10.1073/pnas.0604517103>

- Gunsalus, R. P., Romesser, J. a, & Wolfe, R. S. (1978). Preparation of coenzyme M analogues and their activity in the methyl coenzyme M reductase system of *Methanobacterium thermoautotrophicum*. *Biochemistry*, 17(12), 2374–2377. <https://doi.org/10.1021/bi00605a019>
- He, Z., Wagner, N., Minteer, S. D., & Angenent, L. T. (2006). An Upflow Microbial Fuel Cell with an Interior Cathode: Assessment of the Internal Resistance by Impedance Spectroscopy. *Environ Sci Technol*, 40(17), 5212–7. <https://doi.org/10.1021/es060394f>
- Herrero-Hernandez, E., Smith, T. J., & Akid, R. (2013). Electricity generation from wastewaters with starch as carbon source using a mediatorless microbial fuel cell. *Biosensors and Bioelectronics*, 39(1), 194–198. <https://doi.org/10.1016/j.bios.2012.07.037>
- Hoover, R. (2001). Composition, molecular structure, and physicochemical properties of tuber and root starches: A review. *Carbohydrate Polymers*, 45(3), 253–267. [https://doi.org/10.1016/S0144-8617\(00\)00260-5](https://doi.org/10.1016/S0144-8617(00)00260-5)
- Huang, L., & Logan, B. E. (2008). Electricity generation and treatment of paper recycling wastewater using a microbial fuel cell. *Applied Microbiology and Biotechnology*, 80(2), 349–355. <https://doi.org/10.1007/s00253-008-1546-7>
- Huang, L., Yang, X., Quan, X., Chen, J., & Yang, F. (2010). Amicrobial fuel cell-electro-oxidation system for coking wastewater treatment and bioelectricity generation. *Journal of Chemical Technology and Biotechnology*, 85(5), 621–627. <https://doi.org/10.1002/jctb.2320>
- Ieropoulos, I. A., Stinchcombe, A., Gajda, I., Forbes, S., Merino-Jimenez, I., ... Greenman, J. (2016). Pee power urinal – microbial fuel cell technology field trials in the context of sanitation. *Environ. Sci.: Water Res. Technol.*, 2(2), 336–343. <https://doi.org/10.1039/C5EW00270B>
- Jadhav, G. S., & Ghangrekar, M. M. (2009). Performance of microbial fuel cell subjected to variation in pH, temperature, external load and substrate concentration. *Bioresource Technology*, 100(2), 717–23. <https://doi.org/10.1016/j.biortech.2008.07.041>
- Jang, J. K., Chang, I. S., Hwang, H. Y., Choo, Y. F., Lee, J., ... Neelson, K. H. (2009). Electricity generation coupled to oxidation of propionate in a microbial fuel cell. *Biotechnology Letters*, 32(1), 79–85. <https://doi.org/10.1007/s10529-009-0118-y>
- Jangir, Y., French, S., Momper, L. M., Moser, D. P., Amend, J. P., & El-Naggar, M. Y. (2016). Isolation and characterization of electrochemically active subsurface Delftia and Azonexus species. *Frontiers in Microbiology*, 7(MAY), 1–11. <https://doi.org/10.3389/fmicb.2016.00756>

- Janicek, A., Fan, Y., & Liu, H. (2014). Design of microbial fuel cells for practical application: a review and analysis of scale-up studies. *Biofuels*, 5(1), 79–92. <https://doi.org/10.4155/bfs.13.69>
- Jiang, D., Curtis, M., Troop, E., Scheible, K., McGrath, J., ... Li, B. (2011). A pilot-scale study on utilizing multi-anode/cathode microbial fuel cells (MAC MFCs) to enhance the power production in wastewater treatment. *International Journal of Hydrogen Energy*, 36(1), 876–884. <https://doi.org/10.1016/j.ijhydene.2010.08.074>
- Jung, J.-Y., Lee, S.-M., Shin, P.-K., & Chung, Y.-C. (2000). Effect of pH on phase separated anaerobic digestion. *Biotechnology and Bioprocess Engineering*, 5(6), 456–459. <https://doi.org/10.1007/BF02931947>
- Jung, S., & Regan, J. M. (2011). Influence of External Resistance on Electrogenesis, Methanogenesis, and Anode Prokaryotic Communities in Microbial Fuel Cells. *Applied and Environmental Microbiology*, 77(2), 564–571. <https://doi.org/10.1128/AEM.01392-10>
- Kang, C. S., Eaktasang, N., Kwon, D. Y., & Kim, H. S. (2014). Enhanced current production by *Desulfovibrio desulfuricans* biofilm in a mediator-less microbial fuel cell. *Bioresource Technology*, 165(C), 27–30. <https://doi.org/10.1016/j.biortech.2014.03.148>
- Kannaiah Goud, R., & Venkata Mohan, S. (2013). Prolonged applied potential to anode facilitate selective enrichment of bio-electrochemically active Proteobacteria for mediating electron transfer: Microbial dynamics and bio-catalytic analysis. *Bioresource Technology*, 137, 160–170. <https://doi.org/10.1016/j.biortech.2013.03.059>
- Kapdan, I. K., & Kargi, F. (2006). Bio-hydrogen production from waste materials. *Enzyme and Microbial Technology*, 38(5), 569–582. <https://doi.org/10.1016/j.enzmictec.2005.09.015>
- Kato, S. (2017). Influence of anode potentials on current generation and extracellular electron transfer paths of *Geobacter* species. *International Journal of Molecular Sciences*, 18(1). <https://doi.org/10.3390/ijms18010108>
- Kato, S., Hashimoto, K., & Watanabe, K. (2012). Microbial interspecies electron transfer via electric currents through conductive minerals. *Proceedings of the National Academy of Sciences of the United States of America*, 109(25), 10042–6. <https://doi.org/10.1073/pnas.1117592109>
- Katuri, K. P., Enright, A.-M., O’Flaherty, V., & Leech, D. (2012). Microbial analysis of anodic biofilm in a microbial fuel cell using slaughterhouse wastewater. *Bioelectrochemistry*, 87, 164–71. <https://doi.org/10.1016/j.bioelechem.2011.12.002>

- Kendall, M. M., & Boone, D. R. (2006). The Order Methanosarcinales. *Prokaryotes Vol. 6*, 244–256. https://doi.org/10.1007/0-387-30743-5_12
- Kiely, P. D., Regan, J. M., & Logan, B. E. (2011). The electric picnic: synergistic requirements for exoelectrogenic microbial communities. *Current Opinion in Biotechnology*, 22(3), 378–85. <https://doi.org/10.1016/j.copbio.2011.03.003>
- Kim, H., Kim, B., Kim, J., Lee, T., & Yu, J. (2014). Electricity generation and microbial community in microbial fuel cell using low-pH distillery wastewater at different external resistances. *Journal of Biotechnology*, 186, 175–180. <https://doi.org/10.1016/j.jbiotec.2014.06.012>
- Kim, K.-Y., Yang, W., & Logan, B. E. (2015). Impact of electrode configurations on retention time and domestic wastewater treatment efficiency using microbial fuel cells. *Water Research*, 80, 41–46. <https://doi.org/10.1016/j.watres.2015.05.021>
- Koster, I. W., & Cramer, a. (1987). Inhibition of methanogenesis from acetate in granular sludge by long-chain Fatty acids. *Applied and Environmental Microbiology*, 53(2), 403–9.
- Kotsyurbenko, O. R., Friedrich, M. W., Simankova, M. V., Nozhevnikova, A. N., Golyshin, P. N., ... Conrad, R. (2007). Shift from acetoclastic to H₂-dependent methanogenesis in a West Siberian peat bog at low pH values and isolation of an acidophilic Methanobacterium strain. *Applied and Environmental Microbiology*, 73(7), 2344–2348. <https://doi.org/10.1128/AEM.02413-06>
- Kouzuma, A., Kato, S., & Watanabe, K. (2015). Microbial interspecies interactions: Recent findings in syntrophic consortia. *Frontiers in Microbiology*, 6(MAY), 1–8. <https://doi.org/10.3389/fmicb.2015.00477>
- Lee, H.-S., Parameswaran, P., Kato-Marcus, A., Torres, C. I., & Rittmann, B. E. (2008). Evaluation of energy-conversion efficiencies in microbial fuel cells (MFCs) utilizing fermentable and non-fermentable substrates. *Water Research*, 42(6–7), 1501–1510. <https://doi.org/10.1016/j.watres.2007.10.036>
- Lee, H., Parameswaran, P., Kato-Marcus, A., Torres, C. I., & Rittmann, B. E. (2008). Evaluation of energy-conversion efficiencies in microbial fuel cells (MFCs) utilizing fermentable and non-fermentable substrates, 42, 1501–1510. <https://doi.org/10.1016/j.watres.2007.10.036>
- Lee, Y., & Nirmalakhandan, N. (2011). Electricity production in membrane-less microbial fuel cell fed with livestock organic solid waste. *Bioresource Technology*, 102(10), 5831–5835. <https://doi.org/http://dx.doi.org/10.1016/j.biortech.2011.02.090>

- Leiva, E., Leiva-Aravena, E., & Vargas, I. (2016). Acid Water Neutralization Using Microbial Fuel Cells: An Alternative for Acid Mine Drainage Treatment. *Water*, 8(11), 536. <https://doi.org/10.3390/w8110536>
- Lessner, D. J. (2009). Methanogenesis Biochemistry. *Encyclopedia of Life Sciences (ELS)*, (1), 1–11. <https://doi.org/10.1002/9780470015902.a0000573.pub2>
- Levar, C. E., Chan, C. H., & Mehta-kolte, M. G. (2014). An Inner Membrane Cytochrome Required Only for Reduction of. *mBio*, 5(6), e02034-14. <https://doi.org/10.1128/mBio.02034-14>.Editor
- Levar, C. E., Hoffman, C. L., Dunshee, A. J., Toner, B. M., & Bond, D. R. (2017). Redox potential as a master variable controlling pathways of metal reduction by *Geobacter sulfurreducens*. *The ISME Journal*, 11(3), 741–752.
- Li, W., Yu, H., & He, Z. (2013). Towards sustainable wastewater treatment by using microbial fuel cells-centered technologies. *Energy Environ. Sci.*, 7(3), 911–924. <https://doi.org/10.1039/C3EE43106A>
- Li, X. M., Cheng, K. Y., Selvam, A., & Wong, J. W. C. (2013). Bioelectricity production from acidic food waste leachate using microbial fuel cells: Effect of microbial inocula. *Process Biochemistry*, 48(2), 283–288.
- Liu, F., Rotaru, A.-E., Shrestha, P. M., Malvankar, N. S., Nevin, K. P., & Lovley, D. R. (2012). Promoting direct interspecies electron transfer with activated carbon. *Energy & Environmental Science*, 5(10), 8982. <https://doi.org/10.1039/c2ee22459c>
- Liu, H., Cheng, S., & Logan, B. E. (2005). Power Generation in Fed-Batch Microbial Fuel Cells as a Function of Ionic Strength, Temperature, and Reactor Configuration. *Environmental Science & Technology*, 39(14), 5488–5493. <https://doi.org/10.1021/es050316c>
- Liu, H., Grot, S., & Logan, B. E. (2005). Electrochemically Assisted Microbial Production of Hydrogen from Acetate. *Environmental Science & Technology*, 39(11), 4317–4320. <https://doi.org/10.1021/es050244p>
- Liu, H., Ramnarayanan, R., & Logan, B. E. (2004). Production of electricity during wastewater treatment using a single chamber microbial fuel cell. *Environmental Science & Technology*, 38(7), 2281–5.
- Liu, R., Gao, C., Zhao, Y. G., Wang, A., Lu, S., ... Huang, Q. (2012). Biological treatment of steroidal drug industrial effluent and electricity generation in the microbial fuel cells. *Bioresource Technology*, 123, 86–91.

- Liu, W., & Cheng, S. (2014). Microbial fuel cells for energy production from wastewaters: the way toward practical application. *Journal of Zhejiang University SCIENCE A*, 15(11), 841–861. <https://doi.org/10.1631/jzus.A1400277>
- Liu, Y., & Whitman, W. B. (2008). Metabolic, Phylogenetic, and Ecological Diversity of the Methanogenic Archaea. *Annals of the New York Academy of Sciences*, 1125(1),
- Logan, B. E. (2008). *Microbial Fuel Cells*. Wiley. Retrieved from <http://books.google.com/books?id=cXnc2wmrE9gC>
- Logan, B. E. (2010). Scaling up microbial fuel cells and other bioelectrochemical systems. *Applied Microbiology and Biotechnology*, 85(6), 1665–71. <https://doi.org/10.1007/s00253-009-2378-9>
- Logan, B. E., Hamelers, B., Rozendal, R., Schröder, U., Keller, J., ... Rabaey, K. (2006). Microbial fuel cells: methodology and technology. *Environmental Science & Technology*, 40(17), 5181–92.
- Lovley, D. R. (2006). Bug juice: harvesting electricity with microorganisms. *Nature Reviews. Microbiology*, 4(7), 497–508. <https://doi.org/10.1038/nrmicro1442>
- Lovley, D. R., & Phillips, E. J. P. (1988). Novel Mode of Microbial Energy Metabolism : Organic Carbon Oxidation Coupled to Dissimilatory Reduction of Iron or Manganese. *Applied and Environmental Microbiology*, 54(6), 1472–1480.
- Lu, N., Zhou, S., Zhuang, L., Zhang, J., & Ni, J. (2009). Electricity generation from starch processing wastewater using microbial fuel cell technology. *Biochemical Engineering Journal*, 43(3), 246–251. <https://doi.org/10.1016/j.bej.2008.10.005>
- Majumder, D., Maity, J. P., Tseng, M.-J., Nimje, V. R., Chen, H.-R., ... Chen, C.-Y. (2014). Electricity Generation and Wastewater Treatment of Oil Refinery in Microbial Fuel Cells Using *Pseudomonas putida*. *International Journal of Molecular Sciences*, 15, 16772–16786. <https://doi.org/10.3390/ijms150916772>
- Mansoorian, H. J., Mahvi, A. H., Jafari, A. J., & Khanjani, N. (2014). Evaluation of dairy industry wastewater treatment and simultaneous bioelectricity generation in a catalyst-less and mediator-less membrane microbial fuel cell. *Journal of Saudi Chemical Society*. <https://doi.org/10.1016/j.jscs.2014.08.002>
- Marsili, E., Baron, D. B., Shikhare, I. D., Coursolle, D., Gralnick, J. a, & Bond, D. R. (2008). *Shewanella* secretes flavins that mediate extracellular electron transfer. *Proceedings of the National Academy of Sciences of the United States of America*, 105(10), 3968–73. <https://doi.org/10.1073/pnas.0710525105>

- Mihelcic, J. R. (2009). *Field Guide to Environmental Engineering for Development Workers: Water, Sanitation, and Indoor Air*. American Society of Civil Engineers. Retrieved from <http://books.google.com/books?id=5FJ-qxWRGXoC>
- Min, B., Kim, J., Oh, S., Regan, J. M., & Logan, B. E. (2005). Electricity generation from swine wastewater using microbial fuel cells. *Water Research*, 39(20), 4961–4968. <https://doi.org/10.1016/j.watres.2005.09.039>
- Miyahara, M., Kouzuma, A., & Watanabe, K. (2015). Effects of NaCl concentration on anode microbes in microbial fuel cells. *AMB Express*, 5(1), 123. <https://doi.org/10.1186/s13568-015-0123-6>
- Montgomery, M. A., & Elimelech, M. (2007). Water and sanitation in developing countries: including health in the equation. *Environmental Science & Technology*, 41(1), 17–24. Retrieved from <http://www.ncbi.nlm.nih.gov/pubmed/17265923>
- Morita, M., Malvankar, N. S., Franks, A. E., Summers, Z. M., Giloteaux, L., ... Lovley, D. R. (2011). Potential for Direct Interspecies Electron Transfer in Methanogenic Wastewater Digester Aggregates. *mBio*, 2(4), e00159-11-e00159-11.
- Nevin, K. P., Holmes, D. E., Woodard, T. L., Hinlein, E. S., Ostendorf, D. W., & Lovley, D. R. (2005). *Geobacter bemidjensis* sp. nov. and *Geobacter psychrophilus* sp. nov., two novel Fe(III)-reducing subsurface isolates. *International Journal of Systematic and Evolutionary Microbiology*, 55(4), 1667–1674.
- Nevin, K. P., Richter, H., Covalla, S. F., Johnson, J. P., Woodard, T. L., ... Lovley, D. R. (2008). Power output and columbic efficiencies from biofilms of *Geobacter sulfurreducens* comparable to mixed community microbial fuel cells. *Environmental Microbiology*, 10(10), 2505–14. <https://doi.org/10.1111/j.1462-2920.2008.01675.x>
- Newton, G. J., Mori, S., Nakamura, R., Hashimoto, K., & Watanabe, K. (2009). Analyses of current-generating mechanisms of *Shewanella loihica* PV-4 and *Shewanella oneidensis* MR-1 in microbial fuel cells. *Applied and Environmental Microbiology*, 75(24), 7674–7681. <https://doi.org/10.1128/AEM.01142-09>
- Niessen, J., Schroder, U., & Scholz, F. (2004). Exploiting complex carbohydrates for microbial electricity generation ? a bacterial fuel cell operating on starch. *Electrochemistry Communications*, 6(9), 955–958.
- Oakley, S. M., Gold, A. J., & Oczkowski, A. J. (2010). Nitrogen control through decentralized wastewater treatment: Process performance and alternative management strategies. *Ecological Engineering*, 36(11), 1520–1531.
- Oh, S. E., & Logan, B. E. (2005). Hydrogen and electricity production from a food processing wastewater using fermentation and microbial fuel cell technologies. *Water Research*, 39(19), 4673–82. <https://doi.org/10.1016/j.watres.2005.09.019>

- Oliveira, V. B., Simões, M., Melo, L. F., & Pinto, A. M. F. R. (2013). Overview on the developments of microbial fuel cells. *Biochemical Engineering Journal*, 73(2010), 53–64. <https://doi.org/10.1016/j.bej.2013.01.012>
- Pandey, P., Shinde, V. N., Deopurkar, R. L., Kale, S. P., Patil, S. A., & Pant, D. (2016). Recent advances in the use of different substrates in microbial fuel cells toward wastewater treatment and simultaneous energy recovery. *Applied Energy*, 168, 706–723. <https://doi.org/10.1016/j.apenergy.2016.01.056>
- Parameswaran, P., Torres, C. I., Lee, H.-S., Krajmalnik-Brown, R., & Rittmann, B. E. (2009). Syntrophic interactions among anode respiring bacteria (ARB) and Non-ARB in a biofilm anode: electron balances. *Biotechnology and Bioengineering*, 103(3), 513–23. <https://doi.org/10.1002/bit.22267>
- Parameswaran, P., Zhang, H., Torres, C. I., Rittmann, B. E., & Krajmalnik-Brown, R. (2010a). Microbial community structure in a biofilm anode fed with a fermentable substrate: the significance of hydrogen scavengers. *Biotechnology and Bioengineering*, 105(1), 69–78. <https://doi.org/10.1002/bit.22508>
- Parameswaran, P., Zhang, H., Torres, C. I., Rittmann, B. E., & Krajmalnik-Brown, R. (2010b). Microbial community structure in a biofilm anode fed with a fermentable substrate: the significance of hydrogen scavengers. *Biotechnology and Bioengineering*, 105(1), 69–78. <https://doi.org/10.1002/bit.22508>
- Park, H. S., Kim, B. H., Kim, H. S., Kim, H. J., Kim, G. T., ... Chang, H. I. (2001). A Novel Electrochemically Active and Fe(III)-reducing Bacterium Phylogenetically Related to *Clostridium butyricum* Isolated from a Microbial Fuel Cell. *Anaerobe*, 7(6), 297–306. <https://doi.org/10.1006/anae.2001.0399>
- Park, H. Il, Wu, C., & Lin, L.-S. (2012). Coal tar wastewater treatment and electricity production using a membrane-less tubular microbial fuel cell. *Biotechnology and Bioprocess Engineering*, 17(3), 654–660. <https://doi.org/10.1007/s12257-011-0374-2>
- Patil, S. A., Harnisch, F., Kapadnis, B., & Schröder, U. (2010). Electroactive mixed culture biofilms in microbial bioelectrochemical systems: The role of temperature for biofilm formation and performance. *Biosensors and Bioelectronics*, 26(2), 803–808. <https://doi.org/10.1016/j.bios.2010.06.019>
- Pitter, P., & Chudoba, J. (1990). *Biodegradability of organic substances in the aquatic environment*. Boca Raton: CRC Press LLC.
- Pitts, K. E., Dobbin, P. S., Reyes-Ramirez, F., Thomson, A. J., Richardson, D. J., & Seward, H. E. (2003). Characterization of the *Shewanella oneidensis* MR-1 Decaheme Cytochrome MtrA. *Journal of Biological Chemistry*, 278(30), 27758–27765. <https://doi.org/10.1074/jbc.M302582200>

- Potter, M. C. (1911). Electrical Effects Accompanying the Decomposition of Organic Compounds. *Proceedings of the Royal Society B: Biological Sciences*, 84(571), 260–276. <https://doi.org/10.1098/rspb.1911.0073>
- Rabaey, K., Boon, N., Höfte, M., & Verstraete, W. (2005). Microbial phenazine production enhances electron transfer in biofuel cells. *Environmental Science & Technology*, 39(9), 3401–8.
- Rabaey, K., Clauwaert, P., Aelterman, P., & Verstraete, W. (2005). Tubular microbial fuel cells for efficient electricity generation. *Environmental Science & Technology*, 39(20), 8077–82. Retrieved from <http://www.ncbi.nlm.nih.gov/pubmed/16295878>
- Reguera, G., McCarthy, K. D., Mehta, T., Nicoll, J. S., Tuominen, M. T., & Lovley, D. R. (2005). Extracellular electron transfer via microbial nanowires. *Nature*, 435(7045), 1098–101. <https://doi.org/10.1038/nature03661>
- Reguera, G., Nevin, K. P., Nicoll, J. S., Covalla, S. F., Woodard, T. L., & Lovley, D. R. (2006). Biofilm and nanowire production leads to increased current in *Geobacter sulfurreducens* fuel cells. *Applied and Environmental Microbiology*, 72(11), 7345–8. <https://doi.org/10.1128/AEM.01444-06>
- Reilly, T. E., Dennehy, K. F., Alley, W. M., & Cunningham, W. L. (2008). *Ground-water availability in the United States*. U.S. Geological Survey Circular 1323. Retrieved from <http://pubs.usgs.gov/circ/1323/>
- Revankar, S. T., & Majumdar, P. (2014). *Fuel Cells: Principles, Design, and Analysis*. Boca Raton: Taylor & Francis Ltd.
- Rismani-Yazdi, H., Carver, S. M., Christy, A. D., Yu, Z., Bibby, K., ... Tuovinen, O. H. (2013). Suppression of methanogenesis in cellulose-fed microbial fuel cells in relation to performance, metabolite formation, and microbial population. *Bioresource Technology*, 129, 281–288.
- Rismani-yazdi, H., Christy, A. D., Carver, S. M., Yu, Z., Dehority, B. A., & Tuovinen, O. H. (2011). Effect of external resistance on bacterial diversity and metabolism in cellulose-fed microbial fuel cells. *Bioresource Technology*, 102(1), 278–283.
- Rittmann, B. E., & McCarty, P. L. (2001). *Environmental biotechnology: principles and applications*. McGraw-Hill. Retrieved from <http://books.google.com/books?id=1PMeAQAAIAAJ>
- Rotaru, A.-E., Shrestha, P. M., Liu, F., Markovaite, B., Chen, S., ... Lovley, D. R. (2014). Direct Interspecies Electron Transfer between *Geobacter metallireducens* and *Methanosarcina barkeri*. *Applied and Environmental Microbiology*, 80(15), 4599–4605. <https://doi.org/10.1128/AEM.00895-14>

- Roy, R., & Conrad, R. (1999). Effect of methanogenic precursors (acetate, hydrogen, propionate) on the suppression of methane production by nitrate in anoxic rice field soil. *FEMS Microbiology Ecology*, 28(1), 49–61. [https://doi.org/10.1016/S0168-6496\(98\)00092-0](https://doi.org/10.1016/S0168-6496(98)00092-0)
- Sander, R. (2014). Compilation of Henry's law constants, version 3.99. *Atmospheric Chemistry and Physics Discussions*, 14(21), 29615–30521. <https://doi.org/10.5194/acpd-14-29615-2014>
- Sang, N. N., Soda, S., Ishigaki, T., & Ike, M. (2012). Microorganisms in landfill bioreactors for accelerated stabilization of solid wastes. *Journal of Bioscience and Bioengineering*, 114(3), 243–250. <https://doi.org/10.1016/j.jbiosc.2012.04.007>
- Santos, T. C., Silva, M. A., Morgado, L., Dantas, J. M., & Salgueiro, C. A. (2015). Diving into the redox properties of *Geobacter sulfurreducens* cytochromes: a model for extracellular electron transfer. *Dalton Transactions*, 44(20), 9335–44.
- Schlesinger, W. H. (2009). On the fate of anthropogenic nitrogen. *Proceedings of the National Academy of Sciences*, 106(1), 203–208. <https://doi.org/10.1073/pnas.0810193105>
- Shi, L., Dong, H., Reguera, G., Beyenal, H., Lu, A., ... Fredrickson, J. K. (2016). Extracellular electron transfer mechanisms between microorganisms and minerals. *Nature Publishing Group*, 14(10), 651–662. <https://doi.org/10.1038/nrmicro.2016.93>
- Speers, A. M., & Reguera, G. (2012). Electron donors supporting growth and electroactivity of *geobacter sulfurreducens* anode biofilms. *Applied and Environmental Microbiology*, 78(2), 437–444. <https://doi.org/10.1128/AEM.06782-11>
- Srinivasan, V. N., & Butler, C. S. (2017). Ecological and Transcriptional Responses of Anode-Respiring Communities to Nitrate in a Microbial Fuel Cell. *Environmental Science & Technology*, acs.est.6b06572. <https://doi.org/10.1021/acs.est.6b06572>
- Summers, Z. M., Fogarty, H. E., Leang, C., Franks, A. E., Malvankar, N. S., & Lovley, D. R. (2010). Direct Exchange of Electrons Within Aggregates of an Evolved Syntrophic Coculture of Anaerobic Bacteria. *Science*, 330(6009), 1413–1415.
- Surendra, K. C., Takara, D., Hashimoto, A. G., & Khanal, S. K. (2014). Biogas as a sustainable energy source for developing countries: Opportunities and challenges. *Renewable and Sustainable Energy Reviews*, 31, 846–859.
- Thauer, R. K., Moller-Zinkhan, D., & Spormann, A. M. (1989). Biochemistry of Acetate Catabolism in Anaerobic Chemotrophic Bacteria. *Annual Review Microbiology*, (43), 43–67.

- Torres, C. I., Krajmalnik-Brown, R., Parameswaran, P., Marcus, A. K., Wanger, G., ... Rittmann, B. E. (2009). Selecting anode-respiring bacteria based on anode potential: phylogenetic, electrochemical, and microscopic characterization. *Environmental Science & Technology*, 43(24), 9519–24. <https://doi.org/10.1021/es902165y>
- Torres, C. I., Marcus, A. K., Lee, H.-S., Parameswaran, P., Krajmalnik-Brown, R., & Rittmann, B. E. (2010). A kinetic perspective on extracellular electron transfer by anode-respiring bacteria. *FEMS Microbiology Reviews*, 34(1), 3–17. <https://doi.org/10.1111/j.1574-6976.2009.00191.x>
- Torres, C. I., Marcus, A. K., & Rittmann, B. E. (2007). Kinetics of consumption of fermentation products by anode-respiring bacteria. *Applied Microbiology and Biotechnology*, 77(3), 689–97. <https://doi.org/10.1007/s00253-007-1198-z>
- United Nations, Department of Economic and Social Affairs, P. D. (2015). *World Population Prospects: The 2015 Revision, Key Findings and Advance Tables. Working Paper No. ESA/P/WP.241*. <https://doi.org/10.1007/s13398-014-0173-7.2>
- Vázquez-Larios, A. L., Solorza-Feria, O., Vázquez-Huerta, G., Esparza-García, F., Rinderknecht-Seijas, N., & Poggi-Varaldo, H. M. (2011). Effects of architectural changes and inoculum type on internal resistance of a microbial fuel cell designed for the treatment of leachates from the dark hydrogenogenic fermentation of organic solid wastes. *International Journal of Hydrogen Energy*, 36(10), 6199–6209. <https://doi.org/10.1016/j.ijhydene.2011.01.006>
- Velasquez-Orta, S. B., Yu, E., Katuri, K. P., Head, I. M., Curtis, T. P., & Scott, K. (2011). Evaluation of hydrolysis and fermentation rates in microbial fuel cells. *Applied Microbiology and Biotechnology*, 90(2), 789–98. <https://doi.org/10.1007/s00253-011-3126-5>
- Velvizhi, G., & Venkata Mohan, S. (2012). Electrogenic activity and electron losses under increasing organic load of recalcitrant pharmaceutical wastewater. *International Journal of Hydrogen Energy*, 37(7), 5969–5978.
- Venkata Mohan, S., Mohanakrishna, G., Velvizhi, G., Babu, V. L., & Sarma, P. N. (2010). Bio-catalyzed electrochemical treatment of real field dairy wastewater with simultaneous power generation. *Biochemical Engineering Journal*, 51(1–2), 32–39.
- Wagner, R. C., Call, D. F., & Logan, B. E. (2010). Optimal Set Anode Potentials Vary in Bioelectrochemical Systems, 44(16), 6036–6041.
- Wang, H., Fotidis, I. A., & Angelidaki, I. (2015). Ammonia effect on hydrogenotrophic methanogens and syntrophic acetate-oxidizing bacteria. *FEMS Microbiology Ecology*, 91(11), 1–8. <https://doi.org/10.1093/femsec/fiv130>

- Wang, H., & Ren, Z. J. (2013). A comprehensive review of microbial electrochemical systems as a platform technology. *Biotechnology Advances*, 31(8), 1796–1807.
- Wang, Y., Zhang, Y., Wang, J., & Meng, L. (2009). Effects of volatile fatty acid concentrations on methane yield and methanogenic bacteria. *Biomass and Bioenergy*, 33(5), 848–853. <https://doi.org/10.1016/j.biombioe.2009.01.007>
- Ward, M. H. (2009). Too Much of a Good Thing? Nitrate from Nitrogen Fertilizers and Cancer. *Reviews on Environmental Health*, 24(4), 357–363. <https://doi.org/10.1515/REVEH.2009.24.4.357>
- Wei, J., Liang, P., Cao, X., & Huang, X. (2010). A new insight into potential regulation on growth and power generation of *Geobacter sulfurreducens* in microbial fuel cells based on energy viewpoint. *Environmental Science & Technology*, 44(8), 3187–91. <https://doi.org/10.1021/es903758m>
- White, D. (2007). *The physiology and biochemistry of prokaryotes* (Third). New York, New York: Oxford University Press, Inc.
- WHO/UNICEF Joint Monitoring Program for Water Supply and Sanitation. (2015). *Progress on Sanitation and Drinking Water: 2015 Update and MCG Assessment*.
- Willis, J. L. (2010). *Energy: Technology to Increase Efficiency of Wastewater Treatment*. Gaithersburg, MD.
- Yang, C., Rooke, J. A., Cabeza, I., & Wallace, R. J. (2016). Nitrate and Inhibition of Ruminal Methanogenesis: Microbial Ecology, Obstacles, and Opportunities for Lowering Methane Emissions from Ruminant Livestock. *Frontiers in Microbiology*, 7(FEB), 1–14. <https://doi.org/10.3389/fmicb.2016.00132>
- Zacharoff, L., Chan, C. H., & Bond, D. R. (2016). Reduction of low potential electron acceptors requires the CbcL inner membrane cytochrome of *Geobacter sulfurreducens*. *Bioelectrochemistry*, 107, 7–13.
- Zavarzina, D. G., Sokolova, T. G., Tourova, T. P., Chernyh, N. a, Kostrikina, N. a, & Bonch-Osmolovskaya, E. a. (2007). *Thermincola ferriacetica* sp. nov., a new anaerobic, thermophilic, facultatively chemolithoautotrophic bacterium capable of dissimilatory Fe(III) reduction. *Extremophiles : Life under Extreme Conditions*, 11(1), 1–7. <https://doi.org/10.1007/s00792-006-0004-7>
- Zhang, F., Ge, Z., Grimaud, J., Hurst, J., & He, Z. (2013). Long-Term Performance of Liter-Scale Microbial Fuel Cells Treating Primary Effluent Installed in a Municipal Wastewater Treatment Facility. *Environmental Science & Technology*, 47(9), 4941–4948. <https://doi.org/10.1021/es400631r>

- Zhao, Z., Zhang, Y., Wang, L., & Quan, X. (2015). Potential for direct interspecies electron transfer in an electric-anaerobic system to increase methane production from sludge digestion. *Scientific Reports*, 5(April), 11094. <https://doi.org/10.1038/srep11094>
- Zheng, X., & Nirmalakhandan, N. (2010). Cattle wastes as substrates for bioelectricity production via microbial fuel cells. *Biotechnology Letters*, 32(12), 1809–1814. <https://doi.org/10.1007/s10529-010-0360-3>
- Zhou, M., Wang, H., Hassett, D. J., & Gu, T. (2013). Recent advances in microbial fuel cells (MFCs) and microbial electrolysis cells (MECs) for wastewater treatment, bioenergy and bioproducts. *Journal of Chemical Technology & Biotechnology*, 88(4), 508–518. <https://doi.org/10.1002/jctb.4004>
- Zhou, Z., Meng, Q., & Yu, Z. (2011a). Effects of methanogenic inhibitors on methane production and abundances of methanogens and cellulolytic bacteria in in vitro ruminal cultures. *Applied and Environmental Microbiology*, 77(8), 2634–2639. <https://doi.org/10.1128/AEM.02779-10>
- Zhou, Z., Meng, Q., & Yu, Z. (2011b). Effects of methanogenic inhibitors on methane production and abundances of methanogens and cellulolytic bacteria in in vitro ruminal cultures. *Applied and Environmental Microbiology*, 77(8), 2634–9. <https://doi.org/10.1128/AEM.02779-10>
- Zhuang, L., Chen, Q., Zhou, S., Yuan, Y., & Yuan, H. (2012). Methanogenesis control using 2-bromoethanesulfonate for enhanced power recovery from sewage sludge in air-cathode microbial fuel cells. *International Journal of Electrochemical Science*, 7(7), 6512–6523.
- Zhuang, L., Zheng, Y., Zhou, S., Yuan, Y., Yuan, H., & Chen, Y. (2012). Scalable microbial fuel cell (MFC) stack for continuous real wastewater treatment. *Bioresource Technology*, 106, 82–88. <https://doi.org/10.1016/j.biortech.2011.11.019>
- Zinder, S. H., Anguish, T., & Cardwell, S. C. (1984). Selective Inhibition by 2-Bromoethanesulfonate of Methanogenesis from Acetate in a Thermophilic Anaerobic Digester. *Applied and Environmental Microbiology*, 47(6), 1343–1345.
- Zuo, Y., Maness, P. C., & Logan, B. E. (2006). Electricity production from steam-exploded corn stover biomass. *Energy and Fuels*, 20(4), 1716–1721. <https://doi.org/10.1021/ef060033l>